Deciphering the relationship between Paa1 and remodeler complexes Isw1a and Isw1b

Anne C. Fritsch
München, Deutschland
2020

Aus dem Biomedizinischen Centrum
Lehrstuhl für Physiologische Chemie
Institut der Ludwig-Maximilians-Universität München
Vorstand: Prof. Dr. Andreas Ladurner

Deciphering the relationship between Paa1 and remodeler complexes Isw1a and Isw1b

Dissertation

zum Erwerb des Doktorgrades der Naturwissenschaften

an der Medizinischen Fakultät der

Ludwig-Maximilians-Universität zu München

vorgelegt von

Anne Carina Fritsch

aus

Aachen

2020

Mit Genehmigung der Medizinischen Fakultät der Universität München

Betreuer: Prof. Dr. Michaela Smolle

Zweitgutachter(in): Prof. Dr. rer. nat. Peter Becker

Dekan: Prof. Dr. med. dent. Reinhard Hickel

Tag der mündlichen Prüfung: 23.04.2021

Eidesstattliche Versicherung

Fritsch, Anne Carina Ich erkläre hiermit an Eides statt, dass ich die vorliegende Dissertation mit dem Titel

“Deciphering the relationship between Paa1 and remodeler complexes Isw1a and Isw1b**”**

selbständig verfasst, mich außer der angegebenen keiner weiteren Hilfsmittel bedient und alle Erkenntnisse, die aus dem Schrifttum ganz oder annähernd übernommen sind, als solche kenntlich gemacht und nach ihrer Herkunft unter Bezeichnung der Fundstelle einzeln nachgewiesen habe. Ich erkläre des Weiteren, dass die hier vorgelegte Dissertation nicht in gleicher oder in ähnlicher Form bei einer anderen Stelle zur Erlangung eines akademischen Grades eingereicht wurde.

München, 01. Mai 2021 Anne Fritsch

Ort, Datum Anne Fritsch

Table of contents

Preface

I performed all experiments described in the work here, except for growth assays with the FLO8 reporter strain, which were performed by Ina Koeva. The strains for the Bio-ID super shift assays were transformed and screened by Julia Schluckebier. Libraries for next generation sequencing were prepared by myself and sequenced at LMU Munich (LAFUGA). Bioinformatics were performed by Dr. Tamas Schauer (Biomedical Center Munich, core facility bioinformatics) and myself.

Summary

Nucleosomes represent the basic unit of chromatin, a higher order structure present in eukaryotic nuclei. The presence of nucleosomes prevents access to DNA-binding factors and subsequently prevents DNA transcription and replication. In budding yeast *Saccharomyces cerevisiae* nucleosomes exist in a stereotypical pattern of evenly spaced dyads starting with the +1 nucleosomes following region depleted of nucleosomes, the NDR.

This pattern is maintained by chromatin remodelers. These same remodelers are capable of sliding or evicting of nucleosomes, making way for DNA-binding factors. Remodelers are fueled by ATPase activity and grouped into separate families. The ISWI family in particular is capable of positioning nucleosomes during transcription. One of the family's complexes, Isw1b is also responsible for repressing cryptic transcription originating from within coding regions. It works in tandem with Chd1, retaining histones in the wake of RNA Polymerase II.

Cryptic transcripts are transcripts from promoters located in intragenic, intergenic or antisense regions that are generally non-coding. There are a few exceptions of cryptic transcripts that are translated into peptides with as of yet unknown purpose. Many cryptic transcripts are degraded quickly and their expression is generally repressed in wild type yeast. Cryptic transcription has been implicated in stress response.

Paa1 is a polyamine acetyltransferase that acetylates polyamines in yeast. This leads to the breakdown of polyamines. Polyamines bind nucleic acids and proteins and are thought to stabilize DNA and RNA integrity.

We had reason to believe that Paa1 physically interacts with Isw1a and/or Isw1b. We could not find evidence of this interaction, but we did find several genetic interactions between *ISW1* and *PAA1*. Among these are increased sensitivity to respiratory and replicative stress. We also found that cryptic transcription of certain genes is increased in *Δisw1 Δpaa1*. This is likely an effect of general transcriptional perturbation, as we could observe many changes of expression of both sense and antisense transcription.

These changes of transcription were not limited to specific groups of transcripts but seemingly affected the entire genome uniformly. Transcription was also affected in *Δisw1* but to a lesser extent than in the double mutant. Transcription in *Δpaa1* was mostly unaffected.

Interestingly, these transcriptional changes were not reflected in nucleosome arraying. Nucleosome spacing was mostly unaffected in *Δisw1 Δpaa1*, whereas spacing in *Δpaa1* was subtly shifted towards the TSS. This implies that transcriptional changes are not a result of looser nucleosome arrays, but are more likely caused by changes in remodeler behavior.

Zusammenfassung

Nukleosomen sind die grundlegende Einheit von Chromatin, einer übergeordneten Struktur die sich in eukaryotischen Nuklei findet. Die Anwesenheit von Nukleosomen verhindert Zugriff durch DNA-bindende Faktoren und verhindert demnach DNA-Transkription und Replikation. In Backhefe Saccharomyces cerevisiae existieren Nukleosomen in einem stereotypischen Muster an gleichmäßig angeordneten Dyaden, angefangen mit dem +1 Nukleosom folgend auf eine Nukleosomen-armer Region, der NDR.

Dieses Muster wird von Chromatin-Remodelern aufrechterhalten. Diese Remodeler sind in der Lage dazu Nukleosomen zu verschieben oder zu entfernen, um Platz zu machen für DNA-bindende Faktoren. Remodeler werden von mittels ATPase-Aktivität angetrieben und in verschieden Familien eingeteilt. Die ISWI-Familie im Besonderen spielte eine Rolle in der Anordnung von Nukleosomen während der Transkription. Einer der Komplexe aus der ISWI-Familie, Isw1b ist noch dazu zuständig für die Unterdrückung von Kryptischer Transkription, die aus kodierenden Regionen entspringt. Zusammen mit Chd1 ist Isw1b dafür zuständig um Histone nach der Passage von RNA Polymerase II beizubehalten.

Kryptische Transkripte können von Promotern stammen die inmitten oder in den Flanken eines Genes, oder auf dem antisense Strang liegen. Es gibt wenige Ausnahmen an kryptischen Transkripten, die in Peptide translatiert werden. Die Aufgabe dieser Peptide ist bis jetzt noch unklar. Viele kryptische Transkripte werden schnell abgebaut und ihre Expression ist normalerweise unterdrückt im Hefe Wildtyp. Kryptische Transkription hat unter Umständen etwas mit der Antwort auf Stress zu tun.

Paa1 ist eine Polyamine Acetyltransferase die Polyamine in Hefe acetyliert. Dies führt zum Abbau von Polyaminen. Polyamine binden an Nukleinsäuren und Proteine und sing wahrscheinlich in der Lage dazu die Integrität von DNA und RNA zu stabilisieren.

Wir hatten Grund zur Annahme das Paa1 physisch mit Isw1 und/oder Isw1b interagiert. Wir konnten zwar keinen Beleg für dies Interaktion finden, aber wir konnten einige genetische Interaktionen zwischen *ISW1* und *PAA1* nachweisen. Darunter befinden sich erhöhte Sensibilität zu respiratorischem und replikativem Stress. Wir fanden außerdem, dass kryptische Transkription war erhöht in einigen Genen in *Δisw1 Δpaa1*. Dies ist wahrscheinlich ein Folge von allgemeiner transkriptioneller Perturbation. Expression von sense als auch antisense Transkripten war großflächig betroffen, mit Regulation nach oben und unten.

Diese Änderungen der Transkription waren nicht auf spezifische Gruppen von Transkripten limitiert, sondern schienen das gesamte Genom in etwa gleichmäßig zu betreffen. Transkription war auch in *Δisw1* betroffen, allerdings weniger stark als bei der Doppelmutante. Transkription in *Δpaa1* ist weitgehend unberührt.

Interessanterweise finden sich diese Änderungen nicht in Nukleosomen Abständen wieder. Nukleosomen Abstände war unverändert in *Δisw1 Δpaa1*, wohingegen die Abstände in *Δpaa1* in Richtung des TSS verschoben war. Dies impliziert das Transkriptionsänderungen nicht ein Resultat von veränderter Nukleosomen Anordnung ist, sondern eher durch Änderungen im Benehmen der Remodeler verursacht wird.

1 Introduction

1.1 The biology of chromatin

1.1.1 From DNA to chromosomes - how the genome fits into the nucleosome

DNA is the building block of genetic information (Avery et al., 1944). It is present as long polymers, which poses the problem of fitting long polymer strings into the defined space of a nucleus. This is primarily a problem for eukaryotes with their generally larger genomes, compared to prokaryotes. The entirety of DNA contained in one eukaryotic genome can range from millions of base pairs in yeast (Kullman et al., 2005) to billions of base pairs in humans (Gregory, 2018). All of these have to fit into the limited space of a nucleus, an organelle that is often only a few microns in diameter (Luger et al., 1997).

The nucleus in haploid yeast cells is only about 2 microns in size, whereas the human nucleus reaches up to 10 microns (Milo et al., 2010). First, DNA is wrapped 1.7 times around histone octamers in what is called a nucleosome (Olins and Olins, 1974 and Figure 1-1A). The nucleosome is the minimal repeat unit for higher order structures and multiple nucleosomes, called oligonucleosomes resemble something close to beads on a string. The length of DNA wrapped around a histone octamer is 147 bp (Lutter, 1978) and Figure 1-1C). Nucleosomes are connected by a variable length of DNA called linker DNA that contributes to the shaping of DNA structure (Prunell and Kornberg, 1978; Luger et al., 1997). The linker length often varies between species, ranging from 20 to 90 bp (Perisic et al., 2010).

There are four different types of histones in a canonical histone octamer, histones H2.A, H2.B, H3 and H4 (McGhee and Felsenfeld, 1980 and Figure 1-1A). The octamer itself consists of a histone H3-H4 tetramer and two histone H2A-H2B dimers (Luger et al., 1997 and Figure 1-1A). Histones significantly influence DNA condensation and accessibility and thereby influence a variety of cellular processes, ranging from silencing (Kayne et al., 1988) to transcription activation (Allfrey et al., 1964; Durrin et al., 1991) to promoting chromatin stability (Chavez et al., 2012). Different histone variants also exist and fulfill specialized functions. These variants can have a fundamental impact on chromatin properties. For example, a centromeric histone H3 variant called CENP-A or Cse4 in yeast, is required for the formation of centromeric chromatin (Collins et al., 2004; McKinley and Cheeseman, 2016). Another example, histone H2A.Z is among the most conserved histone variants, showing more sequence similarity across homologs from different species than to histone H2A within the same species (Thatcher and Gorovsky, 1994; Iouzalen et al., 1996). The structure of the histone octamer containing histone H2A.Z is similar to canonical histone H2A. However, changes of some amino acids lead to a subtle destabilization of histone interactions, specifically histone H2A.Z and H3 (Suto et al., 2000). Histone H2A.Z has been found to be involved in transcriptional control (Redon et al., 2002), and alters nucleosome stability (Santisteban, Kalashnikova et al., 2000).

Deposition of any histones requires the activity of histone chaperones; acidic proteins that aid in histone deposition, exchange and eviction (Akey and Luger, 2003; Mavrich et al., 2008), (Ransom et al., 2010). In yeast and most eukaryotes nucleosomes are arrayed in a stereotypical pattern around the Transcription Start Sites (TSS). This pattern is categorized by a nucleosome-depleted region (NDR) just upstream of the TSS. The NDR is flanked by two nucleosomes, -1 upstream of the TSS and +1 near or on the TSS. The latter being followed by arrays of well-spaced nucleosomes along the coding region (Lee et al., 2007; Mavrich et al., 2008 and Figure 1-1B). Histone H2A.Z can be commonly found in nucleosomes surrounding the promoter region (Guillemette, Bataille et al., 2005).

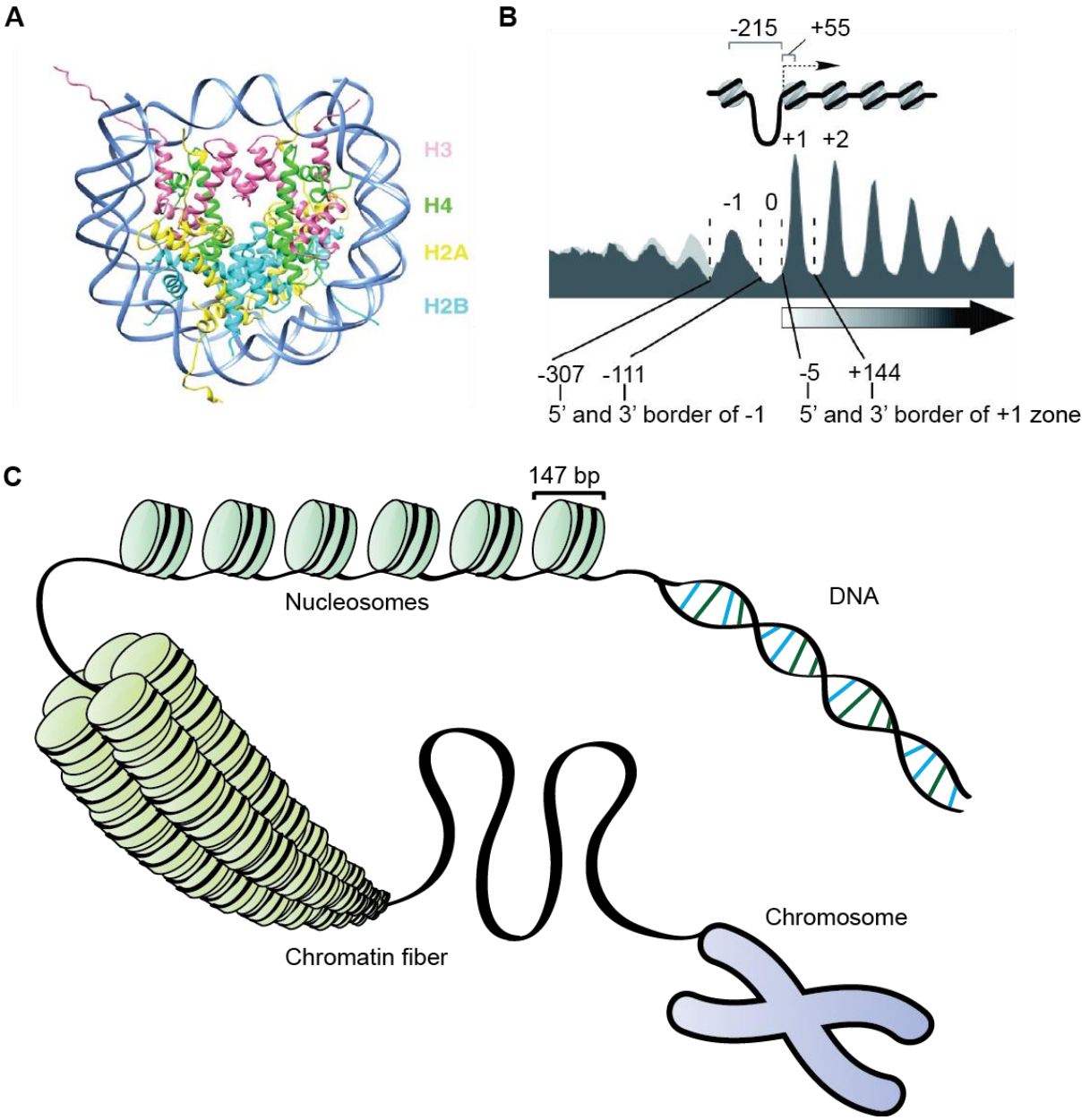

Figure 1-1: From DNA to chromosomes, higher order organization of DNA polymers: (A) Crystal structure of DNA wrapped around a histone octamer. [Reprinted with permission from Elsevier (Zhu and Li 2016)] **(B)** Stereotypical positioning of nucleosomes at the NDR in yeast [Reprinted with permission from BioMed Central Ltd. (Jiang and Pugh 2009)]. **(C)** DNA is wrapped around histones in nucleosomes. These nucleosomes are wound into fibers and then further condensed into chromosomes.

Nucleosomes are then further assembled into helical super-structures that are stabilized by the linker histone H1 (Billett and Barry, 1974; Luger et al., 1997). These super-structures appear as so-called 30 nm fibers, a 30 nm diameter helical structure, whose precise topology is dependent on linker length and exit/entrance angles of DNA on nucleosomes (Wong et al., 2007). This has yet to be observed *in vivo* however and is therefore thought to be an artifact of *in vitro* preparation (Maeshima et al., 2014). Conversely, it has been proposed that chromatin is shaped into primary helices that interdigitize into a larger super-helical structure (Daban and Bermudez, 1998; Robinson and Rhodes, 2006). Chromatin fibers are then further condensed into chromosomes (Figure 1-1C).

1.1.2 Histone modifications are important factors in the regulation of gene expression and maintenance of chromatin structure

Histones can carry a variety of modifications (Zhao and Garcia, 2015) that can directly affect chromatin organization or structure (Bannister and Kouzarides, 2011). Alternatively, they function as recruitment platforms that are recognized by specific effector proteins (Yun et al., 2011) or regulate the transcription of genetic information (Jenuwein and Allis, 2001). Among the most common modifications are acetylation, methylation, phosphorylation, ubiquitination and sumoylation of specific amino acid residues. Modifications can vary between organisms. Typical histone tail modifications in yeast *Saccharomyces cerevisiae* (*S.c.*) are shown in Figure 1-2.

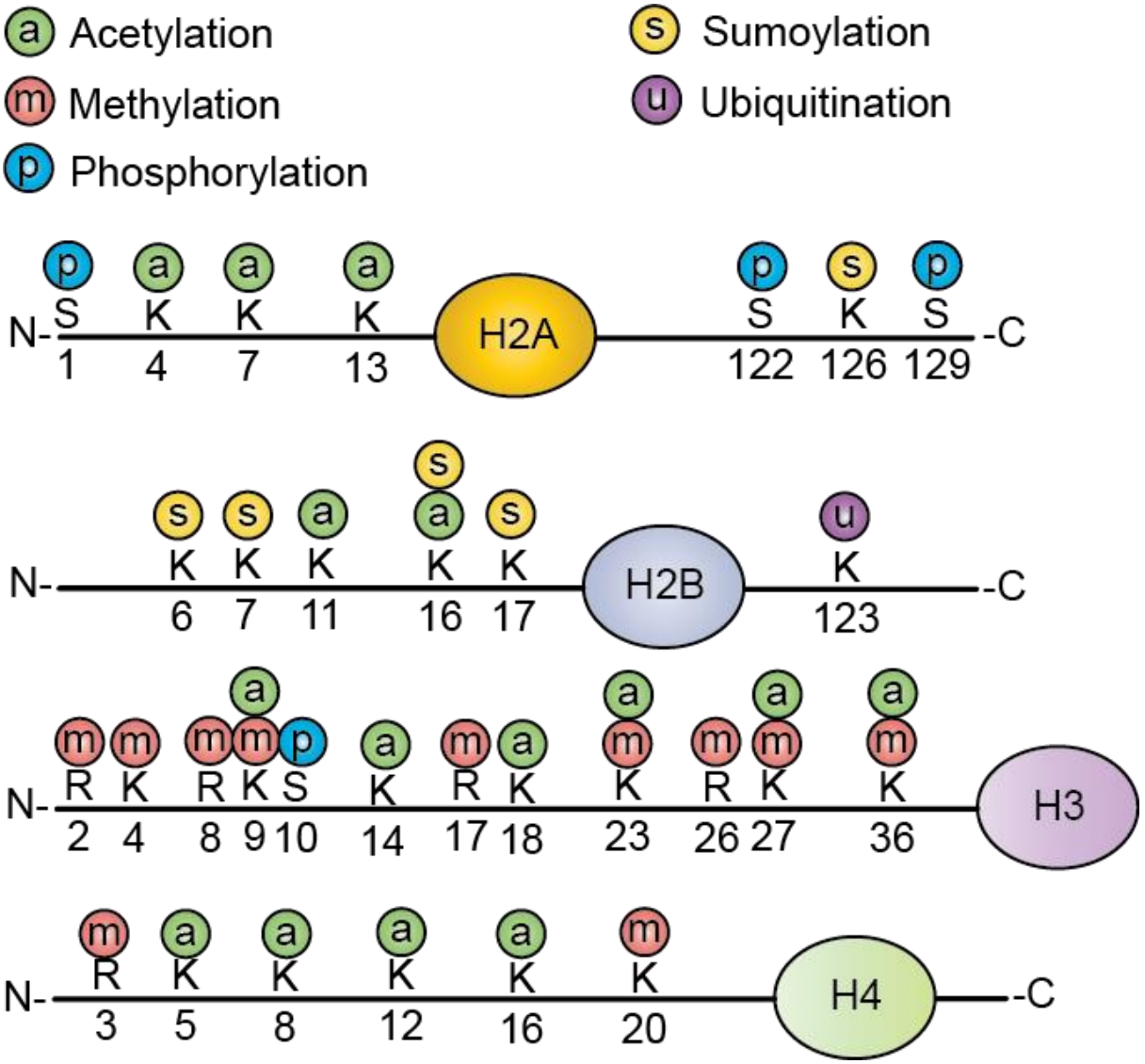

Figure 1-2: Modifications on yeast histone tails. Lysine and arginine residues are among the most commonly modified residues on histone tails. Arginine residues are methylated, whereas lysine residues are methylated, acetylated, ubiquitinated and sumoylated. Serine can carry a phosphorylation mark. Most modifications occur on a histone's N-terminal tail, but H2A and H2B also carry modifications on their C-terminal tail.

Acetylation on lysine residues leads to a "loosening" of chromatin structure, as the acetylation neutralizes the positive charge of the lysine and thereby reduces the electrostatic attraction between histones and DNA (Patrone et al., 2006; Allan et al., 1982). In many instances, multiple acetylation events have additive effects and lead to a gradual increase in DNA accessibility, allowing better access for DNA-binding proteins/transcription factors, the transcriptional machinery and coactivators (Li and Widom, 2004). This loosening and subsequent accessibility is required for active transcription to proceed (Workman and Kingston, 1998). Acetylation marks are also responsible for recruitment of factors (Ferreira et al., 2007). They can be recognized by acetyl-lysine reader modules such as bromodomains (Kanno et al., 2004).

Histone acetyltransferase Gcn5 is responsible for acetylation of H3 lysine residues 9 and 14 (H3K9ac and H3K14ac, Figure 1-2). It is primarily recruited to active promoter regions (Robert, Pokholok et al., 2004). Both H3K9ac and H3K14ac are primarily associated with transcription start sites of active genes (Pokholok et al., 2005).

Both lysine and arginine residues can be methylated. Different methylation states exist. Lysine can be mono-, di- and trimethylated, while arginine can be mono- and dimethylated. Methylated histones are recognized by methyl-binding domains, like PHD fingers, chromodomains or PWWP domains (Shi et al., 2006; Maltby et al., 2012). In contrast to acetylation, methylation has no effect on the positive charges of either lysine or arginine. The consequences of histone methylation are therefore context-dependent. In particular, trimethylation of histone H3 lysine 4 (H3K4me3, Figure 1-2) and histone H3 lysine 36 (H3K36me3, Figure 1-2) are associated with active transcription. H3K4me3 occurs at promoters of active genes (Krogan et al., 2003; Ng et al., 2003) and is mediated by the COMPASS complex (Miller et al., 2001). H3K4me3 only occurs at actively transcribed genes and persists for a time after, functioning as a memory of transcription (Ng et al., 2003).

H3K36me3 on the other hand is a modification mark commonly found in the body of active genes (Li et al., 2002). Set2 is responsible for methylation of lysine 36 (Strahl et al., 2002). The histone deacetylase complex Rpd3S then recognizes H3K36me3 and removes acetylation marks from surrounding histones, increasing chromatin compaction and preventing transcription initiation from internal, cryptic promoter sites (Carrozza et al., 2005; Keogh et al., 2005). Methylated histones are recognized by methyl binding domains, like chromo domains. PHD fingers PWWP domains (Bannister et al., 2001; Shi et al., 2006; Maltby et al., 2012). Taken together, chromatin accessibility can be influenced directly and indirectly in a multitude of ways that affect DNA-based nuclear processes, such as gene expression or DNA replication and repair. As a result, there are many proteins dedicated to regulating chromatin accessibility. Among these are chromatin remodelers, histone chaperones and histone modifying enzymes.

1.2 The role of chromatin remodelers in yeast

Chromatin remodelers can assemble, evict, space or exchange nucleosomes, utilizing energy won from ATP hydrolysis (Bork and Koonin, 1993; Eisen et al., 1995). Most chromatin remodelers are multi-subunit protein complexes. They are grouped into four families by their catalytic subunits: ISWI, CHD, SWI/SNF and INO80 (Witkowski and Foulkes; 2015). They are further grouped into subfamilies based on their other domains and function. Several experiments have shown that some of them work in concert to establish ordered nucleosome structure. Chromatin immunoprecipitation (ChIP) analysis of MNase-digested chromatin has shown cooperative activity between different remodelers to evict and reposition nucleosomes (Rawal et al., 2018). *In vitro* reconstitution of nucleosomes allows examination of nucleosome positioning mechanisms and the resulting order of nucleosome arrays. The presence of remodelers in reconstitution assays can give an indication of individual or cooperative remodeler activity on nucleosome positioning (Garinther and Schultz, 1997; Krietenstein et al., 2016).

INO80 positions +1 nucleosomes and aligns the downstream arrays of nucleosomes. ISWI establishes regular spacing along the array (Krietenstein et al., 2016). The ATPase domain of the INO80 (inositol) family is similar to those from the ISWI family, but functionally they are not related (Bakshi et al., 2004). The INO80 complex has several functions, among which are DNA damage repair (Morrison et al., 2004; Kawashima et al., 2007) and histone placement and exchange (Papamichos-Chronakis et al., 2011). The SWI/SNF (Switch/Sucrose Non-Fermentable) complex can change nucleosome positions on DNA (Whitehouse et al., 1999; van Holde and Yager, 2003). The CHD (Chromodomain-helicase-DNA-binding) family is based on the presence of chromo domains and its members are highly conserved from yeast to humans (Woodage et al., 1997). *In vitro* experiments have shown that Chd proteins are involved in nucleosome sliding (Qiu et al., 2017) and in the assembly and spacing of nucleosome arrays (Lusser et al., 2005). In yeast Chd1 overlaps functionally with the members of the ISWI family (Tsukiyama et al., 1999; Stockdale et al., 2006).

1.3 The complexes of the ISWI family

ISWI (imitation switch) was first described in *Drosophila*, as a relative to the transcriptional activator SWI2 (Elfring et al., 1994). ISWI and SWI2 both contain an ATPase domain, but differ in their domain structure otherwise, indicating that there is no functional homology. ISWI remodelers are highly conserved, with homologs in several eukaryotic organisms from yeast to humans (Elfring et al., 1994; Guschin et al., 2000). Two homologs to *Drosophila* ISWI, Isw1 and Isw2, were identified and purified from yeast (Tsukiyama et al., 1999). Isw2 forms a complex with Itc1, Dls1 and Dpb4 (Gelbart et al., 2001; McConnell et al., 2004), Figure 1-3A). Isw1 was later discovered to form the catalytic subunit of two separate remodeling complexes, Isw1a and Isw1b (Vary et al., 2003 and Figure 1-3A). Isw1a consists of Isw1 and Ioc3. Isw1b consists of Isw1, Ioc2 and Ioc4 (Vary et al., 2003 and Figure 1-3A).

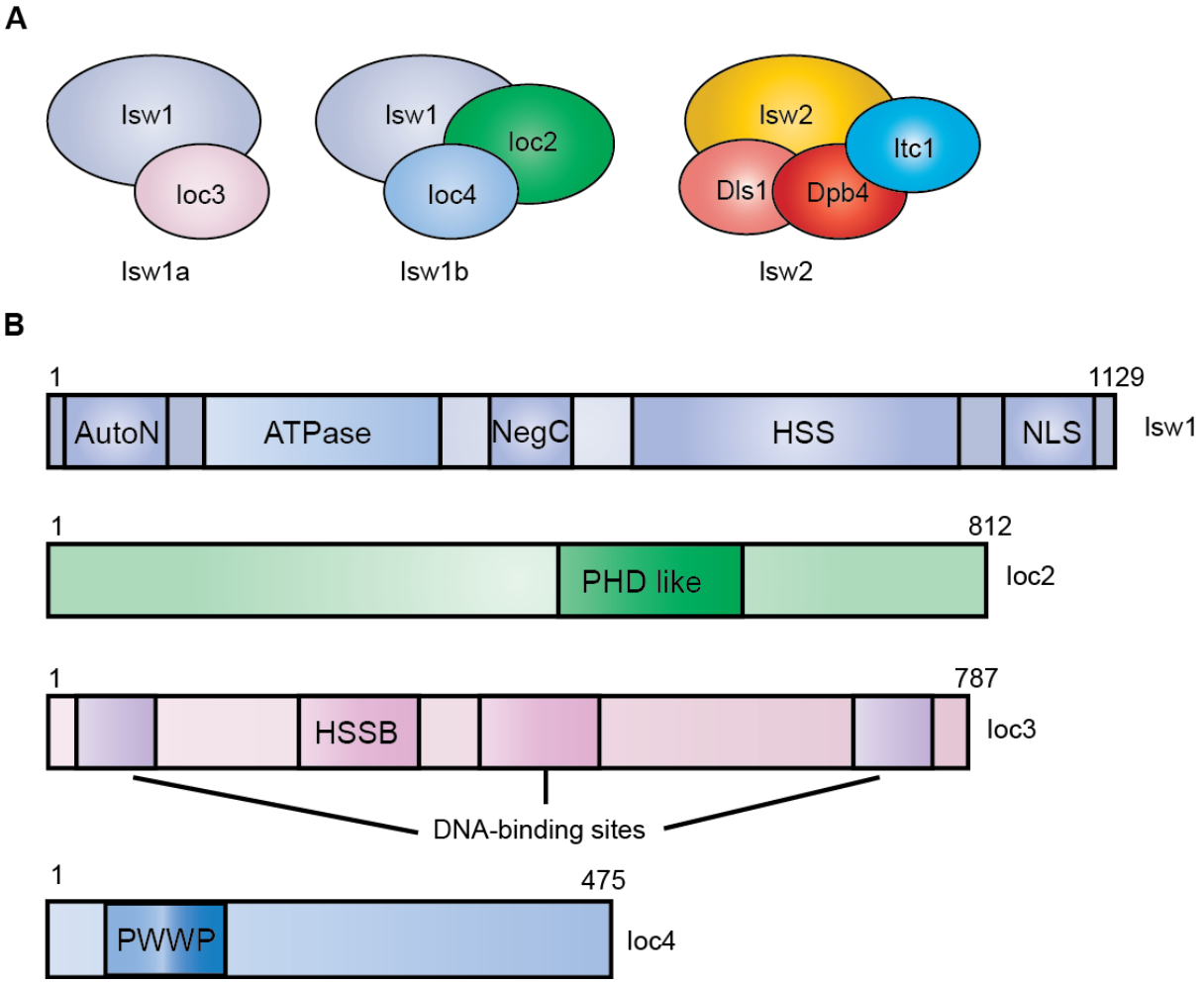

Figure 1-3: The three complexes making up the ISWI remodeler family and the domain structure of the Isw1 complex subunits: (A) The members of the ISWI family are Isw1a, Isw1b and Isw2. Isw1 and Isw2 are the **catalytic** subunits of their respective complexes. Isw1 forms two complexes, Isw1a and Isw1b. **Isw1a** consists of Isw1 and Ioc3 and Isw1b consists of Isw1, Ioc2 and Ioc4, and Isw2 forms a complex with Itc1. **(B)** Isw1 has several domains, the catalytic ATPase domain, an HSS domain, two autoregulatory domains AutoN and NegC and a nuclear localization signal. Ioc2 has a Plant homeodomain like domain. Ioc3 has a HSS-binding domain, and several DNA-binding sites. Ioc4 has a PWWP domain. DNA binding is conferred to the Isw1 complexes through the Ioc subunits. The PWWP domain on Ioc4 binds H3K36me3 and Ioc3 has several DNA-binding sites that also function as a ruler.

1.3.1 Domain structure of Isw1 complexes

Isw1 contains an ATPase domain, which confers catalytic activity through ATP hydrolysis (Tsukiyama et al., 1999). It contains a HAND- SANT-SLIDE (HSS) domain (Grune et al., 2003; Yamada et al., 2011 and Figure 1-3B). The HAND domain confers DNA and nucleosome binding properties. The name derives from the resemblance of the 4-helical structure to a hand. The SLIDE (SANT-like ISWI domain) domain plays a role in DNA-binding and nucleosome recognition (Grune et al., 2003). In this it is functionally related to SANT domains (Yamada et al., 2011; Pinskaya et al., 2009). Function of Isw1 is further regulated by the interplay between two nucleosomal epitopes and two autoregulatory regions on Isw1 (Figure 1-3B). These autoregulatory regions are AutoN, which affects ATP hydrolysis and NegC, which affects the coupling of ATP hydrolysis to DNA sliding. These two epitopes, a basic patch on the H4 tail and a sequence of extranucleosomal linker DNA inhibit the function

of the autoregulatory regions and promote Isw1 activity (Gangaraju and Bartholomew, 2007; Clapier and Cairns, 2012). An NLS (nuclear localization signal) is required for localization to the nucleus (Vasicova et al., 2013 and Figure 1-3B).

Isw1a also contains Ioc3. Ioc3 contains a Helical-Linker-DNA-Binding domain (HLB) and HSS-binding loop (Figure 1-3B). The SLIDE domain of Isw1 plays a role in its interaction with Ioc3, as its absence prevents complex association (Pinskaya et al., 2009). Together with the HSS domain of Isw1, the HLB is thought to function as a protein ruler that measures out nucleosome spacing (Yamada et al., 2011). There is also a Coil-Linker-DNA-Binding motif (CLB) that has been indicated to confer a preference for specific DNA binding sequences to Isw1a (Yamada et al., 2011). Ioc3 preferentially binds TSS and Transcription End Sites (TES), indicating a targeted localization of Isw1a to these sites (Smolle et al., 2012; Yen et al., 2012).

Isw1b contains two other subunits next to its catalytic subunit Isw1. Like in Isw1a, the HSS domain of Isw1 is needed to confer interaction with Ioc2 and Ioc4 (Pinskaya et al., 2009). It has been further shown that both Ioc2 and Ioc4 are required for complex formation, as loss of either will lead to the loss of the other (Vary et al., 2003). Ioc2 contains a Plant HomeoDomain (PHD)-like finger (Vary et al., 2003 and Figure 1-3B). PHDs are made up of a Cys4-His-Cys3 motif that coordinates two zinc ions (Capili et al., 2001). In Ioc2 the PHD like domain contains a 70 amino acid long insert, separating the Cys4-His-Cys3 from the C-terminal end (Vary et al., 2003). Many PHD fingers have been shown to interact with nucleosomes (Ragvin et al., 2004; Sanchez and Zhou, 2011). Its function in interactions with chromatin and/or other proteins is unclear. Ioc4 contains a PWWP (Proline-Tryptophane-Tryptophane-Proline) motif (Vary et al., 2003). PWWP is a member of the royal superfamily that function as lysine methylation reader modules, capable of recognizing both DNA and methylated lysine residues like H3K36me3 or H4K20me3 (Qiu et al., 2002; Maurer-Stroh et al., 2003; Dhayalan et al., 2010; Qin and Min, 2014). PWWP in Ioc4 promotes binding to H3K36me3 and therefore target the Isw1b complex to chromatin (Maltby et al., 2012; Smolle et al., 2012).

1.3.2 Functions of the Isw2 remodeler complex

It has been found that Isw2 plays a role in transcriptional repression *in vivo* (Goldmark et al., 2000), especially repression of antisense transcripts (Whitehouse et al., 2007). Isw2 is responsible for positioning nucleosomes in promoter regions, a function thought to serve as a tool of transcriptional repression (Kent et al., 2001). The Isw2 complex can interact with both naked DNA and nucleosomes arrays (Gelbart et al., 2001). It slides nucleosomes towards the center of DNA, without disrupting the nucleosomes (Kassabov et al., 2002). In comparison to Isw1a, the spacing achieved by Isw2 is less regular (Tsukiyama et al., 1999).

1.3.3 Functions of Isw1 remodeler complexes

Isw1 is capable of sliding nucleosomes (Whitehouse et al., 2003). The ATPase activity of both Isw1 complexes is nucleosome dependent (Tsukiyama et al., 1999; Vary et al., 2003). Both complexes are able to space nucleosomes, although Isw1a has a higher spacing activity than Isw1b. The same holds true in regards to nucleosome sliding. Binding of the complexes to DNA is conferred by the Ioc subunits; Isw1 by itself is incapable of binding DNA or

nucleosomes (Vary et al., 2003). Isw1a prefers binding to nucleosomes containing linker DNA. Isw1b shows no such preference and binds nucleosomes independent of linker DNA (Stockdale et al., 2006). Both Isw1a and Isw1b are capable of sliding nucleosomes, although there are distinct differences between positioning of mono- and dinucleosomes. Isw1a shows a preference for dinucleosomes, whereas Isw1b preferentially binds mononucleosomes (Krajewski, 2014). They also differ in directionality of sliding. Isw1a moves mononucleosomes to more central positions on DNA fragments. Isw1b is capable of positioning mononucleosomes close to the end of DNA (Stockdale et al., 2006).

Isw1a has been proposed as a chromatin ruler, spacing nucleosomes at set distances (Yamada et al., 2011). It has been described initially as a transcriptional repressor, specifically for stress response genes containing a TATA-box (Morillon et al., 2003; Pinskaya et al., 2009). Later data suggests that Ioc3 can be found genome-wide and is enriched at +1 nucleosome positions and at ends of genes (Smolle et al., 2012; Yen et al., 2012). This is achieved by repositioning nucleosomes near promoter sites and therefore preventing access. This may possibly be achieved by potential binding specificity conferred by Ioc3 (Yamada et al., 2011).

Isw1b is responsible for maintaining chromatin structure in the wake of transcription by RNA polymerase II (RNAPII), preventing the initiation of so-called cryptic transcription (Smolle et al., 2012). Isw1b has been found to associate with coding regions of actively transcribed genes (Morillon et al., 2003; Smolle et al., 2012; Maltby et al., 2012).

1.4 Cryptic transcription

1.4.1 Basics of cryptic transcription

Nucleosomes present an obstacle to transcription, by preventing access to underlying DNA. This is at once a problem, barring access to RNAPII, but at the same time also a necessary step to prevent the expression of cryptic promoter sites. These cryptic promoter sites can be found within open reading frames of certain genes (Kaplan et al., 2003), in intergenic regions (Thompson and Parker; 2007) or on antisense strands (Goodman et al., 2013). These cryptic or non-coding transcripts lack coding potential and are rapidly targeted for degradation by the exosome (Goodman et al., 2013). Expression levels of cryptic transcripts are low in wild type cells (Hennig and Fischer; 2014). Several different types of cryptic transcripts have been described.

Wyers et al., (2005) describe cryptic unstable transcripts (CUTs) as transcripts originating from intergenic regions that were previously thought to be silent and that are rapidly degraded by the exosome. Although this was only observed in exosome mutants. Kapranov et al., (2007) propose that stable unannotated transcripts (SUTs) may increase genome complexity and protein diversity. A group of regulatory cryptic transcripts has been described by van Dijk et al., (2011). These transcripts are characterized by degradation by the cytoplasmic 5'-3' Xrn1 exonuclease and have been termed XUTs (Xrn1-sensitive unstable transcripts). XUTs play a repressive role on gene expression and are controlled by Set1-dependent histone methylation.

Another class of regulatory cryptic transcripts are NUTs (Nrd1-unterminated transcripts) that originate from NDRs in the absence of Nrd1 (Schulz et al., 2013). Since these transcripts

deregulate mRNA synthesis, Nrd1 is thought to restrict synthesis of NUTs and prevent genomic deregulation. Cryptic promoter sites have been identified in most eukaryotic organisms, from yeast to humans (Rougemaille and Libri; 2011). In yeast, cryptic promoters can be vastly different; some contain a TATA-Box like *FLO8* (Kaplan et al., 2003), while others, like *STE11*, do not (Pattenden et al., 2010). They are independent from canonical reporters in their regulation, although they do rely on the same transcriptional mechanisms (Pattenden et al., 2010). Transcription of cryptic promotes in wild type yeast is infrequent, due to their general inaccessibility. This requires significant changes in chromatin state to allow cryptic transcription initiation.

1.4.2 Function of cryptic transcription

It is not yet understood what the purpose of these cryptic transcripts is. It has been shown that some cryptic transcripts in fact encode truncated peptides (Brocks et al., 2017) or proteins otherwise absent from the cell (Cheung et al., 2008). However, function of these proteins and peptides is as of yet unclear. Unchecked cryptic transcription leads to genomic instability, which would explain the high rate of conservation of mechanisms that repress cryptic transcription throughout eukaryotes (Nicolas et al., 2007). Several cryptic transcripts have been shown to be involved in transcriptional regulation. For example, *IRT1* is a long non-coding RNA that has been shown to mediate repression of *IME1*, a gene responsible for induction of meiosis (van Werven et al., 2012). Similarly, *IME4* is regulated by *RME2*, a transcript from the antisense strand of *IME4* (Hongay et al., 2006), although the mechanisms of regulation are distinctly different between *IME1* and *IME4*.

It has been shown that stress leads to accumulation of RNAPII near cryptic promoter sites (Kim, Liu et al., 2010), indicating a genome-wide increase of cryptic transcription. In fact, it has been found that stress response genes are enriched for cryptic promoter sites. However, it has also been found that it is not the presence of cryptic transcripts that leads to changes in mRNA (messenger RNA) levels during stress responses (Garcia-Martinez et al., 2012). The field of cryptic transcription has just begun to emerge and there are still large parts that have yet to be understood.

1.4.3 Isw1 and Chd1 maintain chromatin organization and prevent cryptic transcription

Isw1b can be found predominantly on actively transcribed genes, where it serves to maintain histones in the wake of RNAPII (Morillon et al., 2003; Smolle et al., 2012). It is recruited to H3K36me3 through the PWWP domain of its Ioc4 subunit (Maltby et al., 2012). H3K36me3 is mediated by Set2, which is attached to the phosphorylated C-terminal domain (CTD) of RNAPII. Together with Chd1 it facilitates retention of hypoacetylated histones, maintaining chromatin integrity following active transcription (Smolle et al., 2012; Radman-Livaja et al., 2012 and Figure 1-4).

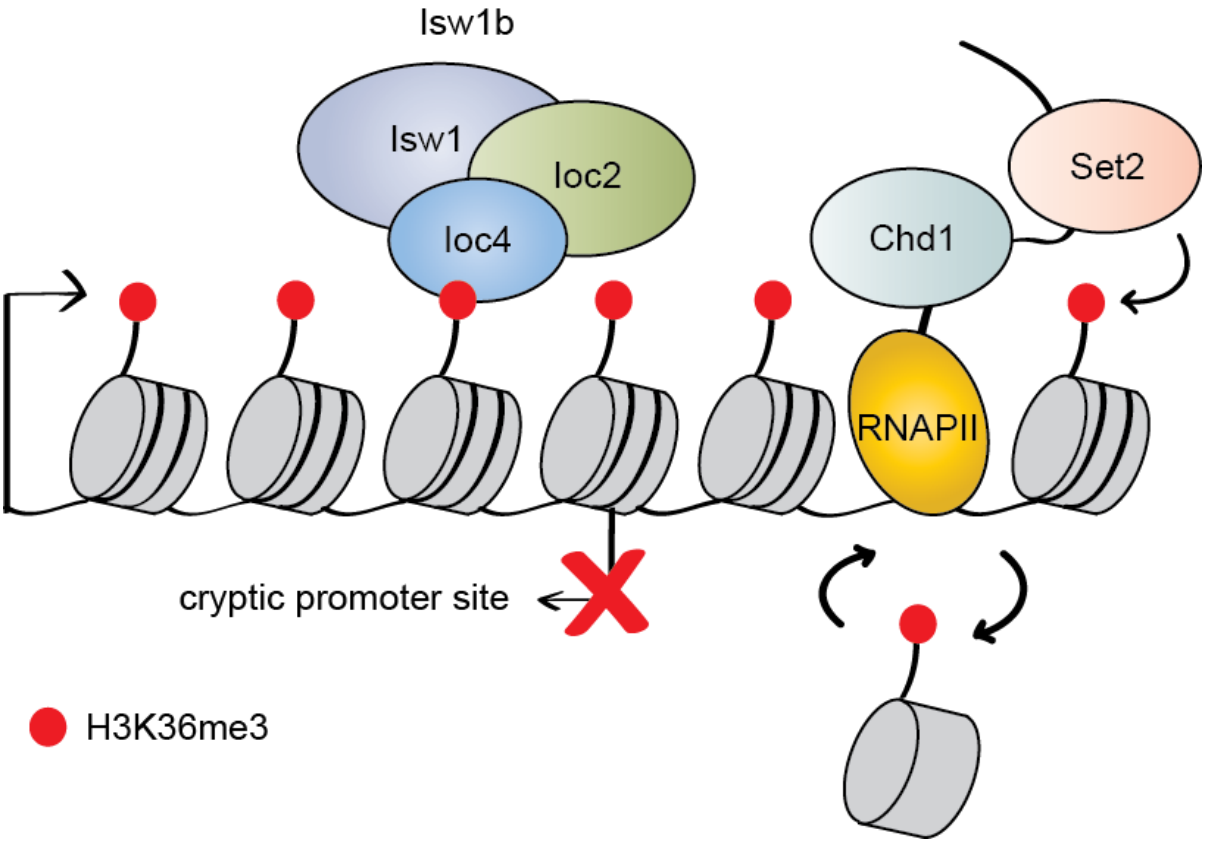

Figure 1-4: Prevention of cryptic transcription by means of histone retention in the wake of RNAPII: Set2 is recruited to the phosphorylated CTD of RNAPII and is responsible for trimethylation of histone H3 lysine 36, which in turn recruits Isw1b. During transcription via RNAPII K36 trimethylated and hypoacetylated histones are retained through the combined effort of Isw1b and Chd1. H3K36me3 is also required for the activity of Rpd3S which deacetylates histones. Chd1 is also associated with RNAPII. The absence of acetylation marks on histones leads to condensation of chromatin, blocking access to so-called cryptic promoter sites within the coding region. These promoter sites cannot be expressed.

In the absence of both of these proteins, cryptic transcription is increased throughout the genome (Smolle et al., 2012). Additionally, H3K36me3 is required for the catalytic activity of Rpd3S histone deacetylase complex (HDAC), which in turn maintains the deacetylated state of histones in the coding region (Joshi and Struhl, 2005; Keogh et al., 2005; Drouin et al., 2010).

1.5 Linking polyamines to ISWI remodelers

1.5.1 Paa1 has been linked to ISWI remodelers by mass spectrometry

A potential link between yeast ISWI remodelers and polyamine metabolism was identified by previous experiments in the lab. Mass spectrometry analysis identified the polyamine acetyltransferase Paa1 as a potential, sub-stoichiometric, yet specific interaction partner of the Isw1b remodeler (Table 1-1).

Table 1-1: MudPIT mass spectrometry analysis of proteins co-purified with Flag-tagged Ioc4: Listed are the spectra and peptide counts for proteins pulled down with Ioc4. Isw1 and Ioc2 are expected as they form the complex Isw1b with Ioc4. Counts and Spectra for Paa1, which is a metabolic enzyme with unrelated function to Isw1b, are highlighted in bold. Paa1 could be shown to pull down with Iotc4 throughout all three replicates. Controls of untagged protein are also shown and were consistently negative for all three replicates (Smolle, unpublished).

	Ioc4-Flag Purification		**Control**	
	Ioc4-Flag	**Ioc4-Flag**	**Control**	**Control**
Protein	**Peptides**	**Spectra**	**Peptides**	**Spectra**
ISW1	139	4475	x	x
IOC2	51	2647	x	x
IOC4	*33*	*2110*	x	x
PAA1	**5**	**20**	x	x

Paa1 is the only polyamine acetyltransferase in yeast, capable of acetylating polyamines. It has first been identified as a functional homolog to the mammalian spermidine/spermine N^1-acetyltransferase (SSAT), by examining yet uncharacterized members of the GNAT (GCN5-related N-acetyltransferase) superfamily in yeast (Liu et al., 2005). This family contains enzymes that acetylate histones, proteins and even sugars. Polyamine acetyltranferases can be found in mammals (Casero and Pegg, 1993) and *Escherichia coli* (*E. coli*), (Fukuchi et al., 1994), indicating a highly conserved status. Paa1 is unable to acetylate histones or small basic proteins, however it is capable of acetylating aryalkylamines like serotonin (Ganguly et al., 2001; Liu et al., 2005). In yeast, the only known substrates for Paa1 are polyamines. Paa1 might play a role in transcription, as *PAA1* has been shown to have genetic interactions with *GCN5* and *SPT8*. Both of these genes encode proteins that are part of histone acetyltransferase complexes that play important roles in transcription activation (Liu et al., 2005).

1.5.2 Characterization of polyamines

Polyamines are small, positively charged molecules that are able to bind DNA, RNA and proteins (Leroy et al., 1997; Bryson and Greenall; 2000; Usherwood; 2000). Acetylation by Paa1 leads to the breakdown and excretion of polyamines (Casero and Pegg; 1993), Figure 1-5B), giving Paa1 a direct role in regulating the levels of polyamines. The most ubiquitous polyamines are spermine, spermidine and putrescine. Prokaryotes contain mostly spermidine and putrescine, while eukaryotes contain significant levels of all three of them (Pollard et al., 1999). In yeast spermine is most abundant (Igarashi and Kashiwagi; 2010). In bacteria polyamines can be commonly found in a polyamine-RNA complex, protecting RNA from degradation (Igarashi and Kashiwagi; 2010). They can further stabilize the structure of higher order condensed chromatin super structures (Belmont et al., 1989; Pollard et al., 1999).

In yeast, spermine was found to bind tRNA, helping establishing adequate folding of tRNA molecules (Kim et al., 1971). Polyamines can fulfill many different roles, ranging from cell proliferation to regulation of gene expression or ion channels (Tabor et al., 1982; Heby and

Emanuelsson, 1981; Celano et al., 1989; Scott et al., 1993). They can influence the composition of chromatin, lead to DNA aggregation and stabilize tRNA (Sato et al., 2003; Plum et al., 1990), (Bolton and Kearns, 1977). Spermine in ageing yeast can inhibit histone acetyltransferase leading to a deacetylation of histone H3, which prevents oxidative stress and necrosis (Eisenberg et al., 2009). This indicates polyamines having a role in longevity, further supported by their ability to induce cellular stress response programs. For example, they protect yeast cells from reactive oxygen species. Yeast cells depleted of polyamines lose their respiratory competence (Balasundaram et al., 1993; Chattopadhyay et al., 2006) and are less resistant to heat shock (Balasundaram et al., 1996).

Polyamines were also found to inhibit cytosine-DNA methyltransferase *in vitro* (Ruiz-Herrera et al., 1995). This is a specific inhibition, as adenine DNA methylases were not affected. In *S. cerevisiae*, spermidine has a major influence on transcriptional expression, in particular by increasing the expression of transcription factors, for example *MET28* and *MET32*, both of which regulate metabolic pathways. This further leads to changes in expression of many metabolic pathway genes, regulated by these transcription factors (Chattopadhyay et al., 2009).

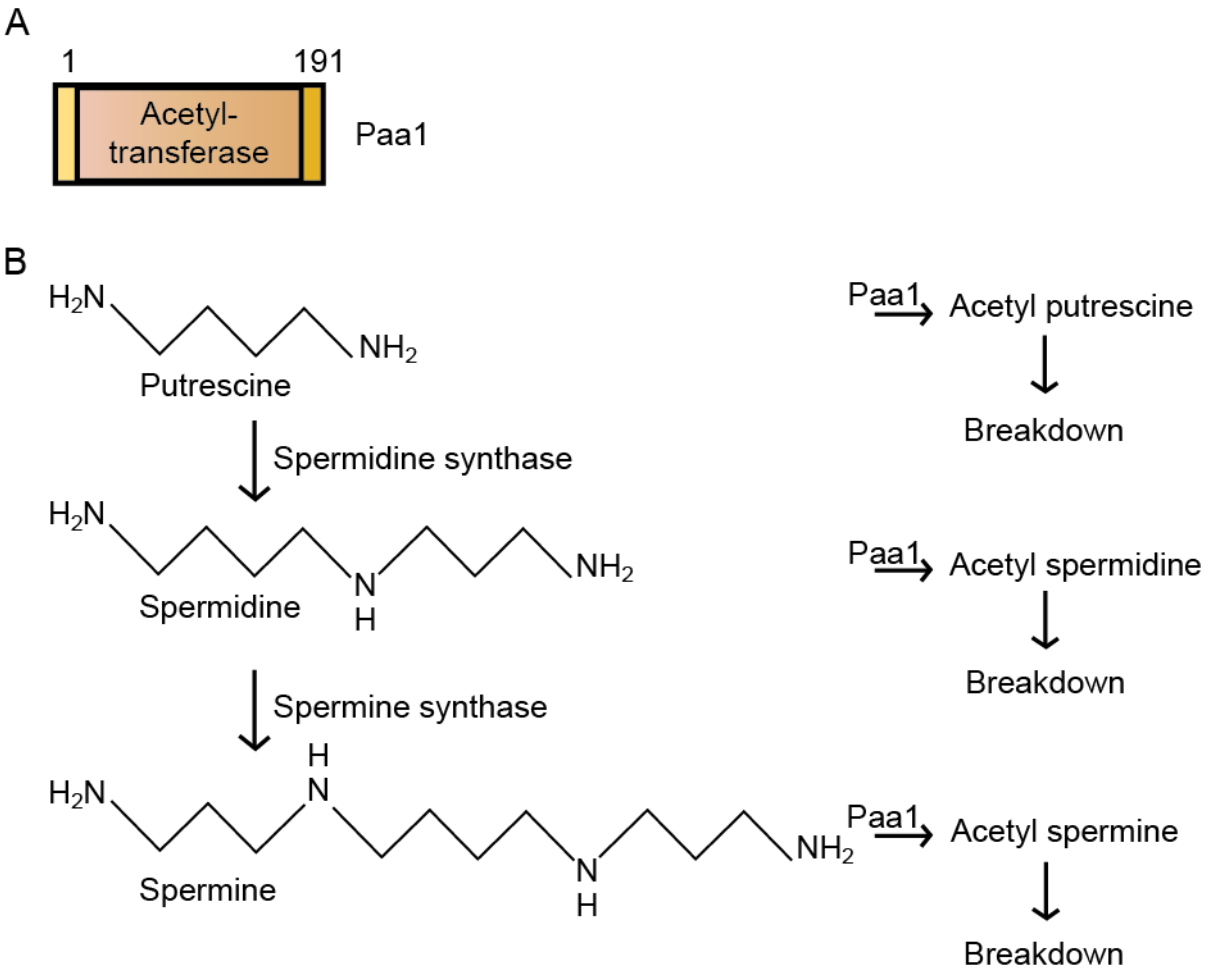

Figure 1-5: Domain organization of polyamine acetyltransferase Paa1 and Polyamine synthesis pathway: (A) Paa1 is a small protein, only containing a domain for its catalytic activity of transferring acetyl-groups. **(B)** Synthesis pathway from putrescine to spermine. All three polyamines can be acetylated by Paa1, which leads to their breakdown and excretion from cells.

Paa1 is thought to regulate polyamine levels on DNA, as the acetylation removes their positive charge that attracts them to DNA. This in turn impacts chromatin condensation, leading to a more open and accessible chromatin state (Raspaud et al., 1999; Liu et al., 2005). However, effects of polyamines on chromatin are ultimately more complex. It has been shown that histone acetylation of nucleosomes is stimulated by low concentrations of polyamines and inhibited at higher concentrations (Dod et al., 1982). A possible explanation for this is that at low concentrations, polyamines outcompete histone tails for the binding to DNA, therefore freeing histone tails for acetylation (Liu et al., 2005). Under these conditions, polyamine binding to DNA would actually lead to a loosening of chromatin state, through the increase of histone acetylation. Furthermore, addition of spermine or spermidine has been shown to increase nucleosome spacing during nucleosome assembly (Blank and Becker; 1995). This makes it difficult to predict the precise effect changes of polyamine levels will have *in vivo*. Polyamines are very versatile and fulfill a multitude of roles. Paa1, having a direct influence on polyamine concentrations, has therefore indirect influence on these processes.

1.6 Project aims

The activities of chromatin remodelers are localized and influenced by their recruitment, ATP levels and availability of (preferred) substrates. For example, SWI/SNF binding is enhanced by acetylation of histone H3 lysine 14 (Hassan et al., 2001; Ferreira et al., 2007).

The Smolle Lab is interested in identifying new regulatory mechanisms that influence ISWI remodeling activities in yeast. Given the preliminary mass spectrometry data we hypothesized that Paa1 may interact and/or modulate the activity of Isw1 chromatin remodelers. The aim of this project was to investigate any potential physical and/or genetic interactions between Isw1 and Paa1. Initially, we sought to confirm the physical interaction identified by mass spectrometry using different biochemical methods, including immunoprecipitations (Chapter 2.1.1) and a biotinylation-based approach (Chapter 2.1.2).

In parallel we also investigated any genetic interactions between *ISW1* and *PAA1*, especially with regards to cryptic transcription. Genetic interaction studies can provide insights into the functional relationship between two genes or their products (Mani et al., 2008). Since an *Δisw1* mutant displays moderate levels of cryptic transcription, we looked at the effects of a *PAA1* deletion on the production of non-coding RNAs alone as well as in combination with a variety of different remodeler mutants (Chapter 2.2.2 and 2.2.4). This analysis was extended onto a genome-wide level using RNA-seq (Chapter 2.3). Finally, we were wondering if transcriptional changes correlated with differences in chromatin structure. Therefore, we performed MNase-seq in order to gain an overview over nucleosome positioning and chromatin organization in these mutant yeast strains (Chapter 2.4).

2 Results

2.1 Investigation of physical interaction between Paa1 and Isw1 remodelers

2.1.1 Co-Immunoprecipitation of Isw1 remodeler subunits and Paa1 shows no interaction

Previously, mass spectrometry analysis had revealed a potential interaction between the Ioc4 subunit of the Isw1b complex and Paa1. The interaction itself was sub-stoichiometric, but could be reliably reproduced in triplicates (Table 1-1). We therefore decided to perform co-immunoprecipitation assays (co-IPs) to further investigate this potential interaction. Ioc4 is part of the Isw1b complex, which shares its catalytic subunits with Isw1a. We therefore decided to investigate all four subunits for their potential interaction with Paa1.

We expressed 3x-Flag tagged Isw1, Ioc2, Ioc3 and Ioc4 with C-terminal Tandem Affinity Purification (TAP) tagged Paa1 in each of these strains. A TAP-tag consists of a calmodulin binding peptide (CBP) and protein A (Rigaut et al., 1999). These two domains are separated by a TEV (Tobacco Etch Virus)-protease cleavage site. CBP binds calmodulin and protein A has a high affinity for IgG, which allows for easy antibody detection. This setup allows for tandem affinity purification, a two-step process that increases purity of the purified protein (Rigaut et al., 1999). For our approach, however, we only performed one pull down step via protein A binding to IgG-sepharose. The 3xFlag-tag consists of three repeats of the Flag sequence DYKDDDDK and can be detected with antibodies specific to this sequence.

We analyzed INput samples (IN), UNbound (UN) and beads carrying Bound protein (B). We then used an anti-Flag antibody to determine the presence of potential 3xFlag-tagged remodeler subunits. We used a TAP-antibody to verify that the pull down was successful, detecting the expected Paa1-TAP, which should be present in only the input and bead fractions, in the case of a complete pull down. Furthermore, we used strains, where only the respective remodeler subunit was tagged, as controls to exclude unspecific binding of Flag-tagged protein and to IgG-sepharose beads.

Here we could show that a very faint band appears in the bound fraction of a pull down of Paa1-TAP with Isw1-3xFlag (Figure 2-1A, band marked with *). Most of the remodeler protein can still be found in the unbound fraction, however. This indicates that a small amount of Isw1 could be pulled down alongside Paa1. However, there is also a small band present in the bound fraction in the Isw1-3xFlag control (Figure 2-1A, top left blot), indicating that there might be unspecific interactions between 3xFlag or Isw1 and IgG-sepharose beads. The pull down itself worked, as can be seen in Figure 2-1A, bottom right blot. Paa1-TAP can only be found in the bound, but not unbound fraction. However, the amount of Isw1-3xFlag that can be observed in the bound fraction is only a small fraction of total protein, the majority of which can be found in the unbound fraction (Figure 2-1A, top left blot). This is not surprising, given the sub-stoichiometric amounts of protein found to have interacted in the MS experiment. Due to the unspecific band present in the negative control, no solid conclusion can be drawn at this point for interaction between Isw1 and Paa1.

We also examined potential interaction between the Ioc subunits and Paa1. Here we can clearly show that there is no interaction between any of the Ioc subunits and Paa1, as none showed a band in the bound fraction (Figure 2-1B-D, top right blots). The pull down worked for all three strains, as can be seen in the bottom right blots of Figure 2-1B-D, with all of the remodeler subunits depleted from the extract, during the pull-down.

Co-IPs proved unsuitable to detect interactions between Paa1 and Isw1 remodeler subunits, as the interaction is likely too transient. This is supported by the initial detection of sub-stoichiometric amounts of protein in the original MS experiments. Therefore, we required a different method to detect more transient interactions.

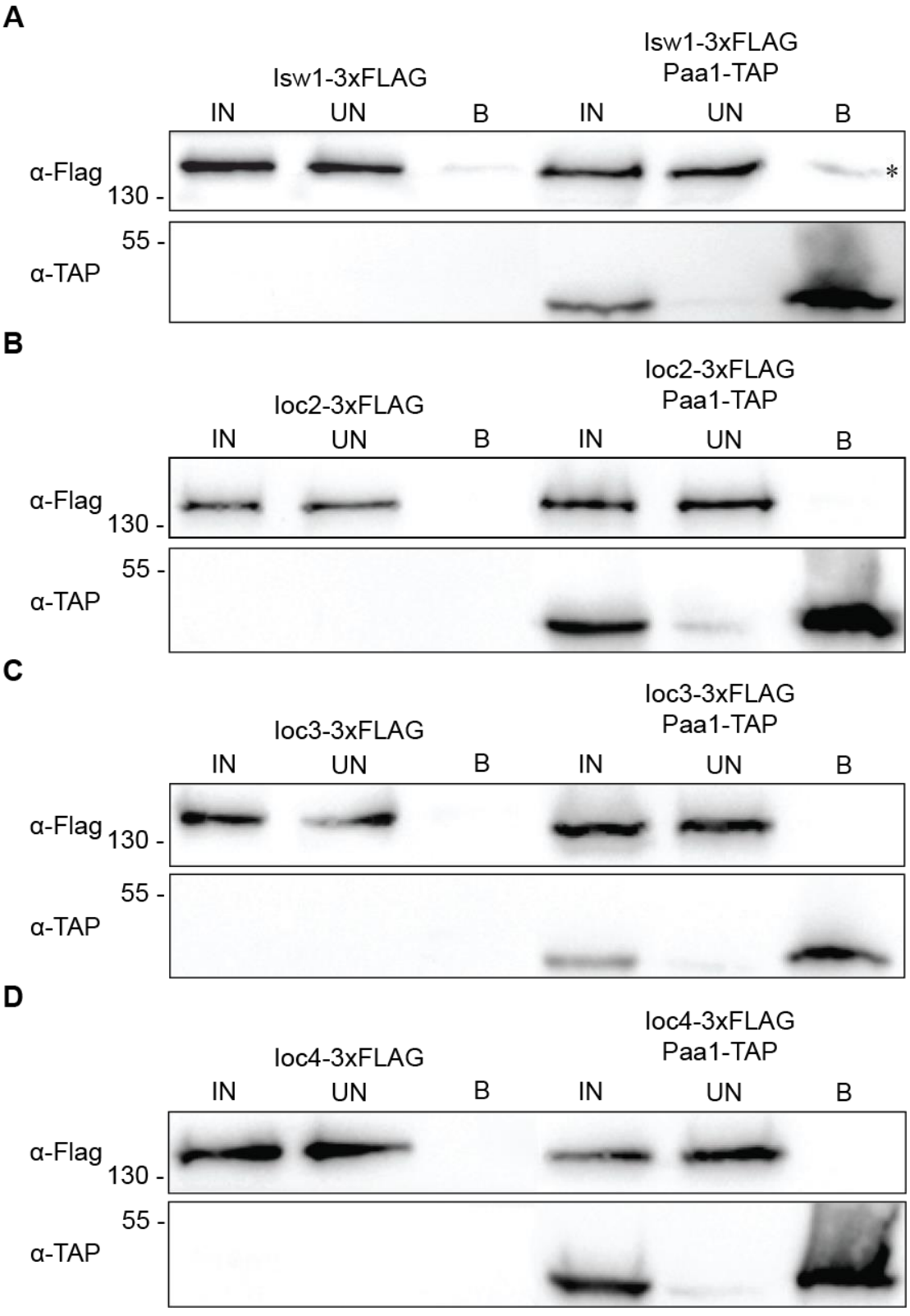

Figure 2-1: Western blots for Co-IPs on TAP-tagged Paa1. TAP-tagged Paa1 was pulled down with IgG-Sepharose beads and potential interactors analyzed by western blotting. Isw1 remodeler subunits were tagged with 3xFlag and detected with a Flag-antibody. Detection with a TAP-antibody served as control for successful pull downs. A sample only containing Flag-tagged protein was used as a negative control. Input (IN), unbound fractions (UN) and bound fractions (B) were compared. **(A)** Pull down of Paa1-TAP and Isw1-3xFlag. A band indicating successful pull down of Isw1-3xFlag is marked with an asterisk. **(B-D)** Pull downs of Paa1-TAP and Ioc2-3xFlag, Ioc3-3xFlag and Ioc4-3xFlag respectively. Representative blots of triplicate experiments are shown.

2.1.2 Bio-ID super shift assay for ISWI remodeler subunits and Paa1 show no interaction

Given the sub-stoichiometric and potentially transient interaction between IgG-sepharose and Isw1-3xFlag, we decided to use a different approach, by using a super shift assay based on Bio-ID. Bio-ID assays exploit the high affinity of the non-covalent bond between biotin and streptavidin, and also one of the strongest non-covalent interactions known (Chaiet and Wolf, 1964; Langer et al., 1981). We employed a super shift assay based on the Bio-ID assay, as described by (Fernandez-Suarez et al., 2008).

We tagged *ISW1*, *IOC3* and *IOC4* each with an *E. coli* biotin ligase, BirA and an HA-tag. We also tagged *PAA1* with an acceptor peptide (AP, GLNDIFEAQKIEWHW) for biotinylation and a TAP-tag, for detection. As negative control, we used a cytosolic protein, Arl1 with a similar expression level as Paa1 (SPELL Version 2.0.3, Hibbs, 2007). As a positive control, we used interaction between Ioc4 and Isw1.

Yeast contains a biotin-apoprotein ligase encoded by *BPL1*, that has been shown to share functional similarities with *E. coli* BirA (Cronan and Wallace, 1995). This means it could potentially biotinylate the acceptor peptide, independent of protein interactions. Therefore, we cultured cells in media without biotin, and then exposed the cells to biotin for a limited amount of time. This ensured that only BirA caused biotinylation on AP. Samples were then incubated with streptavidin, which binds the biotinylated AP-tags and leads to a significant shift in the running size of the protein it is attached to. This allows easy detection of biotinylated AP by detecting the size shift the tagged proteins undergo, upon binding of streptavidin to biotin. The approximate size of streptavidin is 50 kDa. The size shift was compared to samples without streptavidin. The TAP-tag on the prey proteins allows for easy detection by a Peroxidase Anti-Peroxidase (PAP) antibody against protein A. Samples were separated by SDS-PAGE and analyzed by western blotting. The non-covalent bond between streptavidin and biotin is strong enough to withstand treatment with SDS.

The positive control shows that the essay works, as all of Ioc4-AP-TAP has been shifted in the presence of streptavidin (Figure 2-2). Additionally, the negative control also shows that there are no unspecific interactions between Isw1-BirA-HA and Arl1-AP-TAP, as there is no super shift in the presence of streptavidin (Figure 2-2).

No shift of Paa1-AP-TAP could be observed for Ioc3-BirA-HA and Ioc4-BirA-HA respectively in the presence of streptavidin (Figure 2-2), which corroborates our observation from the pull downs that there is most likely no interaction between the pairs.

There is also no shift for Paa1-AP-TAP in the presence of streptavidin, indicating that there is no interaction between Paa1 and Isw1 (Figure 2-2).

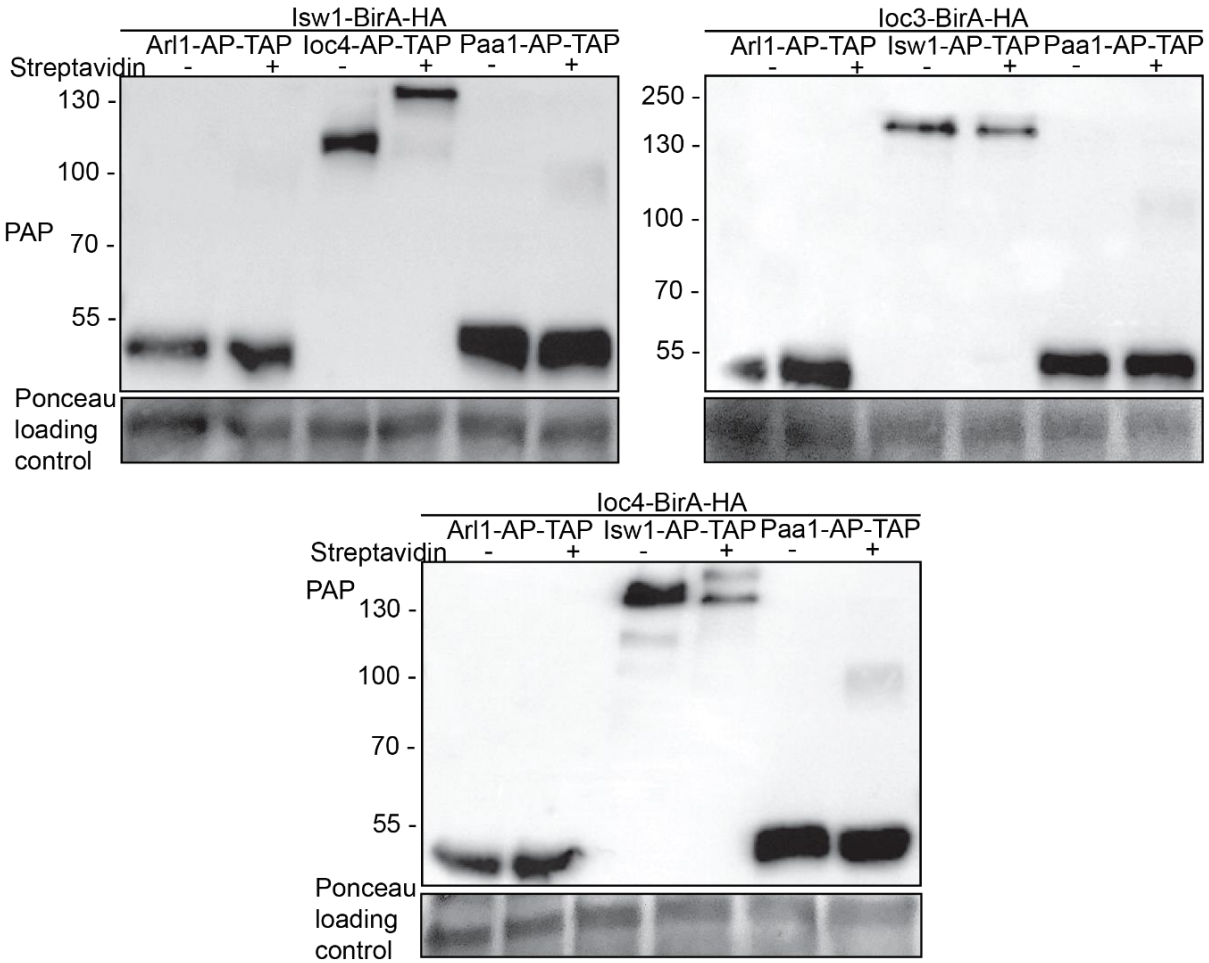

Figure 2-2: Bio-ID based super shift assay of Paa1 and Isw1, Ioc3 and Ioc4. Isw1, Ioc3 and Ioc4 have been tagged with a BirA biotin ligase that specifically biotinylates an acceptor peptide. This peptide has been used to tag *PAA1* and several control proteins to determine if Isw1, Ioc3 and Ioc4 interact with Paa1. Samples were incubated with streptavidin and then analyzed by western blot. Proteins with biotinylated AP were able to bind streptavidin and were therefore shifted significantly in size compared to control samples. Controls used were Arl1, a cytosolic protein, Ioc4 as a positive control for interaction with Isw1. 20% of total extract was loaded. Representative blot of triplicate experiments shown.

2.2 Identification of genetic interactions

2.2.1 Growth assays for phenotyping show genetic interactions between *ISW1* and *PAA1*

Phenotyping is a convenient method to achieve basic understanding of the possible functions of a gene. Deletion of a gene causes a phenotype that often serves to give a first indication as to the function of the gene. Similarly, if two genes are deleted, genetic interactions can be inferred from the resulting phenotype. There are two types of genetic interactions, synthetic and epistatic.

In the case of synthetic interactions, the products of two genes function in different pathways. The deletion of both of these genes and therefore interruption of both pathways leads to a more severe effect than if only one gene were deleted. This can lead to synthetic effects that can range from slow growth phenotypes to synthetic lethality. On the other hand, epistatic interactions occur between two genes whose products function in the same pathway. Deleting both of them will have the same effect as deleting only one, as the pathway is already interrupted. This helps to give an indication of the functional relationship between genes and their gene products.

In an effort to gain an overview over the functional relationship between *ISW1* and *PAA1* we compared growth of a double deletion *Δisw1 Δpaa1* mutant with single deletion mutants and BY4741 wild type under different growth conditions. All conditions were compared to growth in rich media at standard conditions, as seen in Figure 2-3.

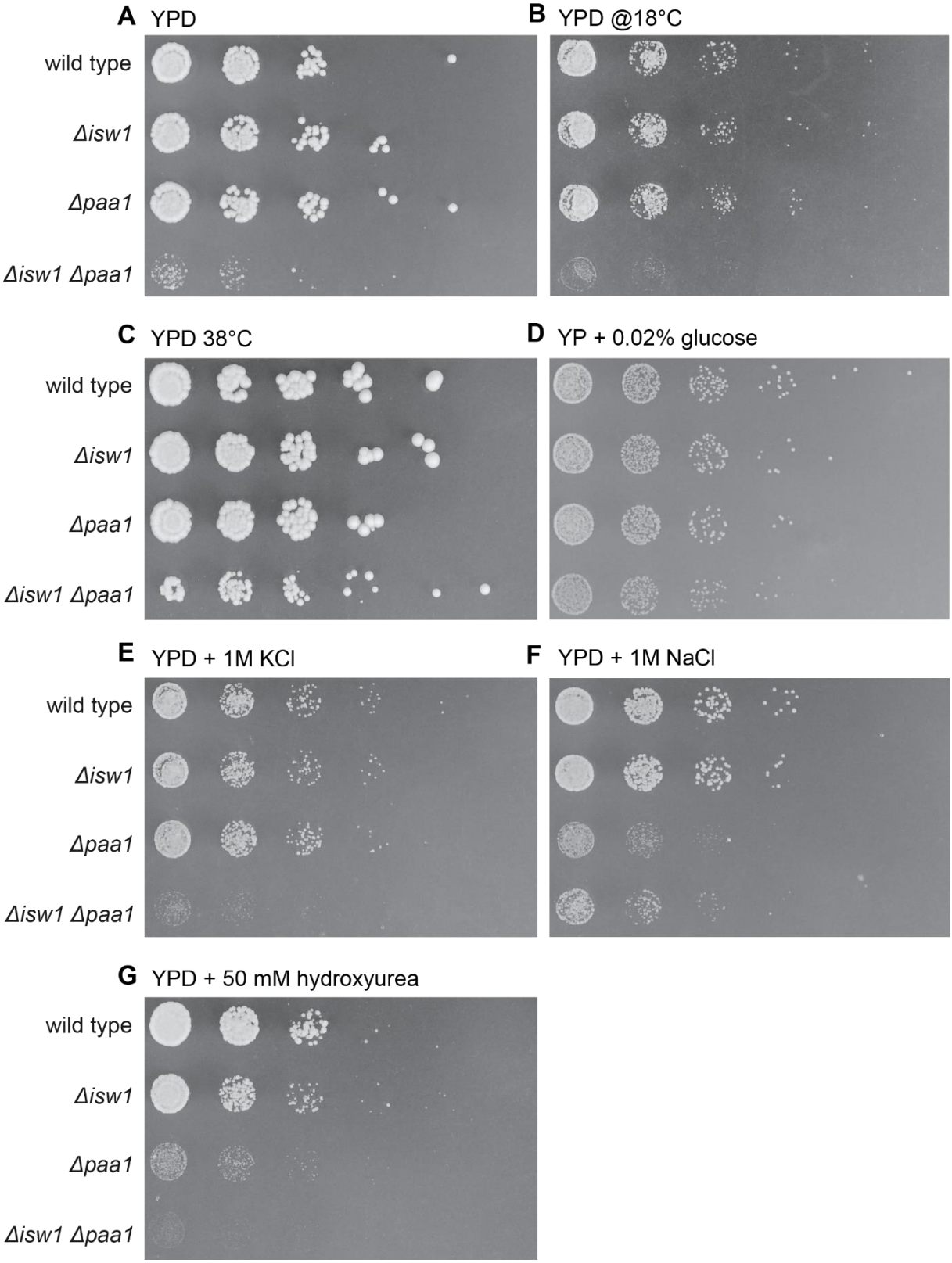

Figure 2-3: Spot dilution assays for Δisw1 Δpaa1 under different growth conditions. Strains were grown in YPD and after harvesting diluted six times with a 5-fold dilution. All six dilutions were spotted onto agar plates and then incubated at 30°C, unless stated otherwise. Growth on YPD at 30°C was chosen as a positive control. Tested conditions included growth on YPD at 18°C or 38°C, growth on YP media with 0.2% glucose growth on YPD supplemented with 1 M KCl, 1 M NaCl or 50 mM hydroxyurea. After 72 hours of growth pictures were taken of the plates. Representative pictures of duplicate experiments are shown.

Growth was scored depending on how well a strain was growing, with (-) scoring for no growth at all and (+++) for growth comparable to wild type growth on rich media (Table 2-1).

Table 2-1: Scored growth of strains for a spot series dilution assay. Growth was scored for wild type, *Δisw1*, *Δpaa1* and *Δisw1 Δpaa1* from no growth (-) to growth better than wild type under control conditions (++++).

Condition	**wild type**	***Δisw1***	***Δpaa1***	***Δisw1 Δpaa1***
YPD	+++	+++	+++	+
Cold shock (18°C)	+++	+++	+++	-
Heat shock (38°C)	++++	++++	++++	++
Starvation (0.02% Glc)	++	++	++	++
YPD, 1M KCl	+++	+++	+++	-
YPD, 1M NaCl	+++	+++	+	+
YPD, 50mM HU	+++	+++	+	-

This revealed a synthetic genetic interaction between *ISW1* and *PAA1*, as *Δisw1 Δpaa1* shows a severe effect on growth, even on rich media (Figure 2-3, YPD). *Δisw1 Δpaa1* grows much worse than the wild type, whereas both single mutants show comparable growth to wild type growth. This effect appears consistently in the controls, but also the heat and cold shock conditions. There was also a general increase of growth for all strains under heat shock conditions (Figure 2-3C, Table 2-1). As it affects all strains, this seems to be more a result of the increased temperature as a strain specific effect. No additional effect on growth could be observed for cold shock (Figure 2-3, YPD @18°C). This clearly shows that *Δisw1 Δpaa1* has a synthetic growth defect.

Growth on Hydroxyurea (HU) is impaired for *Δisw1* and *Δpaa1*, compared to wild type growth, although not to the level of *Δisw1 Δpaa1* (Table 2-1, Figure 2-3, YPD + 50 mM HU) HU prevents the accumulation of dNTPs that are required for cells to enter S-phase, thus arresting cells at the G1/S-phase checkpoint (Koc et al., 2004). *Δpaa1* has been previously reported as being phenotypic for hydroxyurea (Liu et al., 2005), but it is interesting to see that this phenotype is exacerbated by additional deletion of *ISW1*. This is most likely a result of the synthetic genetic interaction between the two, as *Δisw1* by itself is also growing worse than wild type (Table 2-1, Figure 2-3, YPD + 50 mM HU). ISW1 plays a role in replication by helping to reestablish nucleosome arrays behind replication forks (Yadav and Whitehouse, 2016), which can explain why its absence causes a growth phenotype. The absence of Paa1 leads to an increase of polyamine levels (Casero and Pegg, 1993), which could be the reason for the rescue of the *Δisw1* phenotype. Polyamines stabilize DNA and increased stability could help maintain chromatin integrity in the absence of Isw1.

Growth of *Δisw1 Δpaa1* at a lack of glucose is almost at the level of wild type (Figure 2-3, YP + 0.02% glucose). This could be a result of the lower expression of ribosomal proteins in *Δisw1 Δpaa1* we observed in later experiments (Figure 2-15B).

For salinity, there was a decrease of growth for *Δpaa1* and an increase of growth for *Δisw1 Δpaa1* compared to wild type growth on the control plate (Figure 2-3, YPD + 1M NaCl, Table 2-1). Vacuole fragmentation can be observed for *Δisw1* and *Δpaa1* (Michaillat and Mayer, 2013), so it is likely that the growth defect is a result of that, rather than synthetic interactions.

This is further corroborated by growth at osmotic stress, as *Δpaa1* shows a different growth phenotype on KCl plates (Figure 2-3, YPD + 1M KCl). For osmotic stress we can also see a reduced growth phenotype for *Δisw1 Δpaa1* (Figure 2-3, YPD + 1M KCl).

2.2.2 Growth assay for a cryptic transcription reporter strain revealed a cryptic transcription phenotype for *Δisw1 Δpaa1*

In a further attempt to elucidate the functional relationship between *ISW1* and *PAA1*, we performed growth assays with a reporter strain for the detection of cryptic transcription. In this strain the 3' end following the cryptic promoter site of *FLO8* has been replaced by *HIS3*. This *HIS3* gene is out of frame with the canonical transcription start site of *FLO8*. *HIS3* can therefore only be expressed if cryptic transcription occurs (Cheung et al., 2008) and Figure 2-4). This allows for easy detection of cryptic transcription on media lacking histidine.

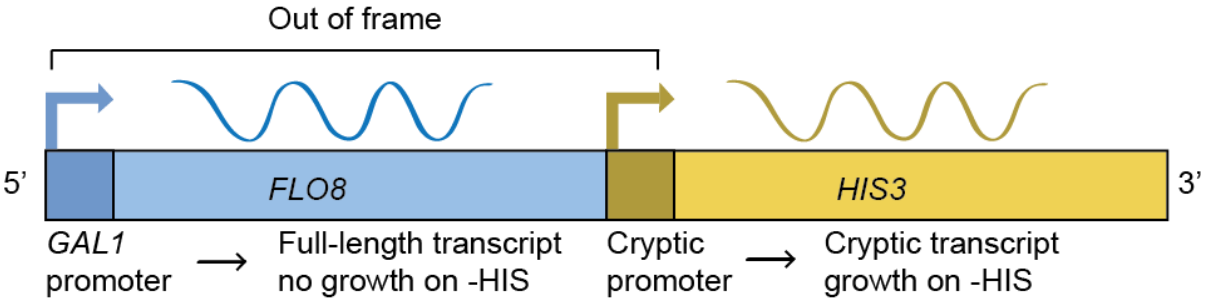

Figure 2-4: FLO8 reporter strain construct for detection of cryptic transcription. *HIS3* has been inserted behind the cryptic promoter site in *FLO8*. The endogenous promoter of *FLO8* has been replace with the *GAL1* promoter. The two promoters are out of frame, which allows for selective growth on -HIS media, depending of cryptic transcription. *HIS3* is only expressed if the cryptic promoter is active. The *GAL1* promoter is repressed in the presence of glucose and active in the presence of galactose.

The strain background is unable to synthesize histidine by itself, due to a 1 kb base pair deletion, removing upstream elements essential for *HIS3* expression (Hope and Struhl, 1985). This means that the strain can only grow on media lacking histidine, if the cryptic promoter site in *FLO8* is active and the downstream-integrated *HIS3* gene is expressed. This makes for easy screening of cryptic transcription in mutant strains.

Additionally, the *FLO8* promoter was replaced with the *GAL1* promoter, which is repressed in the presence of glucose and active in the presence of galactose. Therefore, in the presence of glucose the entirety of the *FLO8::HIS3* gene construct is not actively transcribed. This means any remodeling action needed to free the cryptic promoter site, has to be effective even in closed chromatin state. In the presence of galactose, the *GAL1* promoter is active and *FLO8* is transcribed. Active genes possess a more fluid chromatin state, in order to make room for RNAPII. This makes it easier to access cryptic promoter sites and less stringent remodeler activity is required. This allows for a measured assessment of cryptic transcription and the effect that tested genes have on cryptic promoter activity.

We created a *Δisw1 Δpaa1* double mutant, and *Δisw1* and *Δpaa1* single mutants in the *FLO8* reporter strain background to assess cryptic transcription. We did a series dilution spot assay with 5-fold dilutions on media lacking histidine and complete media as control (Figure 2-5).

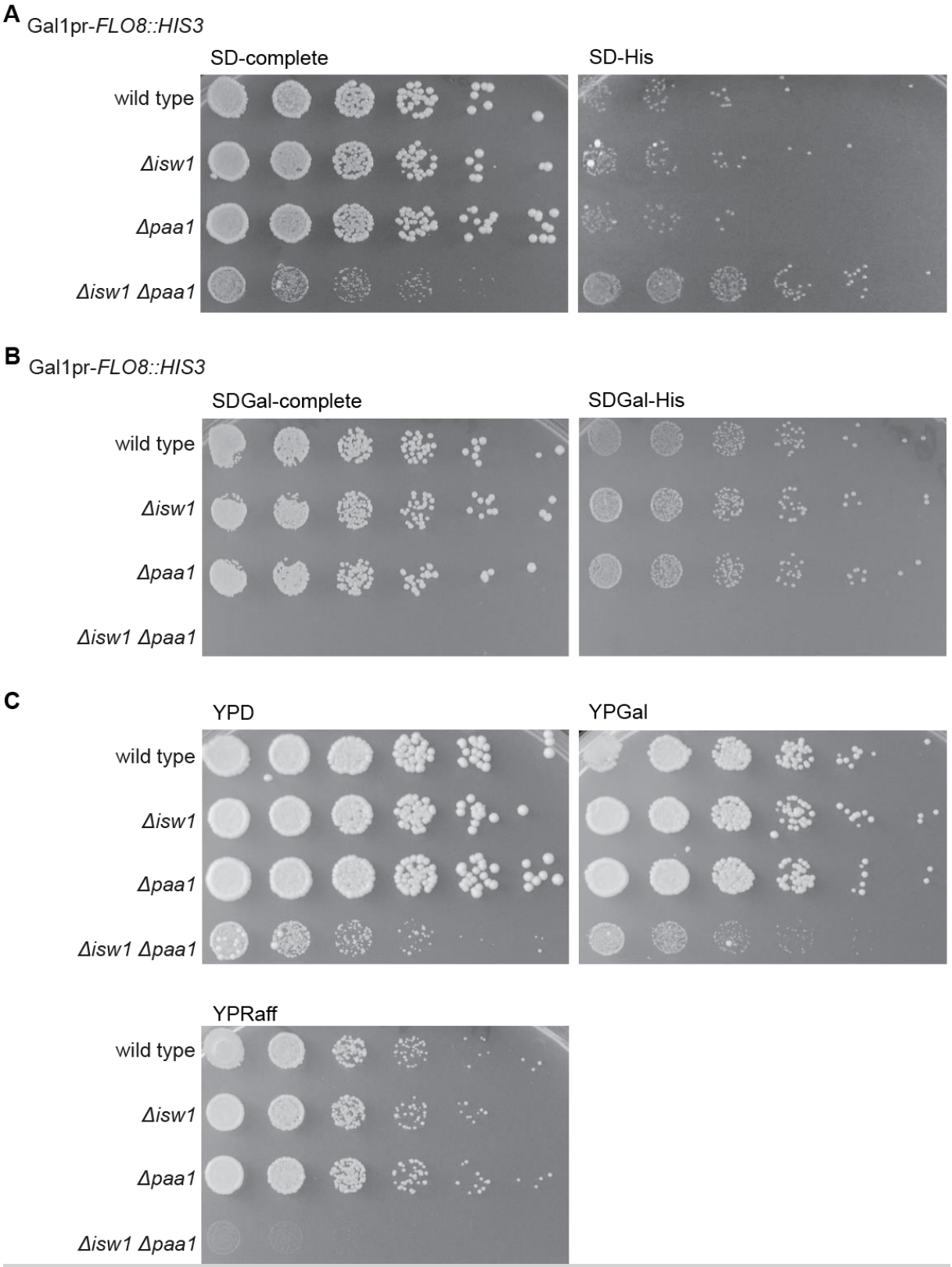

Figure 2-5: Spot dilution spotting assays for Gal1pr-*FLO8*::*HIS3* reporter strain on glucose and galactose media. 5-fold serial dilutions of Gal1pr-*FLO8*::*HIS3* wild type, *Δisw1 Δpaa1*, *Δisw1* and *Δpaa1* were spotted on different media and scored for growth. Small amounts of histidine (0.02%) were supplemented on SD-media lacking histidine to improve readout. **(A)** Strains grown on glucose media with histidine (SD) and without histidine (SD-His). **(B)** Strains grown on galactose media with histidine (SDGal) and without histidine (SDGal-His). **(C)** Strains were grown on YP rich media with different carbon sources, glucose (YPD), galactose (YPGal) or raffinose (YPRaff). A representative picture of triplicate experiments is shown.

We repeated this for both glucose and galactose as a carbon source. Small amounts of histidine were supplemented to -His plates (0.02% histidine), to achieve baseline growth for all strains, in order to improve readout.

Growth was scored from no growth (-) to growth comparable to wild type on SD-complete (Synthetic Defined) media (+++) (Table 2-2).

Table 2-2: Scored growth for Gal1pr-FLO8::HIS3 reporter strain on different media. Growth was scored for Gal1pr-*FLO8*::*HIS3* wild type, *Δisw1*, *Δpaa1* and *Δisw1 Δpaa1* from no growth (-) to growth like wild type under control conditions (+++).

Gal1pr-*FLO8::HIS3*				
Condition	**wild type**	***Δisw1***	***Δpaa1***	***Δisw1 Δpaa1***
SD-complete	+++	+++	+++	++
SD-HIS	+	+	+	++
SDGal-complete	+++	+++	+++	-
SDGal-HIS	+	+	+	-
YPD	+++	+++	+++	+
YPGal	+++	+++	+++	+
YPRaff	+++	+++	+++	-

Growth of *Δisw1 Δpaa1* was impaired on SD-complete media, as well as in liquid overnight cultures. Conversely, growth of *Δisw1 Δpaa1* was improved on SD-His media, compared to empty reporter strain and single mutants, all of which could only grow as the minimal histidine source allowed (Figure 2-5A, Table 2-2). The double mutant on the other hand was able to grow, indicating that cryptic transcription is taking place and *HIS3* is expressed. The double mutant does not grow on SD-media containing galactose as a carbon source (Figure 2-5B, Table 2-2), regardless of histidine content. This is unfortunate, as it means we cannot capitalize on the unique properties of the *GAL1* promoter in determining robustness of a phenotype. We then decided to examine if the growth of *Δisw1 Δpaa1* is affected only on SD plates, or if this also occurs on rich media and other carbon sources.

When grown on YPGal-media, *Δisw1 Δpaa1* shows growth, but it was severely impaired compared to wild type growth (Figure 2-5C). Additionally, *Δisw1 Δpaa1* does not grow on YP with Raffinose at all (Figure 2-5C). The growth of *Δisw1 Δpaa1* is also impaired on SD-complete media, although to a lesser extent than on SGal-complete media. This defect was specific to *Δisw1 Δpaa1*. Wild type, *Δisw1* and *Δpaa1* cells were all able to grow on any carbon source, rich media or synthetic defined media (Figure 2-5).

Unfortunately, the growth phenotype of *Δisw1 Δpaa1* means that we are unable to compare cryptic transcription between active and inactive transcription on *FLO8*, as *Δisw1 Δpaa1* does not grow on galactose. However, as glucose presence requires a stronger phenotype to activate cryptic transcription of *FLO8*, it suggests cryptic transcription does take place in a *Δisw1 Δpaa1* mutant.

2.2.3 Growth assay on lactate and glycerol revealed respiratory deficiency for *Δisw1 Δpaa1*

Yeast growth on carbon sources other than glucose causes de-repression of several genes, among them respiratory genes. This requires cells grown on carbon sources like raffinose or galactose to have a more robust respiratory system than they would require for growth on glucose (Hampsey, 1997). This would explain why *Δisw1 Δpaa1* is incapable of growing on galactose and raffinose media. We therefore decided to grow the strains on media with lactate or glycerol as carbon sources to test *Δisw1 Δpaa1* for respiratory deficiency. Inability to grow on glycerol or lactate indicates a failure to produce respiration-competent mitochondria (Tzagoloff and Dieckmann, 1990). We grew mutants in the wild type BY4741 background, as well as in the Gal1pr-*FLO8::HIS3* reporter strain background to see if potential phenotypes are consistent (Figure 2-6).

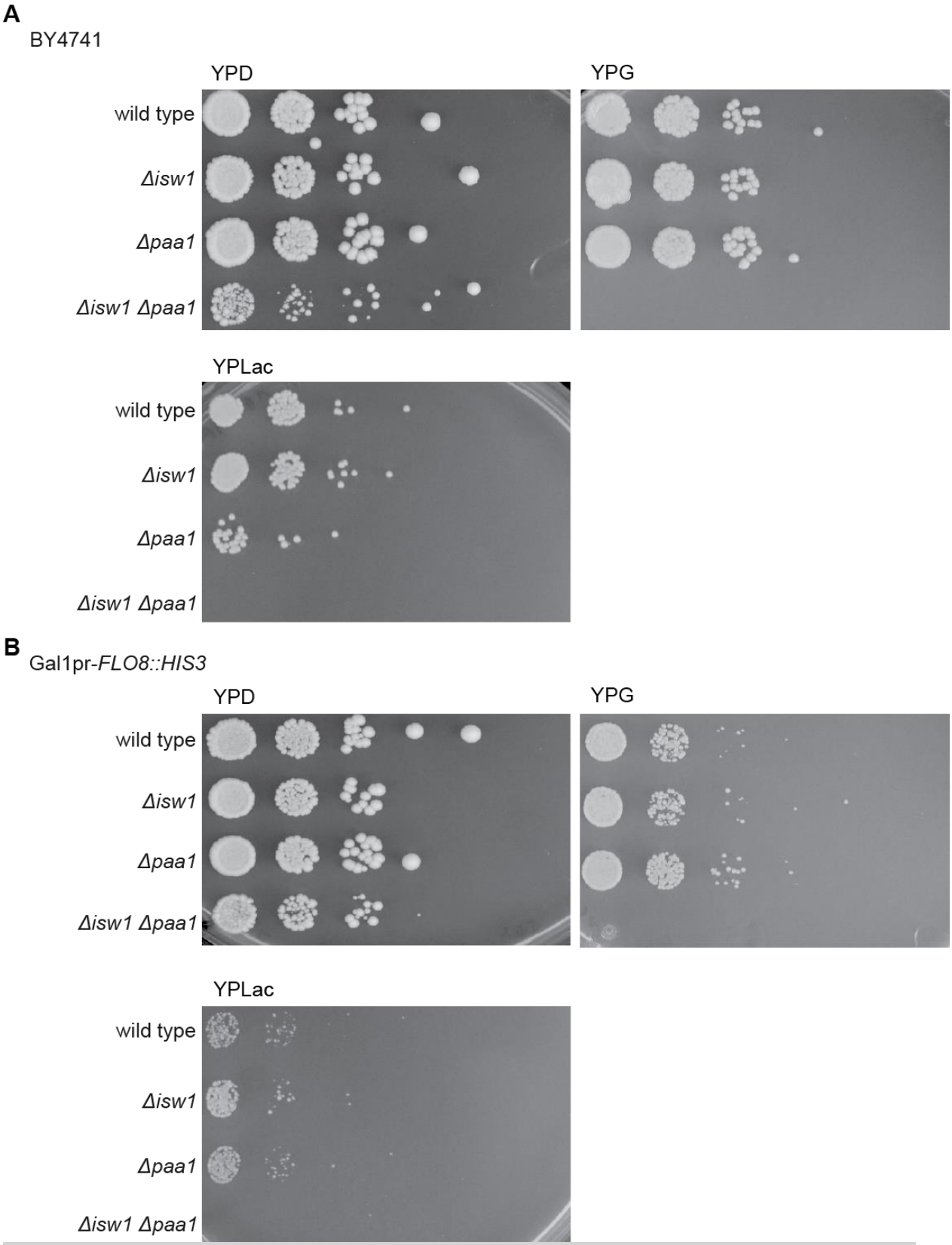

Figure 2-6: Spot dilution spotting assays for Δisw1 Δpaa1 in wild type and reporter strain background on media scoring for respiratory ability. 5-fold serial dilutions of wild type, Δisw1 Δpaa1, Δisw1 and Δpaa1 in BY4741 and reporter strain background were spotted on rich media with different carbon sources. **(A)** Strains in BY4741 background grown on YP media with either glucose (YPD), glycerol (YPG) or lactate (YPLac). **(B)** Strains in Gal1-pr-*FLO8*::*HIS3* reporter strain background grown on YP media with either glucose (YPD), glycerol (YPG) or lactate (YPLac). Representative picture of triplicate experiments is shown.

Results were scored from no growth (-) to growth comparable to wild type on rich media (+++) (Table 2-3).

Table 2-3: Scored growth for Δisw1 Δpaa1 in BY4741 and reporter strain background on media scoring for respiratory deficiency. Growth was scored for wild type, *Δisw1*, *Δpaa1* and *Δisw1 Δpaa1* in BY4741 and reporter strain background. Scores ranged from no growth (-) to growth like wild type under control conditions (+++).

Condition	**wild type**	***Δisw1***	***Δpaa1***	***Δisw1 Δpaa***
YPD	+++	+++	+++	++
YPG	+++	+++	+++	-
YPLac	++	++	+	-
Gal1pr-*FLO8::HIS3*				
YPD	+++	+++	+++	++
YPG	++	++	++	-
YPLac	+	+	+	-

This revealed that in fact neither BY4741 nor Gal1pr-*FLO8::HIS3* background *Δisw1 Δpaa1* can grow on YP-media with either lactate or glycerol as carbon source (Figure 2-6, Table 2-3). Single deletion mutant strains, on the other hand, grow comparable to wild type growth on either carbon source, except for BY4741 *Δpaa1*, which grows less on lactate (Figure 2-6, Table 2-3). This indicates *Δisw1 Δpaa1* is respiratory deficient. Further analysis, however, was inconclusive.

2.2.4 Northern blot analysis confirmed cryptic transcription phenotype for *Δisw1 Δpaa1*

There are many genes besides *FLO8* that possess cryptic promoter sites within their ORFs. This is useful, as it has been described previously that *FLO8* does not work well as a reporter for cryptic transcription in some mutants, like *Δset2* and *Δisw1* (Cheung et al., 2008; Smolle et al., 2012). Therefore, we tested the presence of cryptic transcription in *PCA1* and *SSK22*, two genes that have been identified to have cryptic promoter sites (Lickwar et al., 2009, Smolle, Venkatesh et al., 2012). Remodeler mutants are known to cause cryptic transcription, specifically *Δisw1*, in conjunction with *Δchd1*. Therefore, we decided to assess the impact of *PAA1* deletion on cryptic transcription in *Δisw1*.

RNA was isolated from each strain and analyzed by northern blotting, as it allows easy differentiation between transcripts of different sizes. We picked probes against the 3' end of *PCA1* and *SSK22* respectively. This allows the detection of full-length transcripts and shorter cryptic transcripts. We quantified the signal intensity of each band by densitometry and normalized to *ACT1* as loading control.

2.2.4.1 Cryptic transcription occurs in Δisw1 Δpaa1 mutants

We examined the double mutant *Δisw1 Δpaa1*, as well as single mutants and wild type BY4741 as controls. This revealed a general increase of transcription of *PCA1* in a *Δisw1 Δpaa1* mutant (Figure 2-7A, arrow). The increase of full-length transcription was limited to *PCA1* and did not occur in *SSK22*. For both of them however, an increase in cryptic transcription could be observed. In *PCA1*, signals for bands corresponding to cryptic transcripts were increased

compared to cryptic transcripts in wild type (Figure 2-7A, asterisks and Figure 2-7C). In *SSK22*, an increase in cryptic transcripts could also be observed for *Δisw1 Δpaa1* mutants (Figure 2-7B, asterisk and Figure 2-7D). Additionally, an increase in cryptic transcripts could be observed in *Δisw1* mutants on both *PCA1* and *SSK22*, although the increase was smaller than for the double mutant. This is in accordance with the previous observations of cryptic transcriptions being increased in *Δisw1* mutants in *PCA1* and *SSK22* (Smolle et al., 2012).

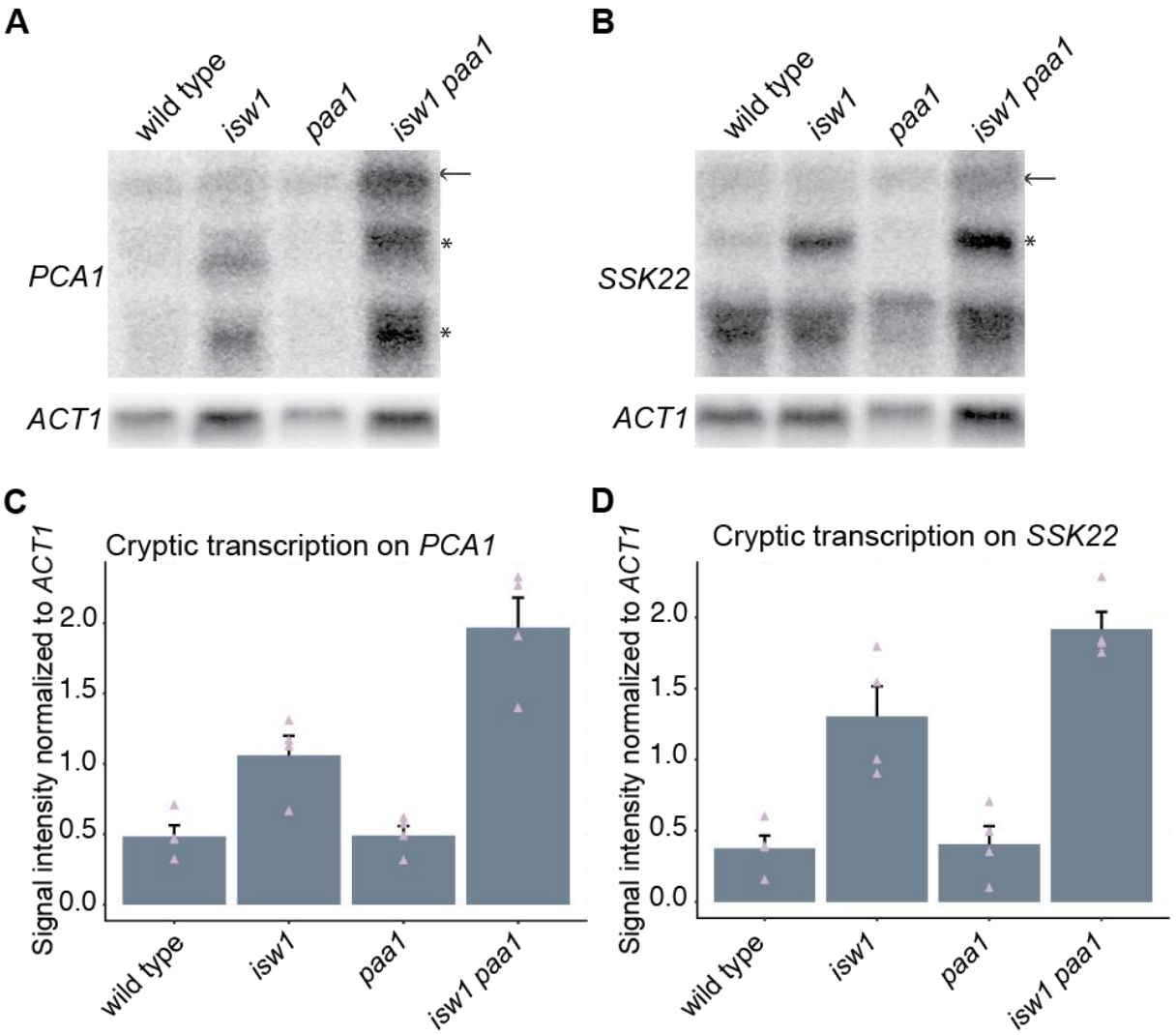

Figure 2-7: Northern blots on *PCA1* and *SSK22* in *Δisw1 Δpaa1* compared to wild type and single mutants. (A-B) Total RNA for each strain was isolated and analyzed by northern blot. The probes targeted the 3' ends of *PCA1* and *SSK22*. *ACT1* was used as loading control. For *SSK22*, a smaller transcript is present in every strain. It has therefore been excluded from analysis. The full-length (←) and cryptic transcripts (*) are indicated. Representative pictures of quadruplicate experiments are shown. **(C-D)** For each strain, all cryptic transcripts were quantified and normalized against *ACT1*. They were then normalized against the daily average of all strains to account for day-to-day variety. Data was plotted as mean ± s.e.m of four independent experiments. Individual data points are shown as triangles.

2.2.4.2 Cryptic transcription in Δioc2 Δioc3 Δpaa1 is limited compared to Δisw1 Δpaa1

Isw1 is the catalytic subunit of Isw1a and Isw1b, two independent remodeler complexes with differing functions. Since deletion of *ISW1* causes cryptic transcription, we wanted to examine if any phenotype could be observed by deletion of either *IOC2* or *IOC3*. If the phenotype is specific for either Isw1a or Isw1b, deletion of *IOC2* or *IOC3* abrogates formation of Isw1a and Isw1b respectively. We repeated northern blots of *Δisw1 Δpaa1* and compared them to *Δioc2 Δpaa* and *Δioc3 Δpaa* mutants.

Furthermore, we tested *Δioc2 Δioc3 Δpaa1* mutants, in order to determine if the effect is dependent on Isw1 alone or the absence of both remodeler complexes. This revealed that the increase of full-length transcription of *PCA1* only occurs in *Δisw1 Δpaa1* and not in *Δioc2 Δioc3 Δpaa1* (Figure 2-8A, arrow). Cryptic transcription of *PCA1* was increased in *Δisw1 Δpaa1*, but not in *Δioc2 Δioc3 Δpaa1* (Figure 2-8A, asterisk and Figure 2-8C). None of the other strains showed a significant change of cryptic transcription on *PCA1* compared to wild type (Figure 2-8A and Figure 2-8C).

We can also observe that cryptic transcription in *Δioc2 Δioc3 Δpaa1* is increased compared to wild type (Figure 2-8B and Figure 2-8D). In general, cryptic transcription on *SSK22* is elevated for most strains, except *Δioc2*, *Δpaa1* and *Δioc2 Δpaa1*. In fact, cryptic transcription is increased in all strains where *IOC3* has been deleted. This effect only occurs on *SSK22* and not on *PCA1*. This suggests that Ioc3 or Isw1a is important for suppressing cryptic transcription specifically at *SSK22*. Isw1a also plays a role in suppressing cryptic transcription (Smolle, unpublished). Due to this effect, we cannot use *SSK22* for meaningful comparison.

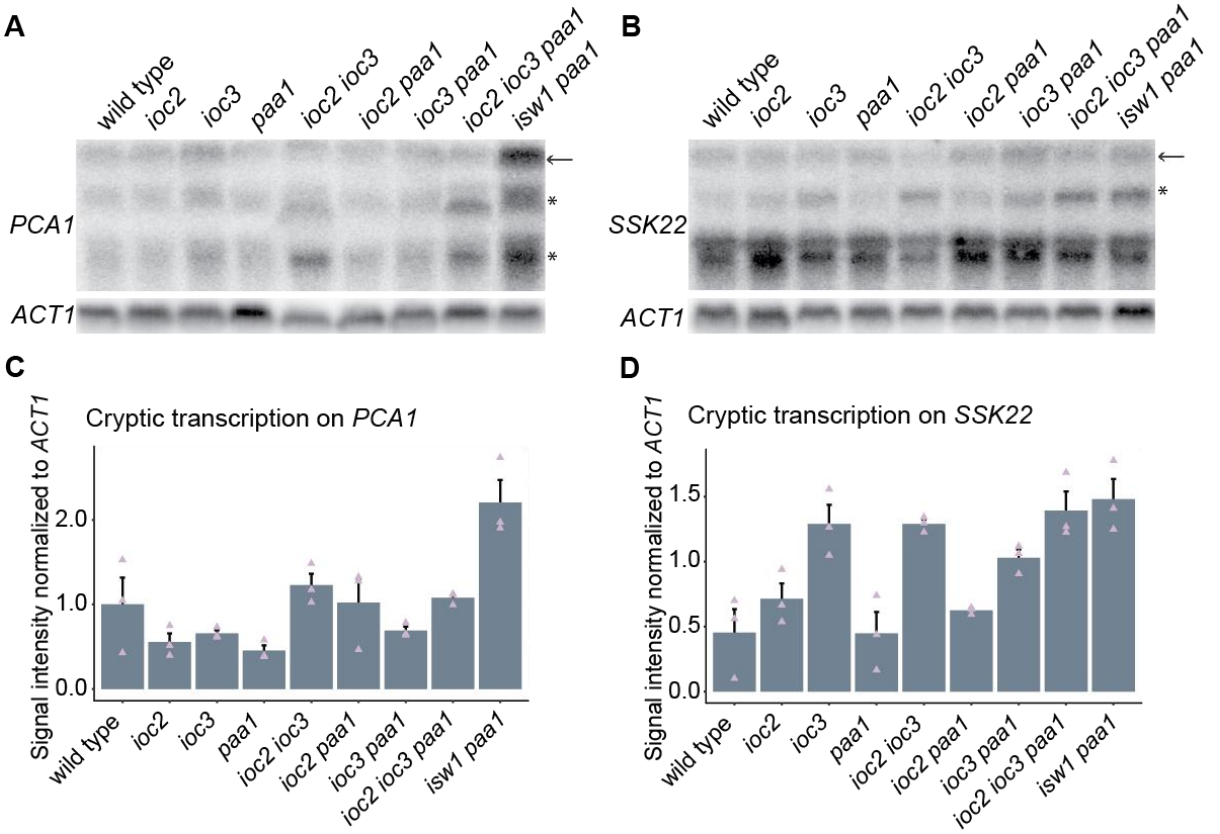

Figure 2-8: Northern blots on *PCA1* and *SSK22* in *Δisw1 Δpaa1* compared to wild type and other Isw1 subunits. (A-B) Total RNA for each strain was isolated and analyzed by northern blot. The probes targeted the 3' ends of *PCA1* and *SSK22*. *ACT1* was used as loading control. For *SSK22*, a smaller transcript is present in every strain. It has therefore been excluded from analysis. The full-length (←) and cryptic transcripts (*) are indicated. Representative pictures of triplicate experiments are shown. **(C-D)** For each strain, all cryptic transcripts were quantified and normalized against *ACT1*. They were then normalized against the daily average of all strains to account for day-to-day variety. Data was plotted as mean ± s.e.m of three independent experiments. Individual data points are shown as triangles.

2.2.4.3 Comparison to homologous remodelers revealed cryptic transcription only occurs in Δisw1 Δpaa1

In another experiment we wanted to determine if these changes to cryptic transcription are unique to Isw1, or if a similar change can be observed for other remodelers. Isw2 and Chd1 in particular are of interest, as they are homologues of Isw1 (Cuperus and Shore, 2002, Kent et al., 2001). Isw2 has been shown to play a role in transcriptional repression *in vivo* (Goldmark et al., 2000). It also possesses ATP-dependent nucleosome spacing activity (Tsukiyama et al., 1999). Chd1 facilitates the retention of hypoacetylated histones together with Isw1b (Smolle et al., 2012; Radman-Livaja et al., 2012). We therefore decided to examine if *Δpaa1* in conjunction with either *Δisw2* or *Δchd1* shows a similar phenotype as *Δisw1 Δpaa1*.

To this end, we performed northern blots for *Δisw2 Δpaa1* and *Δchd1 Δpaa1* and compared them to wild type and *Δisw1 Δpaa1*. Here we could show that there is no increase in transcription for either *Δisw2 Δpaa1* or *Δchd1 Δpaa1* (Figure 2-9, asterisks). This is true for both full-length and cryptic transcription, both on *PCA1* and *SSK22*. Transcription changes for *Δisw1 Δpaa1* are congruent with results obtained in earlier experiments for *PCA1*. This suggests

that the increase of cryptic transcription observed for *Δisw1 Δpaa1* is specific for Isw1 remodelers. Other remodelers cannot substitute for Isw1.

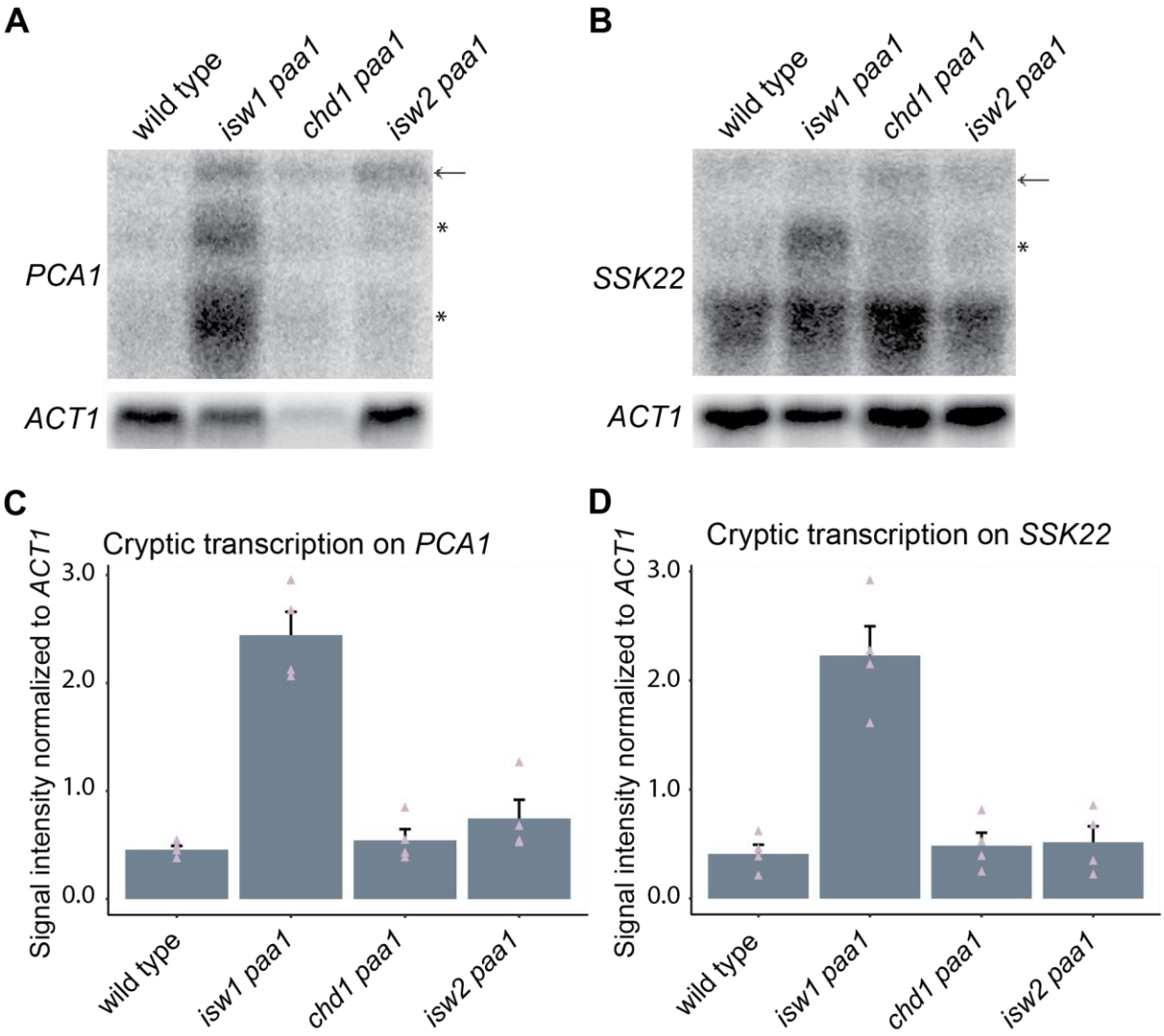

Figure 2-9: Northern blots on *PCA1* and *SSK22* in *Δisw1 Δpaa1* compared to wild type and other remodelers. (A-B) Total RNA for each strain was isolated and analyzed by northern blot. The probes targeted the 3' ends of *PCA1* and *SSK22*. *ACT1* was used as loading control. For *SSK22*, a smaller transcript is present in every strain, regardless of condition. It has therefore been excluded from analysis. The full-length (←) and cryptic transcripts (*) are indicated. Representative pictures of quadruplicate experiments are shown. **(C-D)** For each strain, all cryptic transcripts were quantified and normalized against *ACT1*. They were then normalized against the daily average of all strains to account for day-to-day variety. Data was plotted as mean ± s.e.m of four independent experiments. Individual data points are shown as triangles.

2.3 Defining gene expression by RNA sequencing

2.3.1 Analysis of genome-wide expression in *Δisw1 Δpaa1* by RNA-sequencing revealed strongly affected transcription in *Δisw1 Δpaa1*

Northern blot analysis has revealed a general up-regulation of transcription for *PCA1* in *Δisw1 Δpaa1*, in addition to effects on cryptic transcription in both *PCA1* and *SSK22*. This could indicate a broader effect on transcription caused by *Δisw1 Δpaa1*. Therefore, we decided to examine genome-wide transcription levels by RNA-sequencing (RNAseq) of mRNA. This method gives an overview over the general levels of transcription on all gene loci, as well as cryptic transcripts and allows in-depth analysis of transcription. One major point of interest are changes in cryptic transcripts, a majority of which occur on antisense strands. These transcripts are generally non-coding (Goodman et al., 2013). For this reason, we performed stranded RNAseq.

First, we looked at overall changes in gene transcription. We grouped 2-fold up- or down-regulated genes into Venn diagrams, separated by direction of transcription (Figure 2-10). More transcripts are up-regulated than down-regulated (Figure 2-10). Also, more transcripts in antisense direction are affected than in sense direction (compare Figure 2-10A with Figure 2-10B). Most of the transcripts affected can be found in *Δisw1 Δpaa1*. In sense direction, there are only few changes relative to wild type for *Δisw1* and *Δpaa1*. However, there are quite a few changes in expression in the double mutant and almost all significantly up-regulated genes in *Δisw1* overlap with the double mutant. There has been prior evidence that Isw1 plays a role in transcriptional regulation of certain genes (Tsukiyama et al., 1999; Vary et al., 2003).

In antisense direction there are relatively few changes to down-regulation, comparable to what we have observed in sense direction. There are a larger number of up-regulated transcripts for *Δisw1*. This is as expected, because of its known role in cryptic transcription. Not many changes could be observed for *Δpaa1*, which corroborates our observation from the northern blot experiments Figure 2-7). There are a lot of changes in up-regulation for the double mutant.

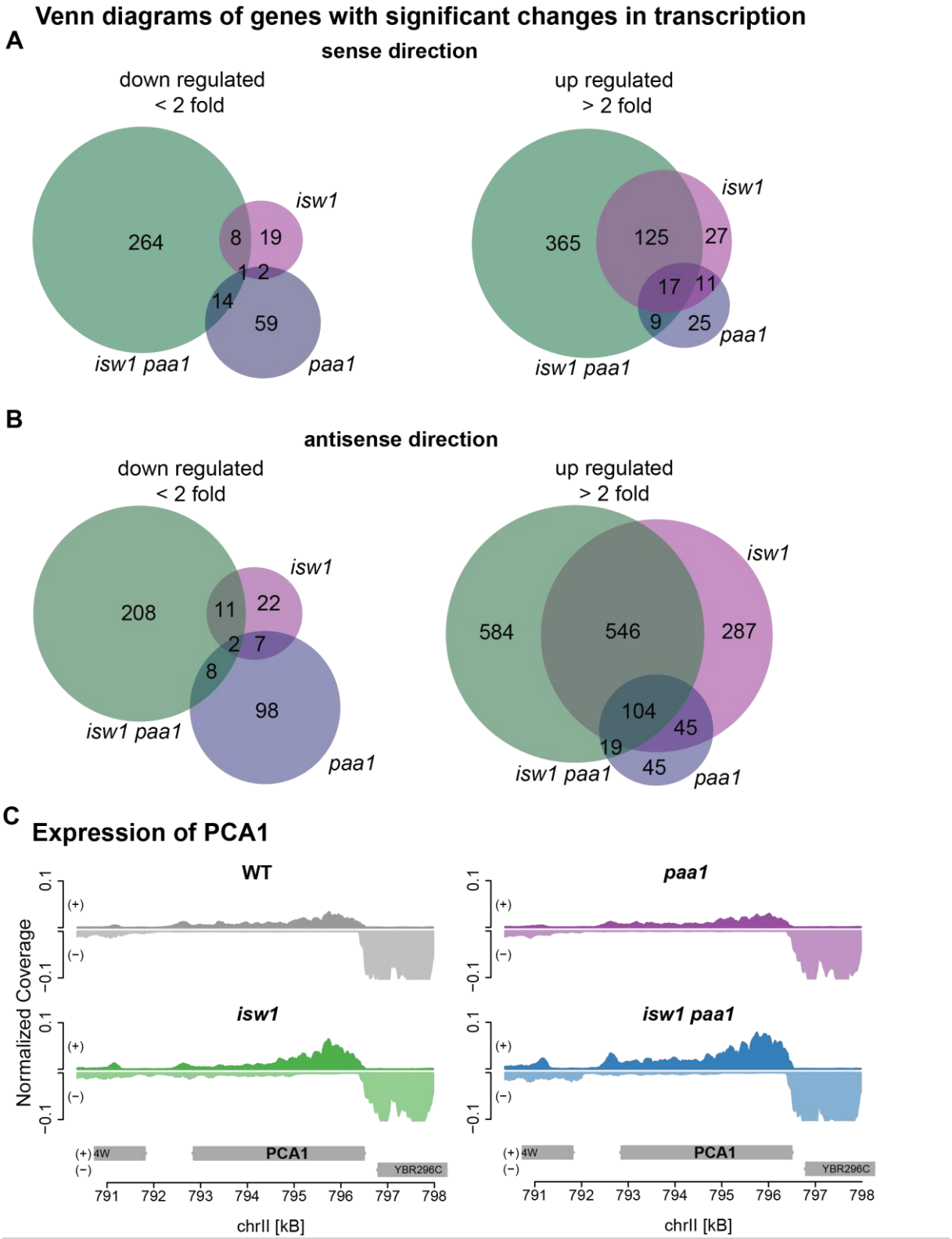

Figure 2-10: Venn diagrams of genes that were significantly changed in transcription rate in *Δisw1*, *Δpaa1* and *Δisw1 Δpaa1*, and traces of *PCA1* expression. The fold change of genes was determined compared to wild type in *Δisw1 Δpaa1*. Here we list all genes whose $\log_2$ fold change was either 2-fold up- or down-regulated. **(A)** Genes with significantly changed expression in sense direction. Genes with less than 2-fold down-regulation (left) are compared to genes with more than 2-fold up-regulation (right). **(B)** Genes with significantly changed expression in antisense direction. Genes with less than 2-fold down-regulation (left) are compared to genes with more than 2-fold up-regulation (right). **(C)** RNASeq traces of the expression of *PCA1* compared for sense and antisense direction between all four strains. Normalized coverage for each strain is shown.

We could observe in our northern blot experiments that overall expression of *PCA1* was increased significantly in *Δisw1 Δpaa1* (Figure 2-7). Similarly, an increase of cryptic transcription could be observed in the same mutant, with a smaller increase of cryptic transcription also observed in *Δisw1* (Figure 2-7). If we look at the traces of *PCA1* expression, we observe the same effect. Transcription near the 3' end of *PCA1* is increased in both *Δisw1* and *Δisw1 Δpaa1*, with a stronger effect in the double mutant (Figure 2-10C). This matches the estimated position of cryptic promoters on *PCA1*. Additionally, transcription along the entire gene is increased for *Δisw1 Δpaa1* (Figure 2-10C).

We then decided to group transcripts by different categories to give us further insight into the pattern of expression changes. We compared transcripts by their total expression levels in Transcripts Per kilobase Million (TPM) and by their $\log_2$ fold change compared to wild type expression.

2.3.1.1 *Expression of cryptic transcripts is widely affected in* Δisw1 Δpaa1

We compared expression of transcripts depending on their class, specifically CUTs, SUTs, ORFs and OTHER (as described in Xu et al., 2009 and in chapter 4 Materials and Methods). The OTHER group contains transcripts that were not classified as CUT, SUT or ORF (Figure 2-11). In sense direction there is overall low total transcription for sense CUTs and SUTs, compared to transcription of ORFs (Figure 2-11A). This is not unexpected, as CUTs and SUTs are predominantly found in intergenic regions and are often antisense to ORFs of protein-coding genes (Wyers et al., 2005; Kapranov et al., 2007). Transcription in *Δisw1 Δpaa1* was increased in sense direction for all classes, compared to wild type (Figure 2-11A). When looking at fold change compared to wild type transcription, transcription is also up-regulated for CUTs and SUTs in *Δisw1* (Figure 2-11B). No changes could be observed for *Δpaa1*.

In antisense direction, transcription is overall much higher for both CUTs and SUTs in both *Δisw1* and *Δisw1 Δpaa1*. There is increased transcription for *Δisw1 Δpaa1* for all classes compared to wild type (Figure 2-11A and B). For *Δpaa1* there are no changes compared to wild type, but for *Δisw1* there is some increase of transcription compared to wild type (Figure 2-11B). This argues for much more pervasive transcription of the yeast genome in the double mutant and perhaps hints at a synthetic effect for *PAA1* and *ISW1*. The fold change of *Δisw1 Δpaa1* shows a much wider spread of transcription levels, in particular for up-regulated transcription. This matches the observations in Figure 2-10.

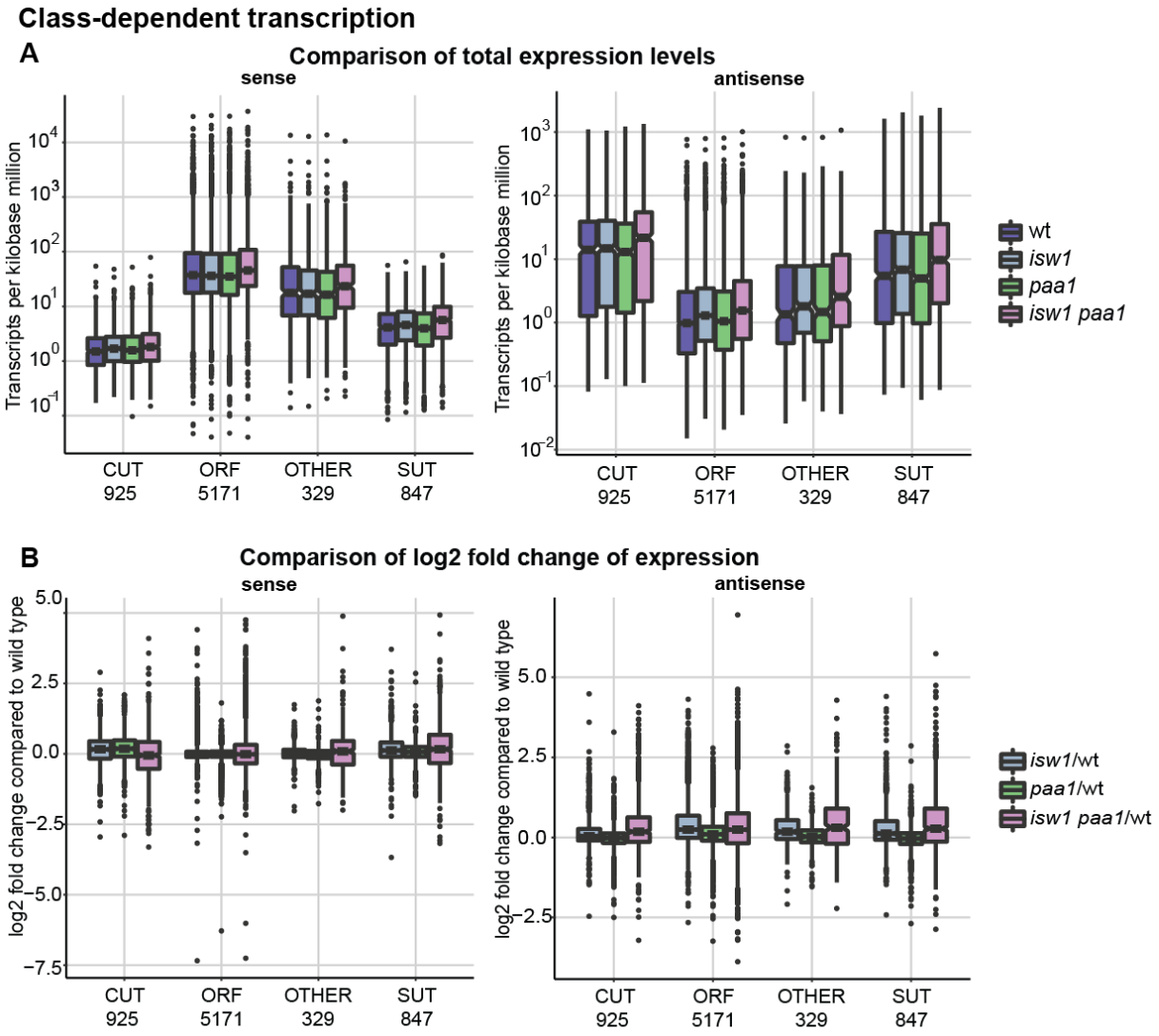

Figure 2-11: Class-dependent transcription in sense and antisense direction. Box plots of transcription in *Δisw1 Δpaa1*, *Δisw1*, *Δpaa1* and wild type was compared for both sense and antisense directed transcription and grouped by class. Box plots show the mean and quartiles. CUT denotes cryptic unstable transcripts, SUT denotes stable unannotated transcripts, ORF is open reading frame and OTHER contains all transcripts that were no classified as CUT, SUT or ORF. Number of transcripts that fall under each category are listed as well. **(A)** Total transcription in *Δisw1 Δpaa1*, *Δisw1*, *Δpaa1* and wild type was compared grouped by class. Total transcription levels are shown as TPMs (Transcripts Per kilobase Million) and represented as $\log_{10}$ values. **(B)** Transcription relative to wild type transcription was compared for *Δisw1 Δpaa1*, *Δisw1* and *Δpaa1*. Transcription compared to wild type is shown as $\log_2$ fold change compared to expression levels in wild type.

2.3.1.2 Transcription in Δisw1 Δpaa1 *decreases with increasing gene length*

We compared expression of transcripts depending on their length, as there is a correlation between high transcription rate and gene length. Many highly transcribed genes are short. Isw1 has been shown to primarily affect long genes and genes with low transcription rates (Tirosh et al., 2010). These genes tend to contain cryptic promoters We looked at genes categorized by length (as described in Holstege et al., 1998).

In sense direction, total transcription decreased with increasing gene length for all strains (Figure 2-12A). Transcription in *Δisw1 Δpaa1* is increased for all lengths compared to the wild type (Figure 2-12A). Additionally, transcription on genes longer than 2000 bp is increased in *Δisw1*, although to a lesser extent than in *Δisw1 Δpaa1*. Looking at changes compared to wild type transcription, it is revealed that again, transcription is changed more strongly for *Δisw1 Δpaa1* than it is for the single mutants. More transcripts overall are changed in transcription, both up and down (Figure 2-12B) for all gene lengths.

In antisense direction there is also a decrease in transcription with increasing gene length. Similar to sense direction, there is an increase of total transcription for *Δisw1 Δpaa1*, although the effect is much more pronounced (Figure 2-12A). Changes of transcription on long genes in *Δisw1* are increased more strongly than in sense direction. Transcription changes for *Δisw1 Δpaa1* are stronger than in the single mutants.

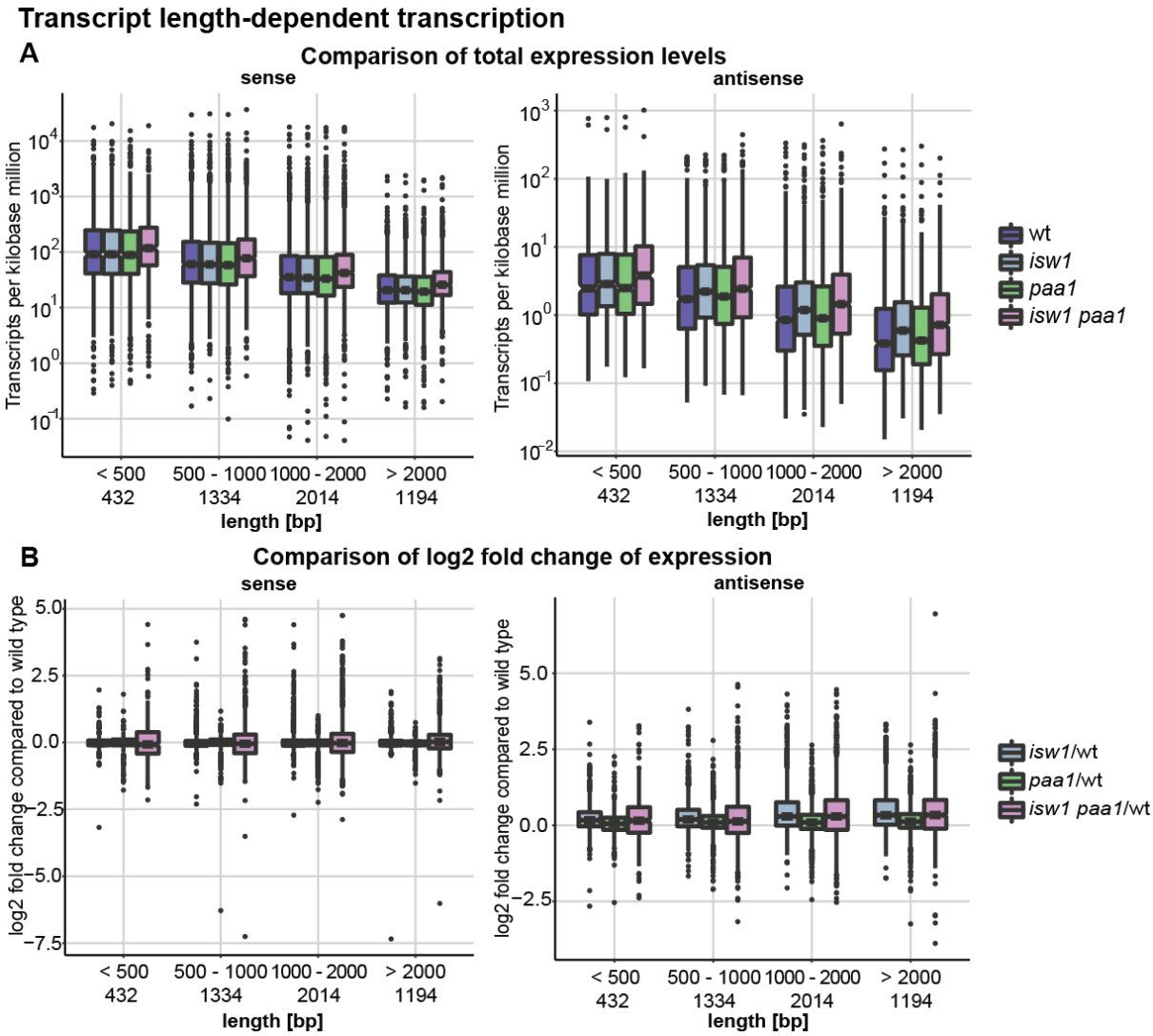

Figure 2-12: Transcript length-dependent transcription in sense and antisense direction. Box plots of transcription in *Δisw1 Δpaa1*, *Δisw1*, *Δpaa1* and wild type was compared for both sense and antisense directed transcription and grouped by transcript length. Box plots show the mean and quartiles. There were four different categories, small transcripts shorter than 500 bp, intermediate length with sizes ranging from 500 to 1000 bp and 1000 to 2000 bp and long transcripts, bigger than 2000 bp. Number of transcripts that fall under each category are listed as well. **(A)** Total transcription in *Δisw1 Δpaa1*, *Δisw1*, *Δpaa1* and wild type was compared grouped by transcript length. Total transcription levels are shown as TPMs (Transcripts Per kilobase Million) and represented as $\log_{10}$ values. **(B)** Transcription relative to wild type transcription was compared for *Δisw1 Δpaa1*, *Δisw1* and *Δpaa1*. Transcription compared to wild type is shown as $\log_2$ fold change compared to expression levels in wild type.

2.3.1.3 Transcription in Δisw1 Δpaa1 *is dependent on transcription rate*

Next, we compared genes grouped by their native transcription rates. Transcription rates were taken from Miller, Schwalb et al., 2011 and used as a basis for comparison. We split transcription rates into five categories from low (< 1 mRNA/hr) to intermediate (5 to 10 mRNA/hr) to high (> 50 mRNA/hr).

As expected, comparison of total transcription in sense direction revealed that transcription is increased for transcripts with high native transcription rates. However, sense transcription in *Δisw1 Δpaa1* is increased compared to wild type transcription for transcripts with low native transcription rates (< 1 mRNA/hr and 1 to 5 mRNA/hr) and intermediate native transcription rates (5 to 10 mRNA/hr). But it is reduced compared to wild type transcription for transcripts with high native transcription rates (> 50 mRNA/hr) (Figure 2-13A). Here, we could also show that transcription in *Δpaa1* is reduced for genes with a low native transcription rate compared to wild type transcription. The number of genes in this category is low, however. Transcription rates were also increased slightly in *Δisw1*, although to a lesser extent than in *Δisw1 Δpaa1* (Figure 2-13A). These results are confirmed when looking at $\log_2$ fold change of transcription compared to wild type. Sense transcription for *Δisw1 Δpaa1* is increased for transcripts with low native transcription rates and decreased for transcripts with high native transcription rates (> 50 mRNA/hr) (Figure 2-13B). Transcription in *Δpaa1* is decreased as it shows a negative $\log_2$ fold change compared to wild type.

In antisense direction, transcription is increased for all native transcription rates in *Δisw1 Δpaa1*, except for the transcripts with the highest native transcription rate, where transcription is down-regulated compared to wild type (Figure 2-13B).

There is also a general trend for strong changes in transcription for *Δisw1 Δpaa1*, as indicated by the size of the boxes for both antisense and sense directed transcription. This implies that there are many genes that are either up or down regulated, especially compared to *Δpaa1*, which in general tends to resemble wild type transcription. A similar observation can be made for *Δisw1*, which is also subject to stronger changes in transcription.

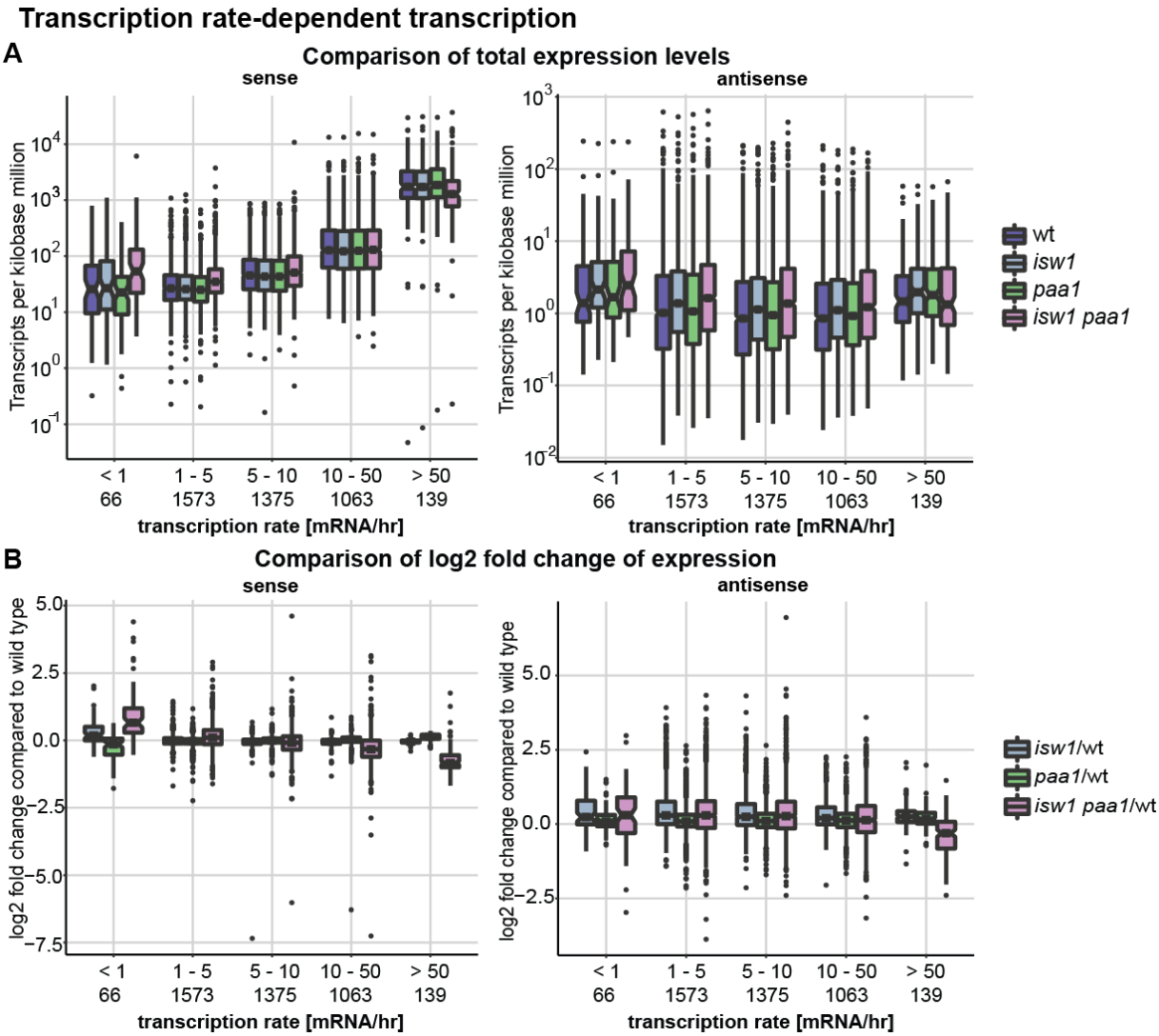

Figure 2-13: Transcription rate-dependent transcription in sense and antisense direction. Box plots of transcription in *Δisw1 Δpaa1*, *Δisw1*, *Δpaa1* and wild type was compared for both sense and antisense directed transcription and grouped by transcription rate. Box plots show the mean and quartiles. Transcripts were categorized as low, with transcription rates smaller than 1 or between 1 and 5 mRNA/hr, intermediate, with transcription rates between 5 and 10 mRNA/hr and high transcription rates, with 10 to 50 and above 50 mRNA/hr. Number of transcripts that fall under each category are listed as well. **(A)** Total transcription in *Δisw1 Δpaa1*, *Δisw1*, *Δpaa1* and wild type was compared grouped by transcription rate. Total transcription levels are shown as TPMs (Transcripts Per kilobase Million) and represented as $\log_{10}$ values. **(B)** Transcription relative to wild type transcription was compared for *Δisw1 Δpaa1*, *Δisw1* and *Δpaa1*. Transcription compared to wild type is shown as $\log_2$ fold change compared to expression.

2.3.1.4 Transcription increases for TATA box genes in sense direction

We also investigated changes of transcription depending on promoter type. In yeast, approximately 20% of genes are under the control, of a TATA box. These genes tend to be regulated by SAGA rather than TFIID (Transcription Factor IID), which is commonly found to regulate TATA-less genes (Basehoar et al., 2004). We decided to investigate if transcription changes dependent on the type of promoter of a gene.

In sense direction, total transcription in *Δpaa1* is reduced for genes with a TATA box, compared to wild type transcription. For genes without a TATA box, total transcription in *Δpaa1* is equal to wild type transcription (Figure 2-14). Additionally, total transcription in *Δisw1 Δpaa1* is increased only for genes with a TATA box, but not for genes without a TATA box (Figure 2-14). Looking at $\log_2$ fold change of transcription in sense direction, it becomes evident that transcription in *Δisw1 Δpaa1* is strongly influenced, regardless of promoter type, with higher changes in both up and down regulation (Figure 2-14). However, SAGA-dependent genes may be slightly more up-regulated than TFIID- dependent genes.

For antisense direction transcripts we observe a slight increase of total transcription in *Δisw1* and *Δisw1 Δpaa1* compared to transcription in wild type, independent of promoter type. Although the effect is more pronounced for *Δisw1 Δpaa1* (Figure 2-14A, right). Here, both SAGA- and TFIID-dependent genes are equally affected. The same is true for expression in antisense direction, where transcription in *Δisw1 Δpaa1* is subject to stronger changes. However, *Δisw1* is also affected, showcasing higher $\log_2$ fold changes for transcripts, both upwards and downwards (Figure 2-14).

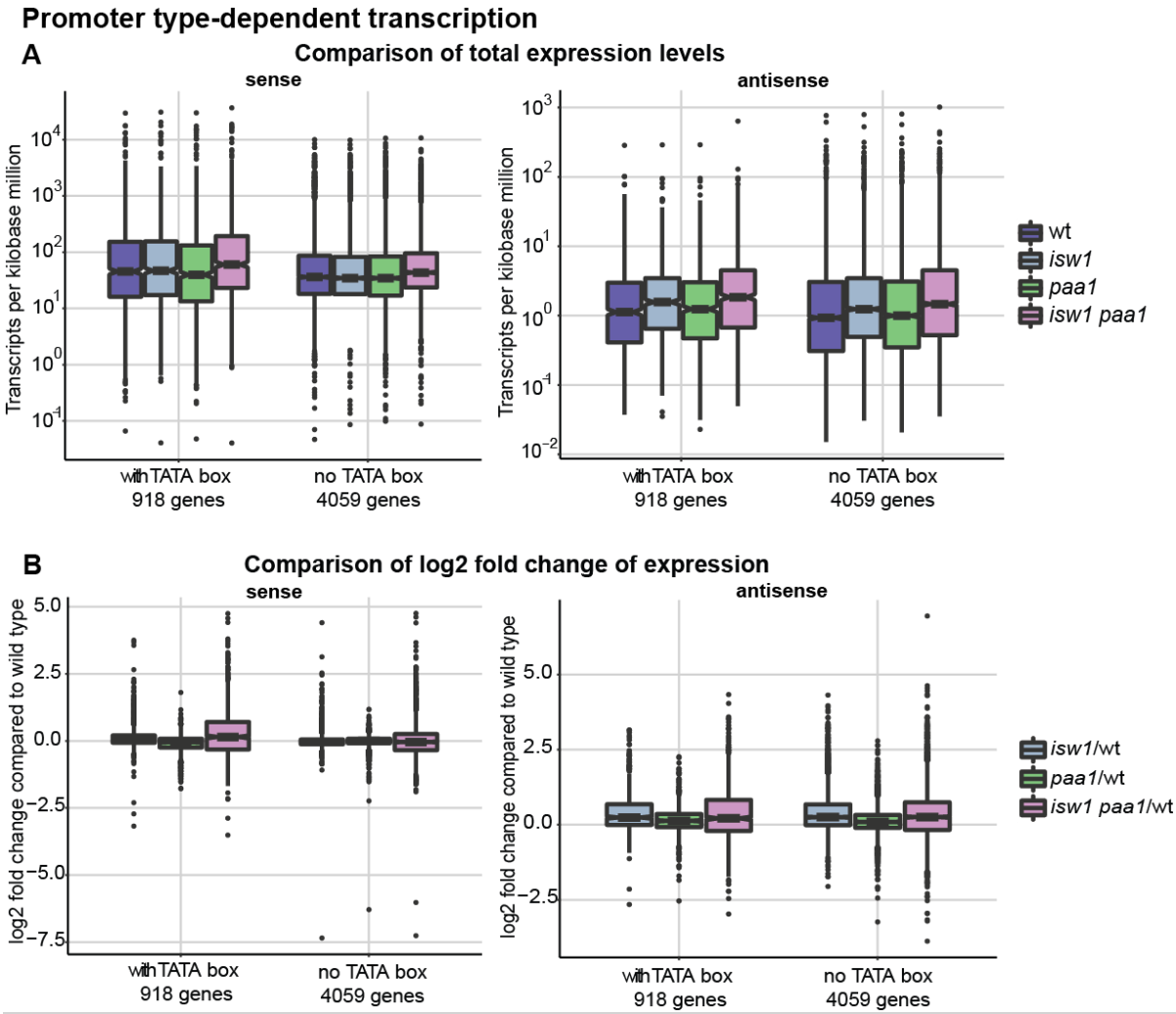

Figure 2-14: Promoter type-dependent transcription in sense and antisense direction. Box plots of transcription in *Δisw1 Δpaa1*, *Δisw1*, *Δpaa1* and wild type was compared for both sense and antisense directed transcription and grouped by promoter type. Box plots show the mean and quartiles. Promoters of genes were either under the control of a TATA box and therefore dependent on SAGA, or were without TATA box and dependent on TFIID. Number of transcripts that fall under each category are listed as well. **(A)** Total transcription in *Δisw1 Δpaa1*, *Δisw1*, *Δpaa1* and wild type was compared grouped by promoter type. Total transcription levels are shown as TPMs (Transcripts Per kilobase Million) and represented as $\log_{10}$ values. **(B)** Transcription relative to wild type transcription was compared for *Δisw1 Δpaa1*, *Δisw1* and *Δpaa1*. Transcription compared to wild type is shown as $\log_2$ fold change compared to expression levels in wild type.

2.3.1.5 Transcription for ribosomal protein genes in Δisw1 Δpaa1 *is down regulated*

We have found indications that the double mutant *Δisw1 Δpaa1* has a respiratory deficiency. This puts cells under substantial stress. Common markers for stress-related changes in gene expression are ribosomal protein genes. Expression of these genes in the mutants seemed to be generally down regulated, if cells are stressed, as could be seen in the RNAseq traces and the example of RPL9A (Figure 2-15A). We therefore chose to examine expression specifically of ribosomal protein genes.

Here we can show that total expression of ribosomal protein genes in sense direction is strongly down regulated in *Δisw1 Δpaa1* compared to wild type expression and expression in the single mutants (Figure 2-15B, left). Expression of ribosomal proteins is unchanged in *Δisw1* compared to the wild type, but slightly increased in *Δpaa1* (Figure 2-15C, left). This indicates stress, since ribosomal protein expression is down-regulated at stress conditions. This is consistent with the observed growth phenotypes (Figure 2-3).

For expression in antisense direction, we can show that expression in *Δisw1 Δpaa1* is down regulated, compared to wild type (Figure 2-15C, right). Expression in the single mutants remains comparable to expression in wild type (Figure 2-15C).

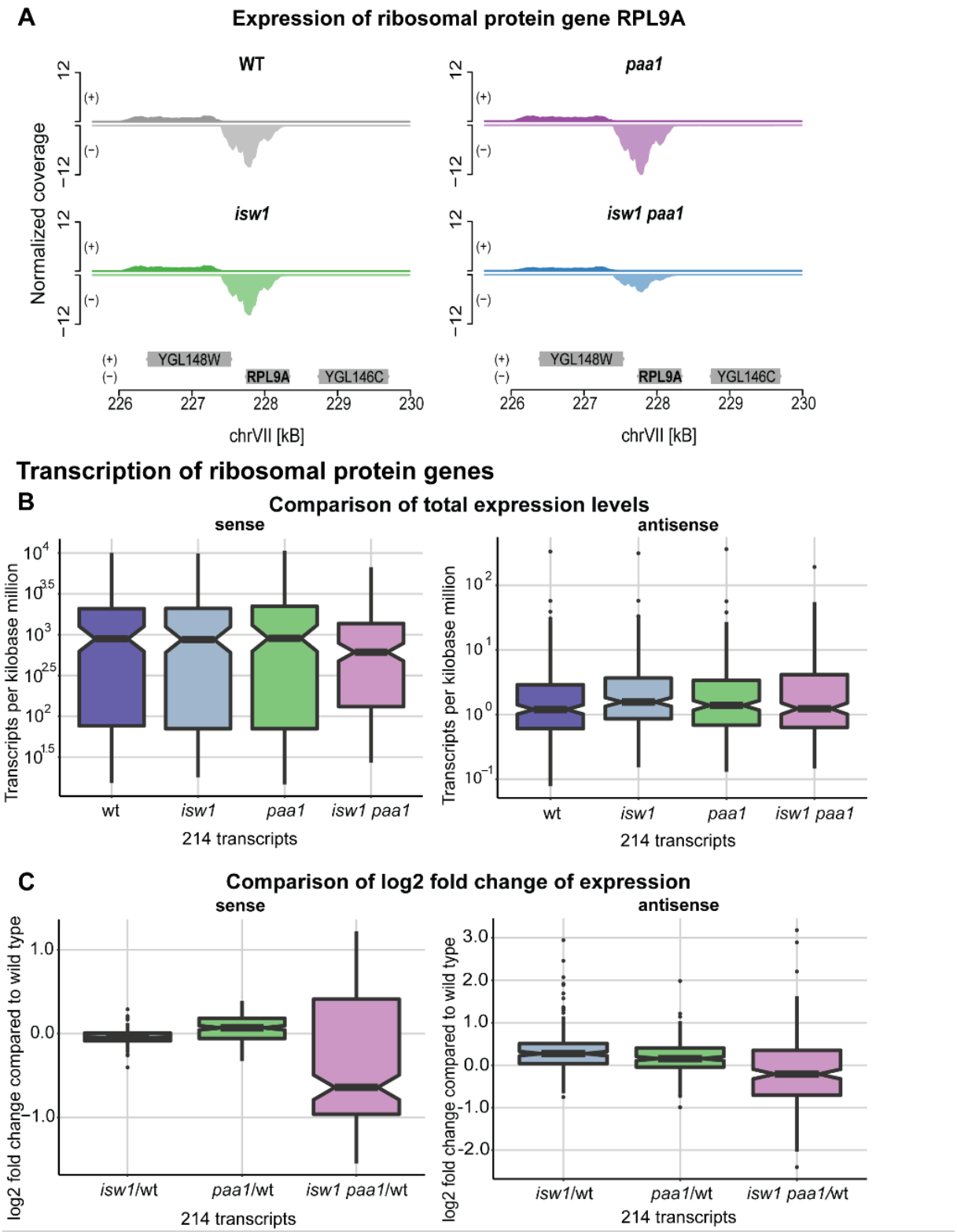

Figure 2-15: Expression of ribosomal protein genes in sense and antisense direction. (A) RNASeq trace of the expression of RPL9A compared for sense and antisense direction between all four strains. Normalized coverage for each strain is shown. **(B)** Box plots of total transcription for ribosomal protein genes in *Δisw1 Δpaa1*, *Δisw1*, *Δpaa1* and wild type in sense and antisense direction. Total transcription levels are shown as TPMs (Transcripts Per kilobase Million) and represented as $\log_{10}$ values. **(C)** Transcription relative to wild type transcription was compared for *Δisw1 Δpaa1*, *Δisw1* and *Δpaa1*. Transcription compared to wild type is shown as $\log_2$ fold change compared to expression levels in wild type from the same replicate. Box plots show the mean and quartiles. Amounts of transcripts are listed as well.

2.3.1.6 Transcription for mitochondrial protein genes in Δisw1 Δpaa1 *is unaffected*

We also decided to look at expression of mitochondrial protein genes. Changes in expression of mitochondrial protein genes, down-regulation in particular would explain the respiratory phenotype we observed in the growth assays in the double mutant (Figure 2-3). There were no changes in transcription in *Δisw1* and *Δpaa1* compared to the wild type in sense direction (Figure 2-16A and B). We could also not observe any down-regulation of transcription for *Δisw1 Δpaa1*. It seems to be that expression is slightly up-regulated (Figure 2-16A and B). This is unexpected, given our results from the growth assays. It also shows that mitochondrial protein genes are expressed and that the mitochondrial genome is likely intact.

In antisense direction, *Δpaa1* also shows no changes in expression compared to wild type (Figure 2-16A). *Δisw1* shows slight up-regulation compared to wild type (Figure 2-16B, right). The double mutant is also up-regulated compared to wild type (Figure 2-16B).

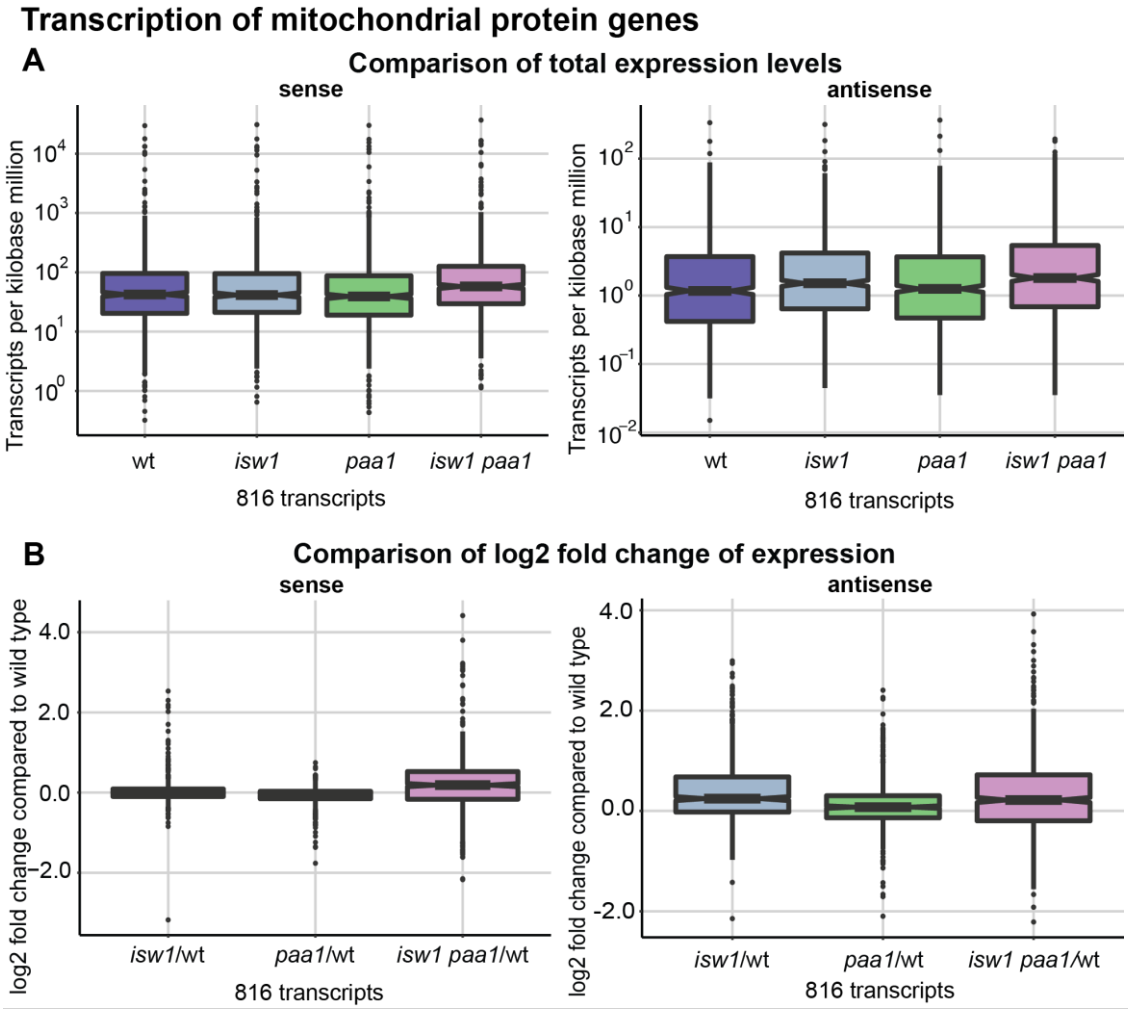

Figure 2-16: Expression of mitochondrial protein genes in sense and antisense direction. Box plots of transcription of mitochondrial protein genes in *Δisw1 Δpaa1*, *Δisw1*, *Δpaa1* and wild type was compared for both sense and antisense directed. Box plots show the mean and quartiles. Number of transcripts that fall under each category are listed as well. **(A)** Transcription of mitochondrial protein genes in *Δisw1 Δpaa1*, *Δisw1*, *Δpaa1* and wild type was compared. Total transcription levels are shown as TPMs (Transcripts Per kilobase Million) and represented as $\log_{10}$ values. **(B)** Transcription of mitochondrial protein genes relative to wild type transcription was compared for *Δisw1 Δpaa1*, *Δisw1* and *Δpaa1*. Transcription compared to wild type is shown as $\log_2$ fold change compared to expression levels in wild type.

2.3.1.7 Transcription for genes with increased histone turnover in Δisw1 Δpaa1 *is unaffected*

Certain genes show an increase in histone turnover in a *Δisw1* deletion mutant at the mid to 3' end of genes (Smolle et al., 2012). We decided to examine if these genes also show an increase of expression as a result of the increased histone turnover, compared to genes with no increased histone turnover.

In sense direction, there is a change of overall transcription for *Δisw1 Δpaa1* (Figure 2-17A and B) Transcription of *Δpaa1* is unaffected. Transcription is also unaffected for *Δisw1* (Figure 2-17A and B).

Transcription in antisense direction is slightly increased for *Δisw1 Δpaa1*, with a more pronounced effect in *Δisw1 Δpaa1* (Figure 2-17A and B). Transcription in *Δpaa1* remains similar to wild type transcription. Antisense transcription in *Δisw1* is increased slightly, but to a lesser extent than in the double mutant. This could be a result of the increased histone turnover, but unlikely as the change in expression occurs in both gene classes, independent of turnover rate. Additionally, there are no changes in expression in sense direction for *Δisw1*. This indicates that the changes in expression are not a result of increased histone turnover.

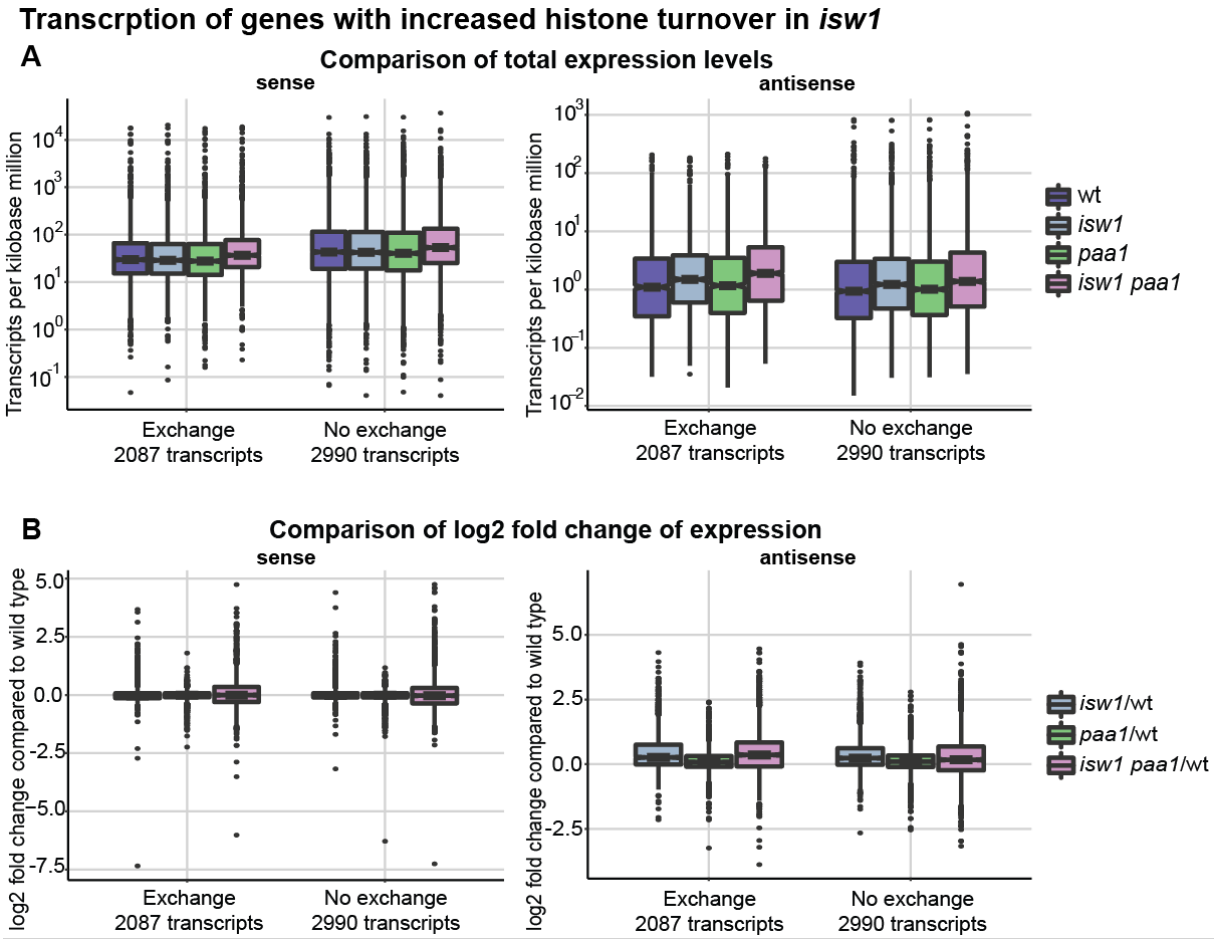

Figure 2-17: Expression of genes that have increased histone turnover in *Δisw1*. Box plots of transcription levels of genes with increased histone exchange rates in *Δisw1* in *Δisw1 Δpaa1*, *Δisw1*, Δpaa1 and wild type were compared for both sense and antisense directed transcription. Amounts of transcripts were listed as well. Box plots show the mean and quartiles. (A) Total transcription for genes with increased histone turnover rates in *Δisw1* in *Δisw1 Δpaa1*, *Δisw1*, *Δpaa1* and wild type in sense and antisense direction, compared to transcripts with no change in exchange rate. Total transcription levels are shown as TPMs (Transcripts Per kilobase Million) and represented as log10 values. (B) Transcription relative to wild type transcription was compared for *Δisw1 Δpaa1*, *Δisw1* and *Δpaa1*. Transcription compared to wild type is shown as $\log_2$ fold change compared to expression levels in wild type.

We also had a look at the top and bottom 10 percentile of genes with histone turnover changes to see if we can observe a stronger effect in these groups, but the results were similar to what we observed in Figure 2-17 (results not shown).

2.3.2 Changes in antisense transcription are more likely to occur on genes with changes in sense expression

We also wanted to examine how changes in sense and antisense transcription correlate. We therefore plotted the $\log_2$-fold changes of mutants compared to wild type, comparing sense and antisense transcription (Figure 2-18). Genes were grouped by whether they are up- and/or down-regulated in sense and antisense direction.

For *Δpaa1* we can see only a few small differences between the changes of transcription in sense and antisense direction. The overall changes of transcription in sense direction are relatively low. The same is true for changes of transcription in antisense direction, although here the trend leans towards more up-regulation (Figure 2-18).

For *Δisw1* there is more antisense transcription of genes that are both slightly down- or up-regulated in sense direction. In general, more transcripts are up-regulated in antisense direction. In contrast, there are fewer transcripts that were down-regulated in antisense direction, with again an equal split between up- and down-regulated genes (Figure 2-18).

Something similar can be observed for *Δisw1 Δpaa1*, although the changes in sense transcription are more pronounced (Figure 2-18). Overall, transcription is much more strongly affected in the double mutant. Particularly when it comes to transcriptional changes in antisense direction, the double mutant shows more pronounced changes, affecting more genes overall. This is true for both up- and down-regulated genes, although down-regulation is affected more strongly, when compared to the two single mutants. This observation is in line with previous analyses showing that for some genes there is a much stronger down-regulation in *Δisw1 Δpaa1*.

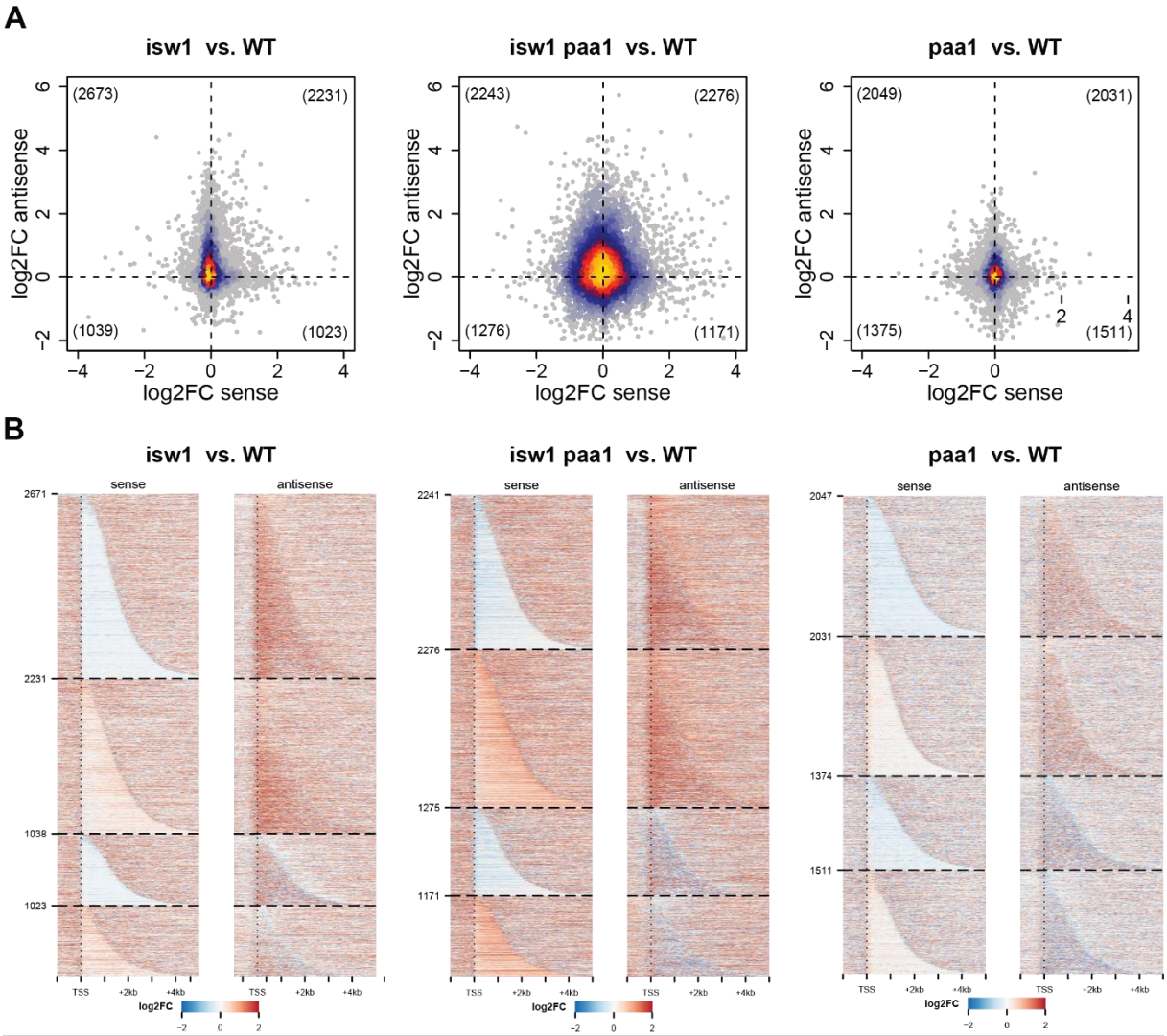

Figure 2-18: log_2-fold change comparisons for *Δisw1*, *Δpaa1* and *Δisw1 Δpaa1* (A) Density colored scatterplots comparing log_2-fold change of sense and antisense transcripts between *Δisw1*, *Δpaa1* and *Δisw1 Δpaa1* and wild type. The number of genes in each quadrant is indicated. **(B)** Heatmaps of log_2-fold changes aligned to TSS for *Δisw1*, *Δpaa1* and *Δisw1 Δpaa1* vs. wild type. Genes are grouped by whether they are up- or down- regulated in sense and antisense direction (numbers of each group are given). The number of genes in each group matches the number of genes in the quadrants of **A**. Genes are ordered by length.

2.4 Defining nucleosome positions by MNase sequencing

2.4.1 Genome-wide analysis of nucleosome positioning and spacing revealed increase of spacing in *Δpaa1* and a shift of nucleosome positioning in *Δisw1 Δpaa1*

Nucleosome occupancy is known to block access to expression sites (Knezetic and Luse, 1986), although this is best described for metabolic genes like *PHO*. Genes are generally covered by nucleosome arrays, which are influenced by remodelers (Bork and Koonin, 1993; Eisen et al., 1995). The absence of remodelers, as in *Δisw1 Δchd1*, leads to a reduction of regularly spaced nucleosome arrays. *Δisw1 Δchd1* is also a mutant with considerate levels of antisense transcription (Smolle et al., 2012). Therefore, we wanted to examine if *Δisw1 Δpaa1* leads to reduction in nucleosome arrays or promoter occupancy, as this could be a cause for the increase of cryptic transcription we observed earlier (2.2.2 and 2.2.4.1).

We decided to perform MNase-sequencing experiments (MNase-seq). To this end, we isolated nuclei from BY4741 wild type cells, as well as *Δisw1*, *Δpaa1* and *Δisw1 Δpaa1* deletion mutants. We titrated different concentrations of MNase to gain a better overview of digestion efficiency (Figure S1). The different concentrations chosen were 16, 32 and 64 U/ml. These were compared to samples without any added MNase for comparison to undigested chromatin. Here we can show a nice nucleosome ladder for all four strains at lower MNase concentrations and over digestion and reduction of the ladder pattern at increased amounts of MNase.

Samples that were picked for library preparation had to have a 1 to 5 ratio of dinucleosomes to mononucleosomes (Figure S1, see samples marked with asterisk). We plotted the dyad density for all genes in all strains, centered on the +1 nucleosome position according to (Chereji, Ramachandran et al., 2018) to give an overview of nucleosome array formation on a genome-wide level (Figure 2-19A).

Nucleosome positions in the wild type and *Δisw1* match what has been previously observed (Gkikopoulos et al., 2011; Ocampo et al., 2016). There is a slight shift of nucleosome positions away from the TSS in *Δpaa1* (Figure 2-19A). Similar to *Δisw1*, overall nucleosome positions for *Δisw1 Δpaa1* remain comparable to those in the wild type.

We then compared nucleosome spacing of individual genes to a regular array of Gaussian distributions of idealized spacing, as described in Ocampo et al., 2016 (Figure 2-19B). The example given is for nucleosome spacing on *SSK22* in the wild type (Figure 2-19B). From there we calculated a cross-correlation (r) between the Gaussian distribution and the nucleosome spacing of each gene. A higher cross-correlation indicates that the spacing of the gene is closer to the one given by the regular Gaussian distribution, and therefore more regular. A lower cross-correlation indicates that the spacing of the respective gene is different from the Gaussian distribution and therefore less regular. We then plotted the cross-correlations of all genes (Figure 2-19C). Cross-correlation values for *Δisw1* and *Δpaa1* are close to the wild type, indicating that nucleosome spacing is unaffected by the single mutants. For *Δisw1 Δpaa1* however, cross-correlation values are slightly shifted to the left, indicating that nucleosome spacing is less regular in the double mutant than in the wild type.

The Gaussian distribution gives an idealized nucleosome repeat length (NRL) that can be used to calculate NRL for individual genes. We plotted the NRLs for all genes, as given by the Gaussian distributions to give an idea of average repeat length of all genes (Figure 2-19D). This showed that *Δisw1* and *Δisw1 Δpaa1* remain close to wild type spacing of 160 bp, whereas *Δpaa1* spacing is wider at around 170 bp.

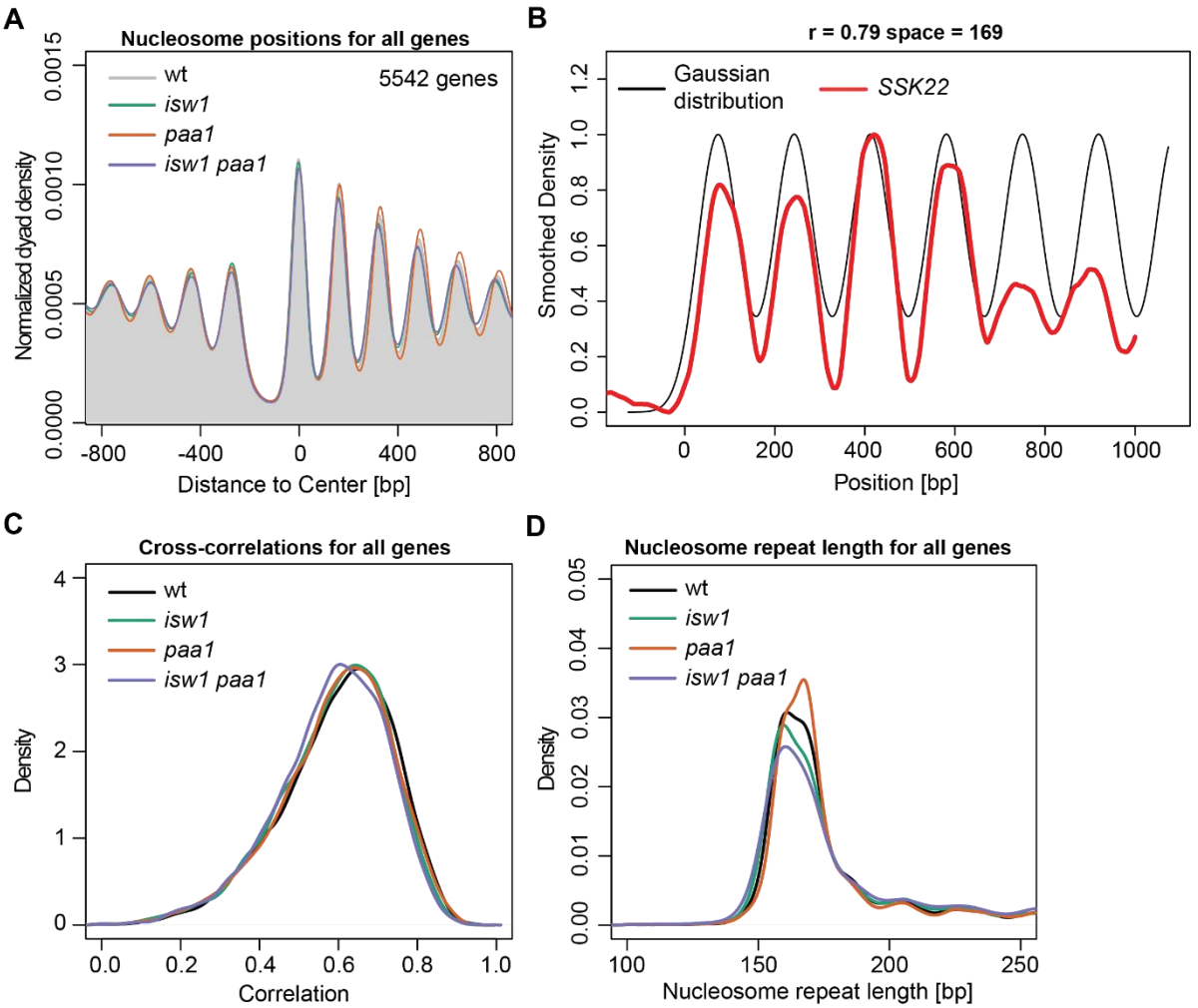

Figure 2-19: Nucleosome positions and repeat lengths for all genes. (A) Nucleosome positions of all genes, aligned to the +1 nucleosome position, as determined by Chereji et al., (2018). Positioning of wild type nucleosomes is shown as a grey background. The y-axis gives the dyad density, a readout for the number of nucleosomes found at any given position. Spacing tends to be more organized closer to the TSS, a fact reflected by the generally higher dyad density closer to the center. **(B)** Alignment of nucleosome positioning in *SSK22* to a periodic Gaussian distribution. Correlation coefficient (r) and spacing based off the Gaussian distribution are given (space). **(C)** Plotted cross-correlation values for all genes, as determined by correlation to Gaussian distributions. **(D)** Nucleosome repeat length for all genes.

We observed several effects on transcription in our RNAseq data. Different groups of genes are affected differently by *Δisw1 Δpaa1*. We used these same groups of genes to analyze in our MNase-seq data set.

2.4.1.1 Nucleosome positions of genes with cryptic promoter sites remain unaffected in Δisw1 paa1

Cryptic transcription is associated with increased histone turnover and higher acetylation levels of histones over ORFs. The insertion of acetylated histones leads to a loosening of chromatin structure, which makes cryptic promoter sites accessible to the transcriptional machinery. We plotted the dyad coverage of genes with known cryptic promoter sites to see if we could track these changes (Figure 2-20). Changes in dyad coverage could indicate that fewer nucleosomes can be found at this position. We could not observe any differences in dyad coverage for any of the mutants on *PCA1*, *SSK22*, *FLO8* or *STE11*. *Δisw1*, *Δpaa1* and *Δisw1 Δpaa1* were all comparable to wild type pattern (Figure 2-20).

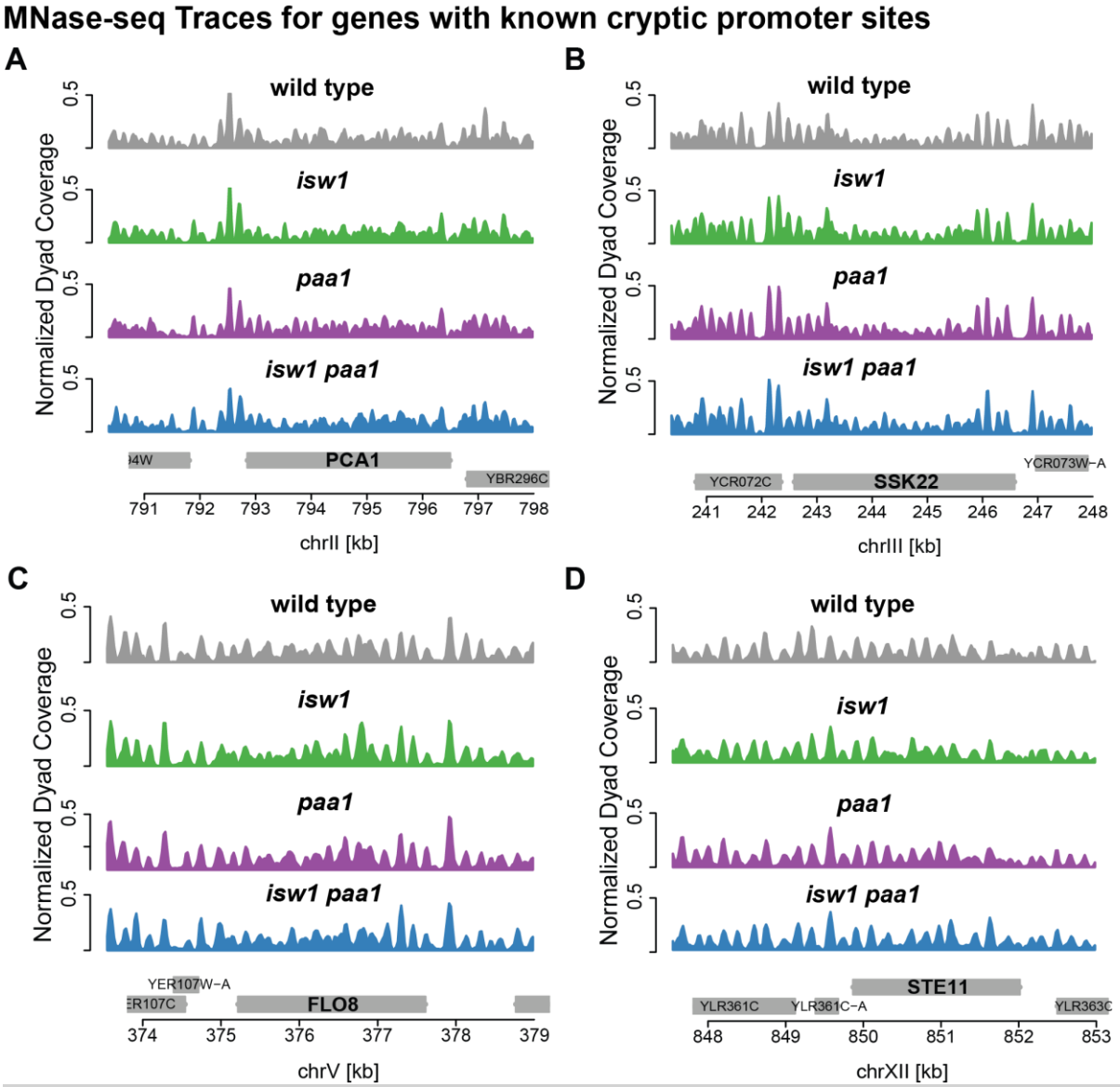

Figure 2-20: MNase-seq traces of four different genes with known cryptic promoter sites for wild type, *Δisw1*, *Δpaa1* and *Δisw1 Δpaa1*. (A) MNase-seq trace of the nucleosome pattern of *PCA1* for all four strains. Normalized dyad coverage for each strain is shown. **(B)** MNase-seq trace of the nucleosome pattern of *SSK22* for all four strains. Normalized dyad coverage for each strain is shown. **(C)** MNase-seq trace of the nucleosome pattern of *FLO8* for all four strains. Normalized dyad coverage for each strain is shown. **(D)** MNase-seq trace of the nucleosome pattern of *STE11* for all four strains. Normalized dyad coverage for each strain is shown. One representative replicate is shown for each.

2.4.1.2 Gene length has no effect on nucleosome spacing

When we looked at changes in expression of genes of different sizes, it was revealed that transcription in *Δisw1 Δpaa1* was generally increased compared to the wild type, independent of gene length (as observed in Figure 2-12). When looking at nucleosome positioning grouped by gene length, we could show that, in all cases, nucleosome positions are shifted away from the TSS in *Δpaa1* (Figure 2-21). This occurs in all genes, independent of length, although the effect is more pronounced for larger genes (Figure 2-21C and D). In *Δisw1 Δpaa1* and *Δisw1* nucleosome position are comparable to wild type for gene lengths smaller than 1000 bp (Figure 2-21A and B). Positions of nucleosome are shifted closer to the TSS for genes longer than 1000 bp in *Δisw1* and *Δisw1 Δpaa1*, although this shift is rather small (Figure 2-21C and D).

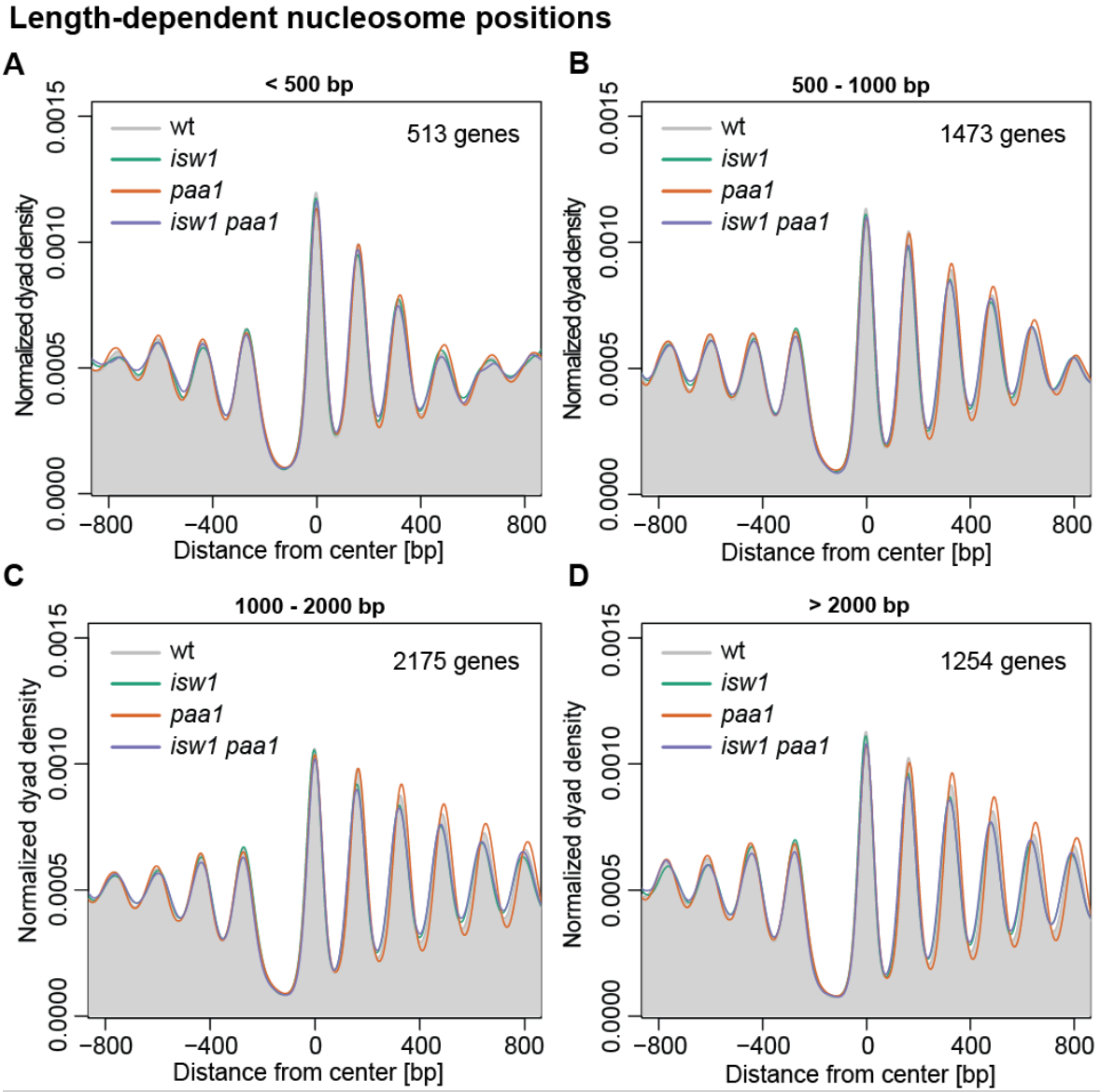

Figure 2-21: Nucleosome positions dependent on gene length. Positioning of nucleosomes aligned to the +1 nucleosome of each gene was determined as described by Chereji et al., (2018). Genes were grouped by length and the spacing compared for wild type, *Δisw1*, *Δpaa1* and *Δisw1 Δpaa1*. **(A)** Spacing for genes smaller than 500 bp. **(B)** Spacing for genes between 500 and 1000 bp. **(C)** Spacing for genes between 1000 and 2000 bp. **(D)** Spacing for genes larger than 2000 bp. The total number of genes is given for each group.

This becomes even more obvious when looking at nucleosome repeat lengths. NRLs for genes larger than 1000 bp have a second, higher peak in *Δpaa1* (Figure 2-22, bottom). Whereas genes smaller than 1000 bp in *Δpaa1* share about the same nucleosome repeat length as the wild type (Figure 2-22A). In *Δisw1 Δpaa1* and *Δisw1* nucleosome repeat lengths are comparable to wild type in all genes (Figure 2-22). Interestingly, this indicates that for *Δisw1 Δpaa1* and *Δisw1*, nucleosome repeat length remains unchanged with perhaps a small shift of nucleosome positions, while in *Δpaa1* both nucleosome repeat length and nucleosome positions have changed.

Length-dependent nucleosome spacing

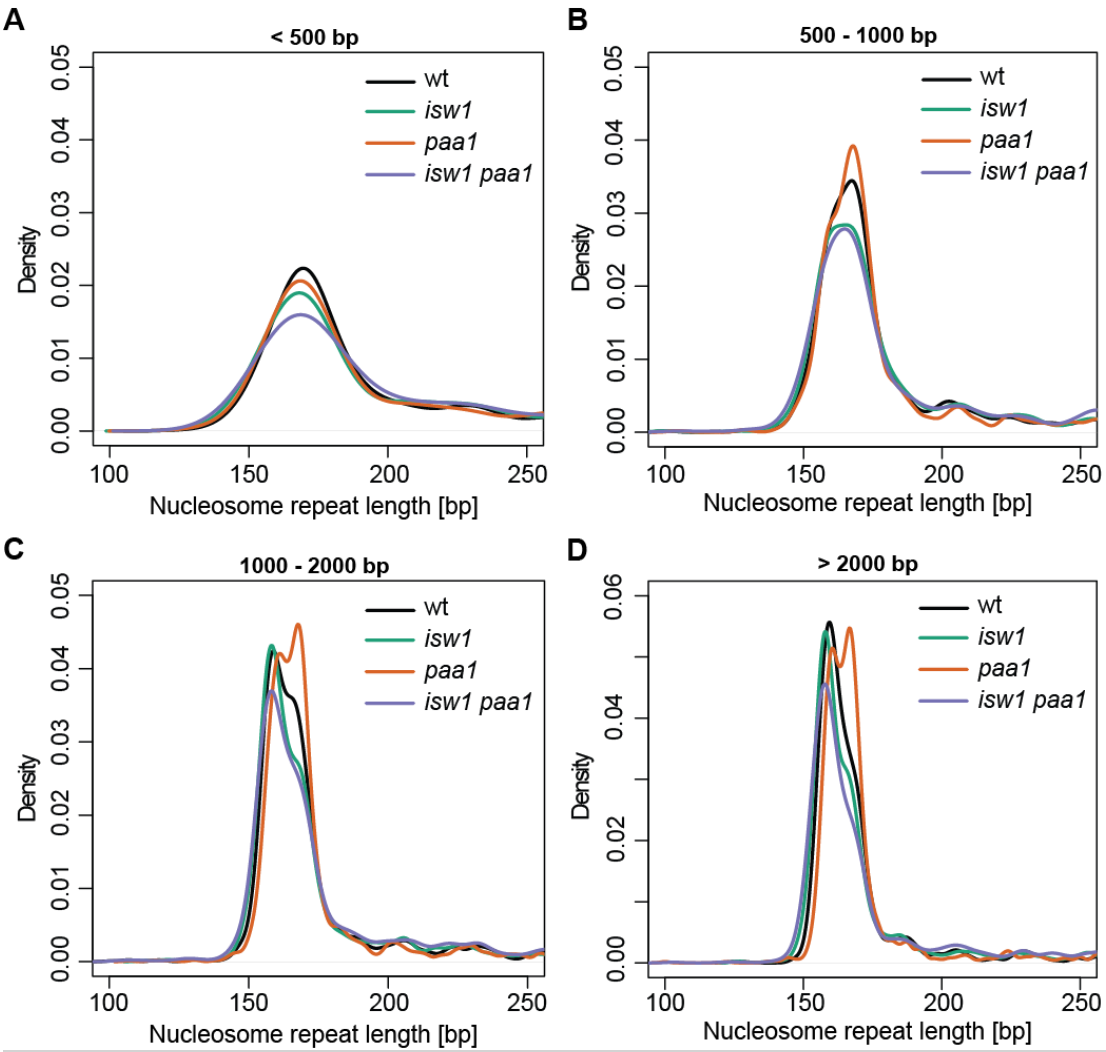

Figure 2-22: Nucleosome repeat length dependent on gene length. Nucleosome repeat length determined as described by Ocampo et al., (2016). Genes were grouped by length and compared for wild type, *Δisw1*, *Δpaa1* and *Δisw1 Δpaa1*. **(A)** Nucleosome repeat length for genes smaller than 500 bp. **(B)** Nucleosome repeat length for genes between 500 and 1000 bp. **(C)** Nucleosome repeat length for genes between 1000 and 2000 bp. **(D)** Nucleosome repeat length for genes larger than 2000 bp.

2.4.1.3 Genes with intermediate transcription rate have slightly changed nucleosome patterns

We could observe an interesting trend of transcription changes in our RNAseq data for genes with different native transcription rates. Transcription in *Δisw1 Δpaa1* compared to wild type was increased more in genes with low native transcription rates and decreased in genes with high native transcription rates in both sense and antisense direction (as observed in Figure 2-13).

Looking at the nucleosome patterns (Figure 2-23), we see the same trend repeated here. that we observed when looking at nucleosome positions in all genes. The positions of nucleosomes in *Δpaa1* are shifted away from the TSS. In *Δisw1* and *Δisw1 Δpaa1* there is no or a very small shift closer to the TSS compared to wild type positioning. However, in genes with a very low (< 1 mRNA/hr) or very high (> 50 mRNAs/hour) native transcription rate the pattern for *Δpaa1* is comparable to the wild type (Figure 2-23). Nucleosome positioning in *Δisw1* and *Δisw1 Δpaa1* was also mostly affected in genes with intermediate native transcription rates (1 - 5, 5 - 10 and 10 - 50 mRNA/hr) and less in genes with either very high or very low native transcription rates (Figure 2-23).

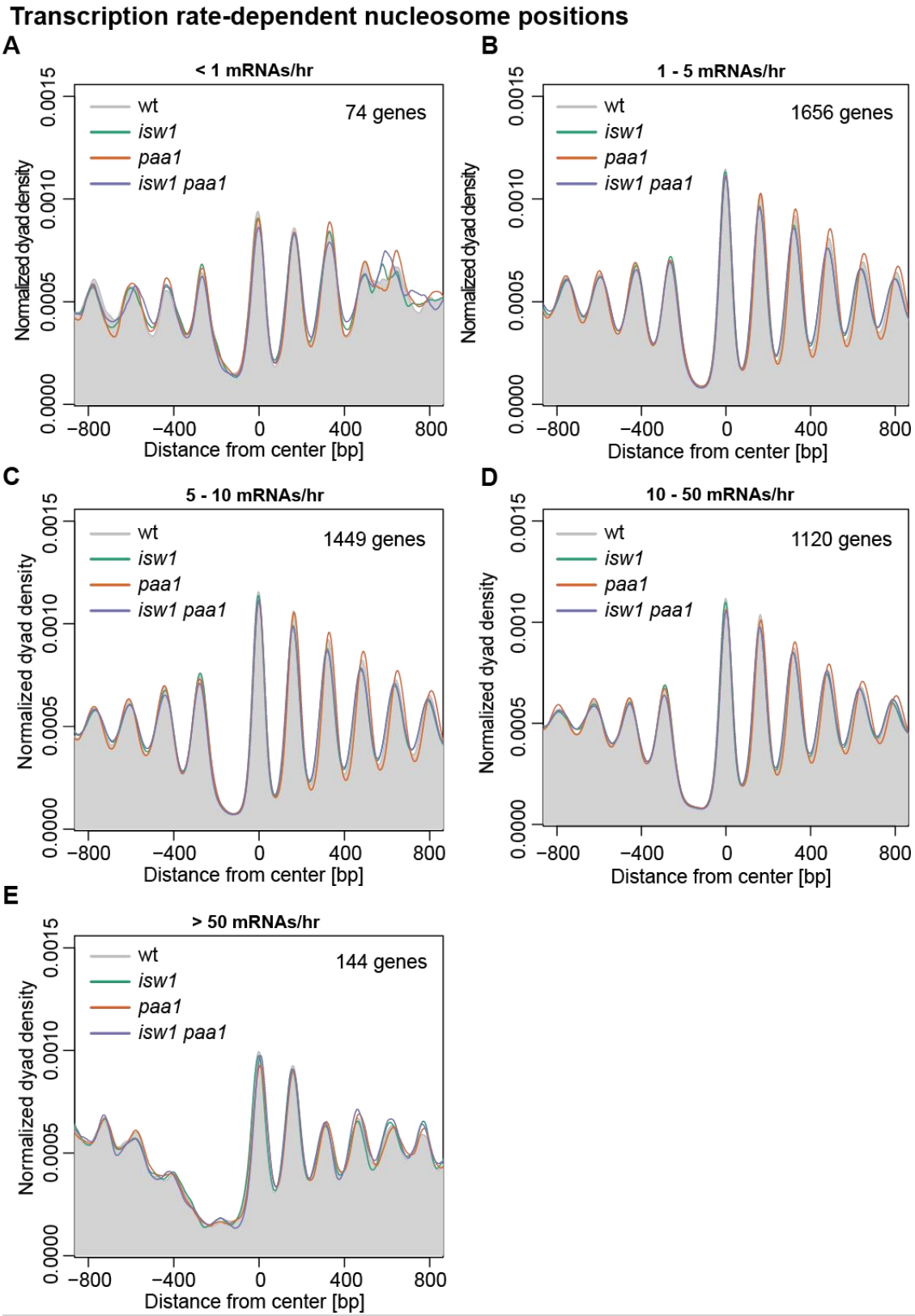

Figure 2-23: Nucleosome positions dependent on native transcription rate. Positioning of nucleosomes aligned to the +1 nucleosome of each gene was determined as described by Chereji et al., (2018). Genes were grouped by transcription rate and the spacing compared for wild type, *Δisw1*, *Δpaa1* and *Δisw1 Δpaa1*. **(A)** Spacing for genes with a transcription rate of < 1 mRNA/hr. **(B)** Spacing for genes with a transcription rate of 1 - 5 mRNA/hr. **(C)** Spacing for genes with a transcription rate of 5 - 10 mRNA/hr. **(D)** Spacing for genes with a transcription rate of 10 - 50 mRNA/hr. **(E)** Spacing for genes with a transcription rate of > 50 mRNA/hr. The total number of genes is given for each group.

Nucleosome repeat length in genes with low native transcription rate (< 1 mRNA/hr) is around the same size in all four strains, at around 170 bp (Figure 2-24A). For genes with a higher native transcription rate, only *Δpaa1* has a peak at this size (Figure 2-24). Although *Δpaa1* and the other three strains have an NRL at around 160 bp in genes with very high native transcription rates (> 50 mRNA/hr). It is interesting to note that there is a second, smaller peak in *Δpaa1* for genes with a native transcription rate between 5 and 50 mRNA/hr (Figure 2-24C and D), putting a large number of genes at a spacing length closer to wild type spacing.

In the wild type, *Δisw1* and *Δisw1 Δpaa1* the average NRL for all genes lies around 160 bp (Figure 2-24). Nucleosome repeat length in *Δisw1* is relatively close to that in wild type overall. Similar to what we observed in the length-dependent analysis, only *Δpaa1* seems to differ from wild type spacing, indicating that genes in this mutant are subject both to changes in positioning and spacing of nucleosomes. No changes of NRL could be observed for either *Δisw1* or *Δisw1 Δpaa1,* indicating that the difference in spacing we observed in Figure 2-23 is a result of a shift of the entire nucleosome arrays, as opposed to changes of individual nucleosome positions.

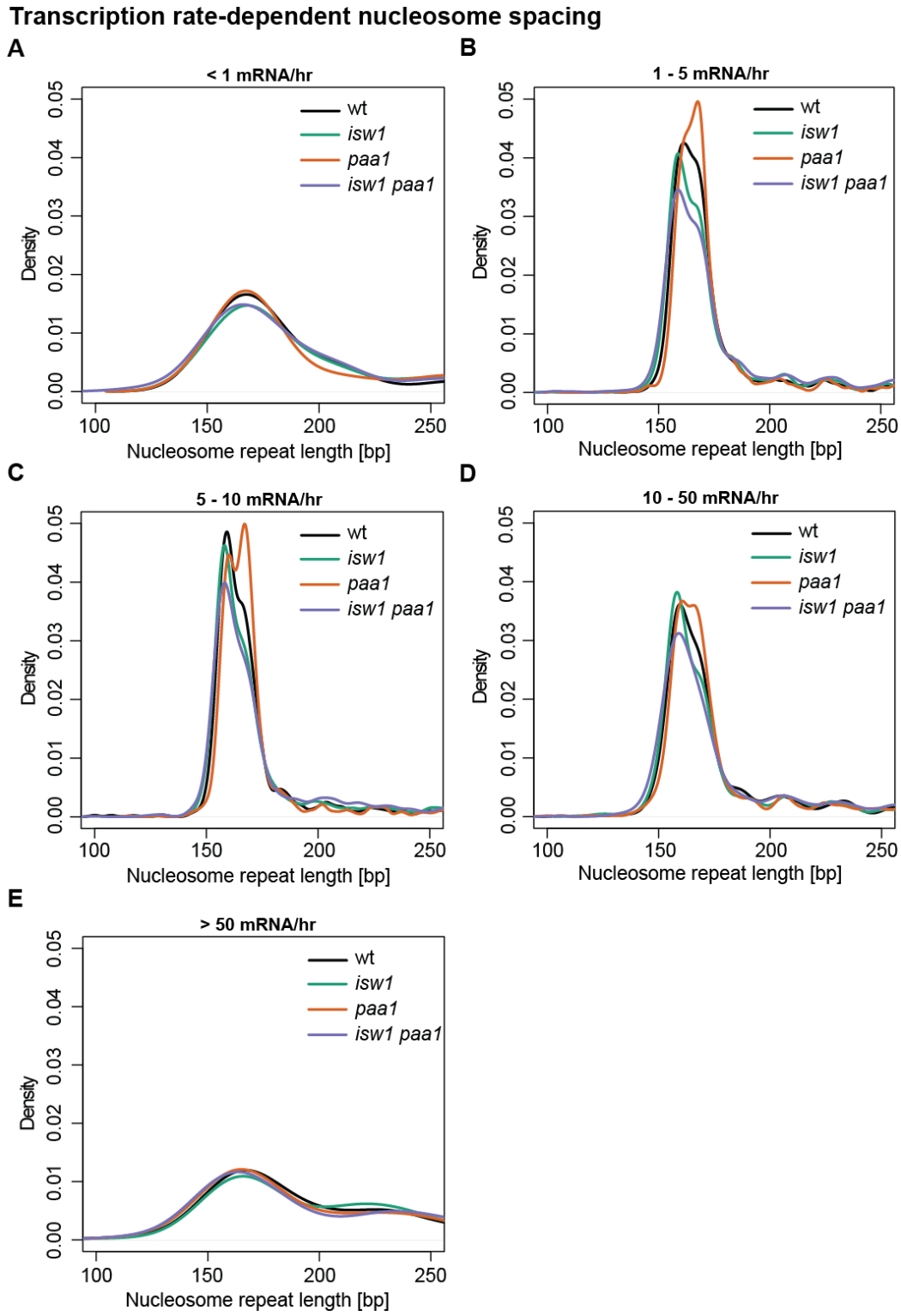

Figure 2-24: Nucleosome repeat length dependent on native transcription rate. Nucleosome repeat length determined as described by Ocampo et al., (2016). Genes were grouped by length and compared for wild type, *Δisw1*, *Δpaa1* and *Δisw1 Δpaa1*. **(A)** Spacing for genes with a transcription rate of < 1 mRNA/hr. **(B)** Spacing for genes with a transcription rate of 1 - 5 mRNA/hr. **(C)** Spacing for genes with a transcription rate of 5 - 10 mRNA/hr. **(D)** Spacing for genes with a transcription rate of 10 - 50 mRNA/hr. **(E)** Spacing for genes with a transcription rate of > 50 mRNA/hr. The total number of genes is given for each group.

2.4.1.4 Genes with no TATA have shifted nucleosome spacing in Δpaa1

Expression in sense direction was significantly increased in *Δisw1 Δpaa1* only for genes with a TATA box. Overall expression was much stronger affected for genes with a TATA box, with several genes being either significantly up- or-down regulated. Expression in antisense direction was affected independently of promoter type (as observed in Figure 2-14).

When looking at nucleosome positioning, we could observe no change in pattern in either *Δisw1* or *Δisw1 Δpaa1* compared to wild type in genes with a TATA box (Figure 2-25A, left). For *Δpaa1* we can observe a shift of the pattern away from the TSS for both TATA genes and genes without a TATA box (Figure 2-25A), which is consistent with previous observations. When looking at precise NRL, we can observe that for all strains, there is little change in repeat length compared to the wild type for genes with a TATA box (Figure 2-25B, left). The NRL for genes in *Δpaa1* is at around 170 bp, compared to the 160 bp of wild type repeat lengths (Figure 2-25B, right). Here, we can also observe a second, smaller peak for genes in *Δpaa1* that puts them closer to wild type spacing. Interestingly, there is also a small shoulder for wild type, *Δisw1* and *Δisw1 Δpaa1* at around 170 bp, which puts them close to the peak for *Δpaa1* (Figure 2-25B, right). This indicates that spacing is not uniform within TATA-lacking genes.

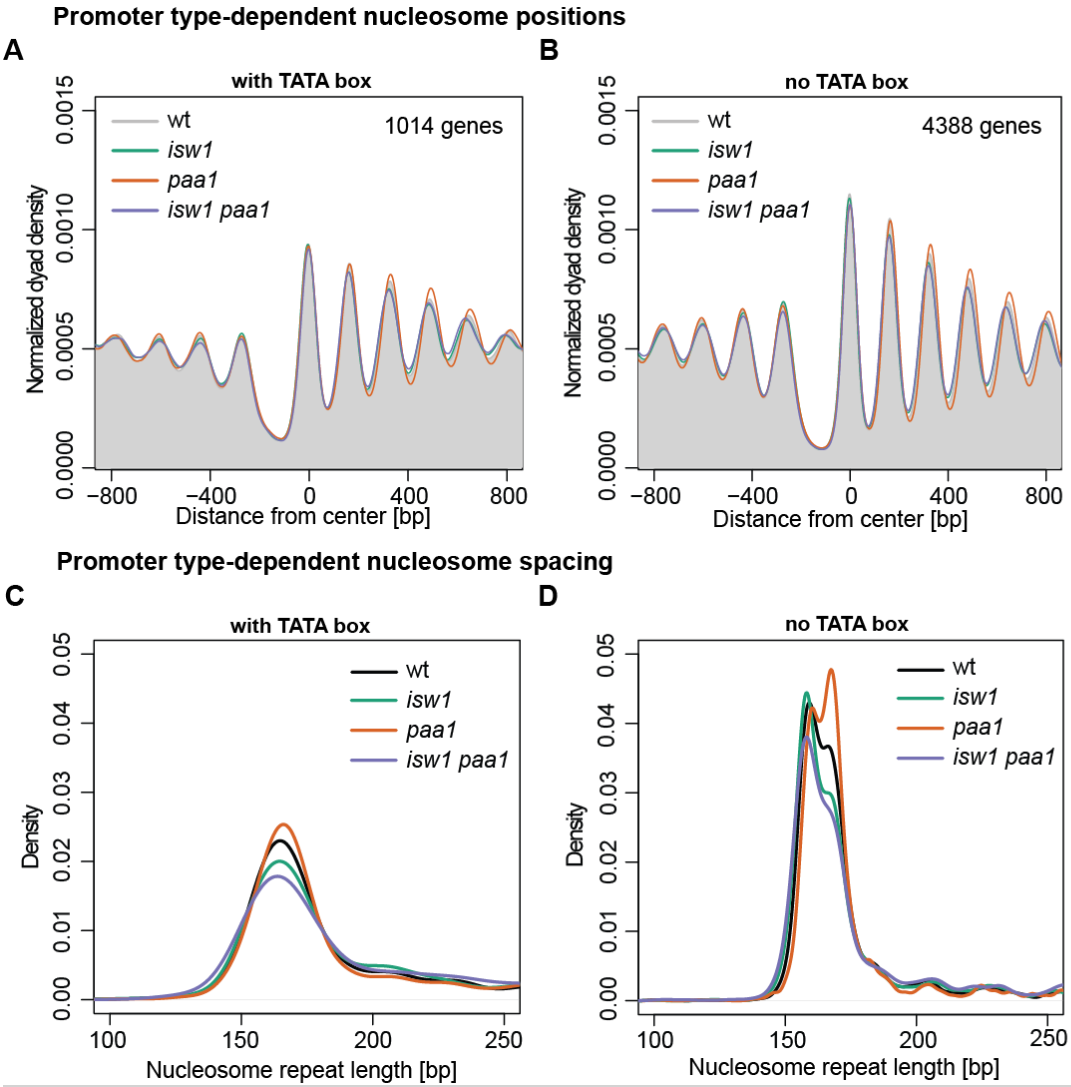

Figure 2-25: Nucleosome positions and repeat length dependent on promoter type. Genes were grouped by promoter type and the nucleosome positions compared for wild type, *Δisw1*, *Δpaa1* and *Δisw1 Δpaa1*. **(A-B)** Positioning of nucleosomes aligned to the +1 nucleosome of each gene was determined as described by Chereji et al., (2018). The total amount of genes is given for each group. **(C-D)** Nucleosome repeat length for genes grouped by promoter type was determined and plotted as described by Ocampo et al., (2016).

2.4.1.5 Ribosomal protein genes have the same nucleosome pattern as the rest of the genome

For ribosomal protein genes we could observe a significant decrease of transcription in sense direction and a less pronounced decrease of transcription in antisense direction (as observed in Figure 2-15). Repression of transcription of ribosomal protein genes is a common marker for stressed cells. Nucleosome positioning in ribosomal protein genes is only very marginally shifted away from the TSS in *Δpaa1* (Figure 2-26A). Conversely, nucleosome positioning in *Δisw1* and *Δisw1 Δpaa1* is the same as it is in wild type (Figure 2-26A). NRLs remain the same as in wild type for all three of the strains (Figure 2-26C). This indicates that the entire array of nucleosomes is shifted in *Δpaa1* as opposed to individual changes of nucleosome positions.

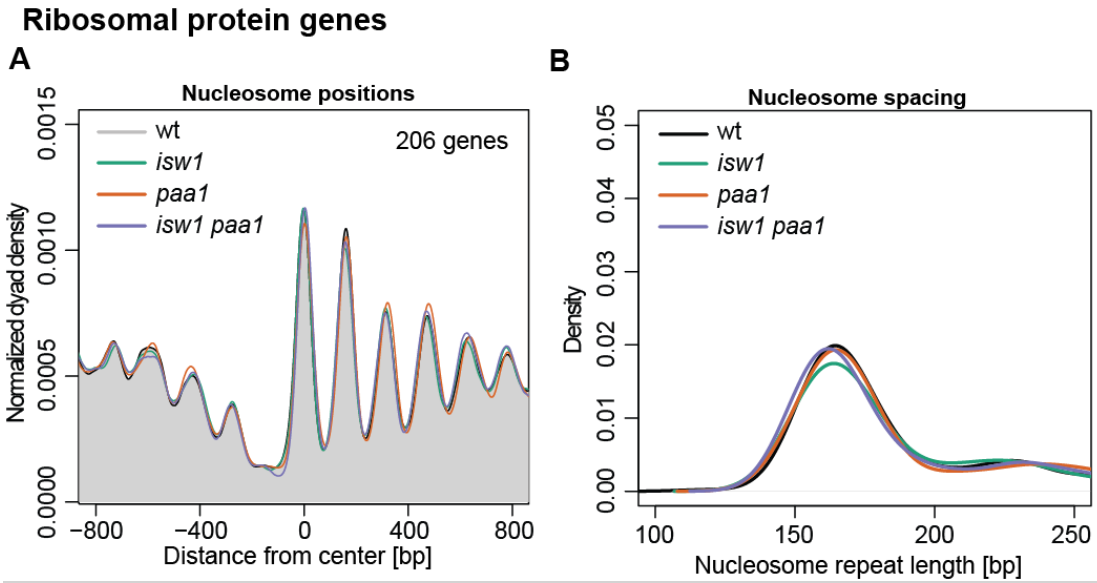

Figure 2-26: Nucleosome positions and repeat length for ribosomal protein genes. Nucleosome spacing was compared for wild type, *Δisw1*, *Δpaa1* and *Δisw1 Δpaa1*. **(A)** Nucleosome positioning for ribosomal protein genes in wild type, *Δisw1*, *Δpaa1* and *Δisw1 Δpaa1* centered on +1 nucleosome position. **(B)** Nucleosome repeat length for ribosomal protein genes was determined and plotted as described by Ocampo et al., (2016).

2.4.1.6 Genes with increased histone turnover upon deletion of Δisw1 *have the same nucleosome pattern as the rest of the genome*

We also examined genes that showed an increase of histone turnover in *Δisw1* in (Smolle et al., 2012). Here we could see a general increase in transcription in antisense direction for *Δisw1* and *Δisw1 Δpaa1*, but not *Δpaa1* (as observed in Figure 2-17). However, we could not observe changes of expression dependent on histone turnover rate.

When looking at nucleosome positioning, we can show that nucleosome positions in *Δisw1* and *Δisw1 Δpaa1* are shifted closer to the TSS than they are in the wild type, and nucleosome positions in *Δpaa1* are shifted away from the TSS compared to wild type (Figure 2-27B). When looking at NRLs, we can observe no difference in length in *Δpaa1* between genes with increased histone exchange and genes without increased histone exchange (Figure 2-27C and D). In both groups, the NRL is around 170 bp in length. The NRLs in *Δisw1* and *Δisw1 Δpaa1* are comparable to wild type.

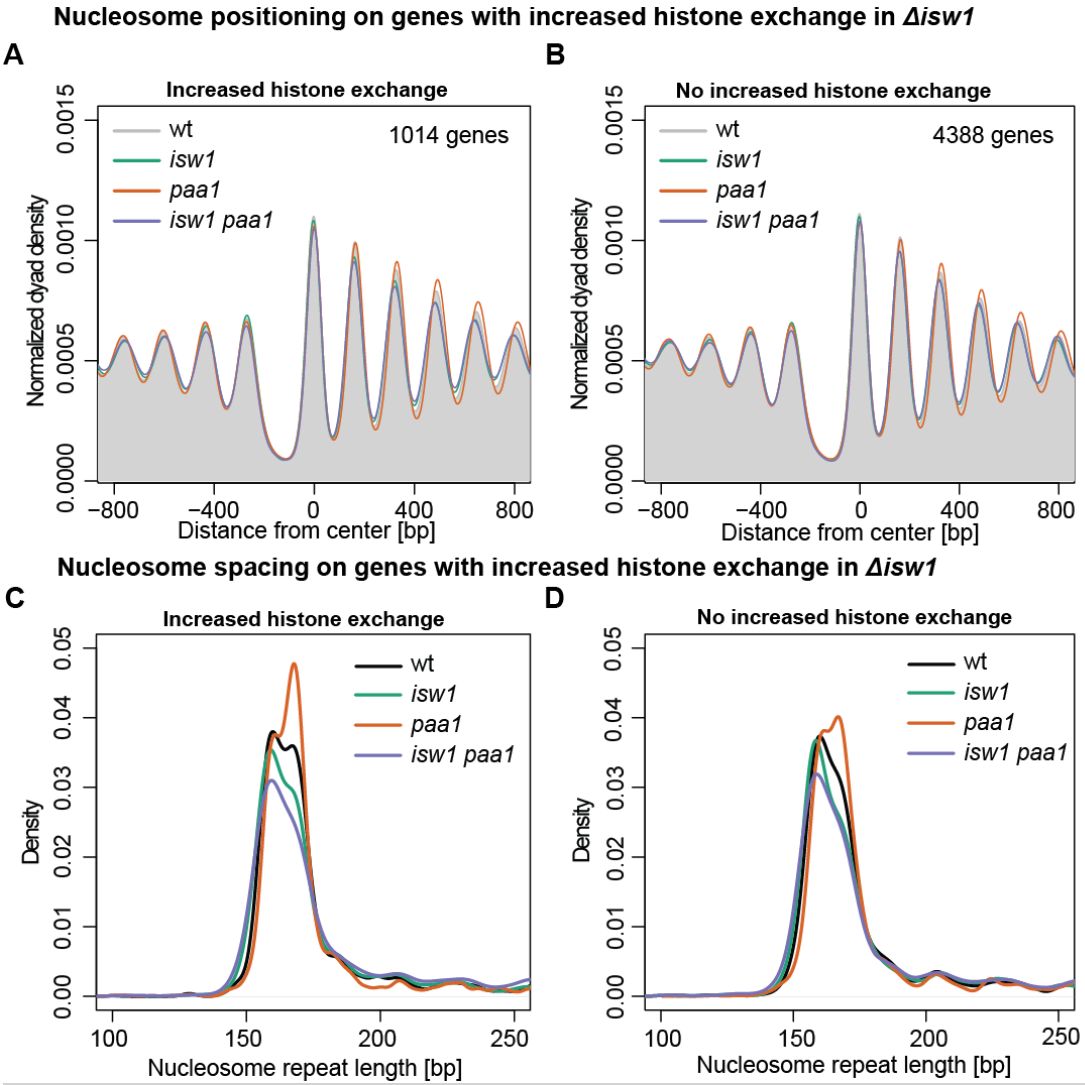

Figure 2-27: Nucleosome positions and repeat length for genes with increased histone turnover in *Δisw1*. Data sets of genes with increased histone exchange rates in *Δisw1* were obtained from Smolle et al., (2012). Nucleosome spacing was compared for wild type, *Δisw1*, *Δpaa1* and *Δisw1 Δpaa1*. **(A-B)** Nucleosome positioning for genes with increased histone turnover in *Δisw1* in wild type, *Δisw1*, *Δpaa1* and *Δisw1 Δpaa1* strains. The total amount of genes is given for each group. **(C-D)** Nucleosome repeat length for genes with increased histone turnover in *Δisw1* in wild type *Δisw1*, *Δpaa1* and *Δisw1 Δpaa1* strains was determined and plotted as described by Ocampo et al., (2016).

2.4.1.7 Nucleosome spacing in genes whose expression was significantly changed in Δisw1 Δpaa1 *is the same as genome-wide spacing*

We then decided to look at nucleosome positions in those genes that were significantly changed in overall transcription compared to wild type in our RNAseq experiments. Here we can show that, as before, nucleosome positions in *Δpaa1* are shifted away from the TSS, and nucleosome positions in *Δisw1* and *Δisw1 Δpaa1* are shifted towards the TSS. This is true for all genes, regardless if they are up or down regulated (Figure 2-28A and B). Interestingly, when looking at NRLs we can see very little difference between wild type and *Δpaa1* for both up and down regulated genes (Figure 2-28C and D). There is also no notable difference between wild type repeat length and *Δisw1* and *Δisw1 Δpaa1* (Figure 2-28C and D).

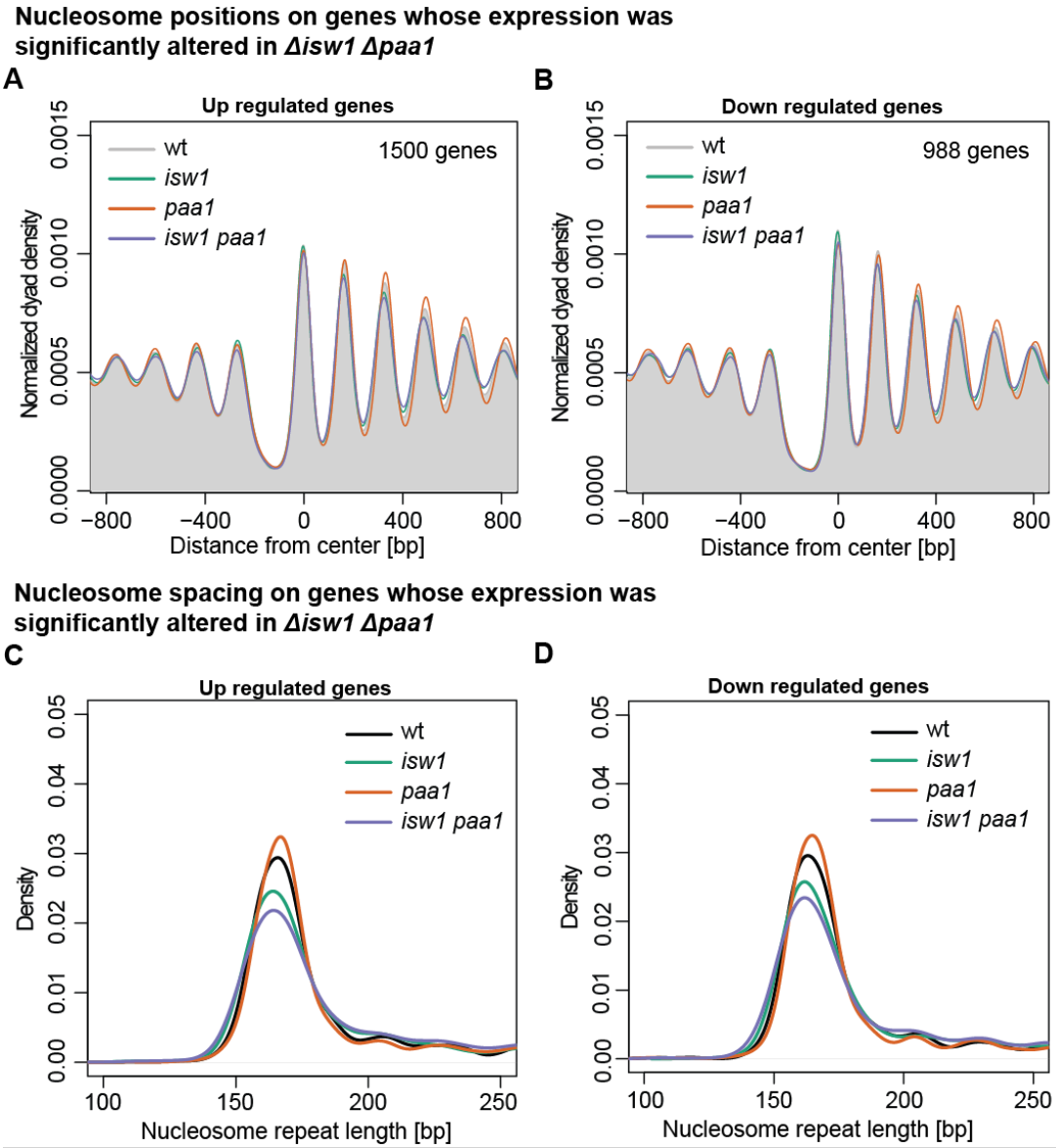

Figure 2-28: Nucleosome positions and repeat length for genes with significantly changed expression in *Δisw1 Δpaa1*. Data sets of genes with significantly changed expression in *Δisw1 Δpaa1* were obtained from our RNASeq data. Nucleosome spacing was compared for wild type, *Δisw1*, *Δpaa1* and *Δisw1 Δpaa1*. **(A-B)** Nucleosome positions for genes with significantly changed transcription in *Δisw1 Δpaa1*, separated by up and down regulation. Nucleosomes were aligned to +1 nucleosomes as described by Chereji et al., (2018). The total amount of genes is given for each group. **(C-D)** Nucleosome repeat length for genes with significantly changed expression in *Δisw1 Δpaa1* in wild type *Δisw1*, *Δpaa1* and *Δisw1 Δpaa1* strains was determined and plotted as described by Ocampo et al., (2016).

2.4.1.8 Nucleosome spacing in genes whose expression was significantly changed in Δpaa1 *is the same as genome-wide spacing*

We consistently observed a shift and widening of nucleosome spacing for all genes in *Δpaa1*. We therefore decided to take a look at genes whose expression was significantly changed in *Δpaa1*. Here it does not seem that nucleosome positions are changed in any of the mutant strains compared to wild type, although due to the small number of genes analyzed, the overall pattern is less smooth (Figure 2-29A and B). This trend is confirmed when looking at nucleosome spacing, as the peaks of all curves align with the peak of the wild type curve, putting the NRLs of all genes at about the same number (Figure 2-29C and D).

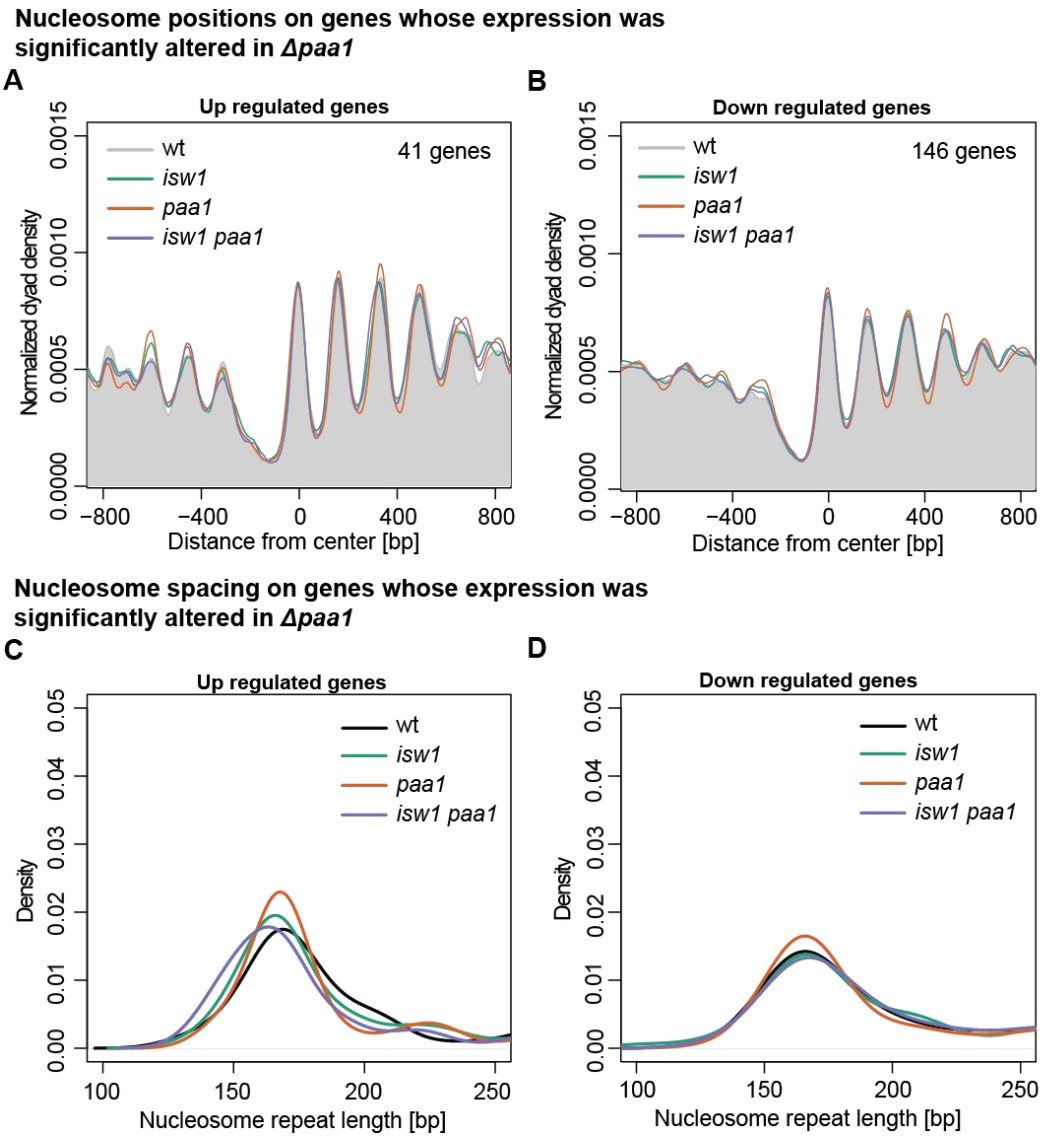

Figure 2-29: Nucleosome positions and repeat length for genes with significantly changed expression in *Δpaa1*. Data sets of genes with significantly changed expression in *Δpaa1* were obtained from our RNASeq data. Nucleosome spacing was compared for wild type, *Δisw1*, *Δpaa1* and *Δisw1 Δpaa1*. **(A-B)** Nucleosome positions for genes with significantly changed transcription in *Δpaa1*, separated by up and down regulation. Nucleosomes were aligned to +1 nucleosomes as described by Chereji et al., (2018). The total amount of genes is given for each group. **(C-D)** Nucleosome repeat length for genes with significantly changed expression in *Δpaa1* in wild type *Δisw1*, *Δpaa1* and *Δisw1 Δpaa1* strains was determined and plotted as described by Ocampo et al., (2016).

2.4.1.9 Summary of RNA-sequencing results

Most changes occur for *Δpaa1*. The NRL for *Δpaa1* increases over a large number of genes compared to the wild type by up to 10 bp. However, there are barely any changes in transcription for *Δpaa1*. Deletion of *PAA1* does cause higher polyamine levels in yeast (Casero and Pegg, 1993), and we can assume that the changes in nucleosome repeat length is due to that. In *Δisw1 Δpaa1* the deletion of *ISW1* rescues the phenotype of longer NRLs in *Δpaa1*, leading to NRLs similar to wild type. However, there are a lot of changes in transcription in both sense and antisense direction. It seems that the nucleosome arrays are not affecting transcription or affect changes of transcription.

3 Discussion

3.1 There is no significant physical interaction between ISWI remodelers and Paa1

There is no interaction between Paa1 and either the Ioc3 or Ioc4 subunits (Figure 2-1B-D), but we observed weak interactions between Isw1 and Paa1 in our Co-IP experiments. However, unspecific binding could be observed in the negative control (Figure 2-1A). Therefore, we used a Bio-ID-based assay in order to assess more transient interactions.

The Bio-ID super shift assay is very sensitive and capable of detecting more transient interactions. In fact, it has been observed by Fernandez-Suarez et al., (2008) that the background biotinylation is high on AP, due to the high affinity of AP to the biotin ligase BirA. The yeast biotin-apoprotein ligase encoded by *BPL1* has also been shown to share functional similarities with *E. coli* BirA (Cronan and Wallace, 1995) and could potentially biotinylate AP as well. We reduced this background biotinylation by growing the strains in biotin-depleted media and only added biotin prior to blotting. We can clearly show that there is no interaction between Isw1, Ioc3 or Ioc4 and Paa1 (Figure 2-2).

3.2 Characterization of genetic interaction between ISW1 and PAA1

We undertook several experiments to determine the genetic interactions between *ISW1* and *PAA1*. Genetic interaction between two genes can reveal functional relationships between these genes or their products (Mani et al., 2008). Two types of genetic interactions have been described, epistatic and synthetic interactions. Synthetic interaction describes the relationship between two genes and their products in different pathways. The combined effect of deleting both genes will be more severe compared to the effect of single deletions. This can lead to several synthetic effects, that only occur when two genes are deleted, but are absent if only one of the genes is deleted. Epistatic interactions occur when two genes of the same pathway are deleted and therefore are characterized by no added effect in the double deletion compared to single deletions. Depending on the precise nature of the functional relationship between two genes, this may also lead to the double deletion rescuing the phenotype of one of the single deletions. This makes genetic interaction studies a useful tool to understand the functional relationship between two genes or their products.

3.2.1 Phenotyping of *Δisw1 Δpaa1* revealed respiratory deficiency

In our phenotyping studies we observed several synthetic genetic interactions between *ISW1* and *PAA1*. Growth in *Δisw1 Δpaa1* was severely impeded even on rich media. This effect was increased on media with galactose or raffinose as a carbon source (Figure 2-5C). Growth on carbon sources other than glucose causes de-repression of several genes important for cellular respiration. This means that strains grown on media other than glucose require a more robust respiratory system. Lack of growth on media with galactose or raffinose as carbon sources can indicate respiratory defects (Hampsey, 1997). Indeed, when we grew the double deletion mutant on media with lactate or glycerol as carbon source, the strain was not able to

grow on either media (Figure 2-6). This inability to grow is an indication of failure to produce respiratory-competent mitochondria (Tzagoloff and Dieckmann, 1990).

We did attempt to further determine if the respiration defects might be due to a ρ^0 phenotype of *Δisw1 Δpaa1*. Strains with a ρ^0 phenotype have been depleted of mitochondrial DNA, leading to respiratory defects in these strains. Cross of a wild type ρ^0 strain with *Δisw1 Δpaa1* leads to rescue of the ρ^0 phenotype, if *Δisw1 Δpaa1* has functional mitochondria. Alternatively, the phenotype cannot be rescued because *Δisw1 Δpaa1* is also lacking mitochondrial DNA. Unfortunately, results from these crossing experiments remained inconclusive and did not reveal further insights, as crossing was unsuccessful (data not shown).

3.2.2 *Δisw1 Δpaa1* has improved resistance to high salinity

Growth under control conditions is impaired for *Δisw1 Δpaa1*, but growth on YPD media with NaCl had been recovered, especially compared to growth of the single *Δpaa1* mutant. Growth of *Δpaa1* on NaCl is inhibited, compared to wild type growth (Figure 2-3). Growth on NaCl is commonly used to score for resistance to high salinity and osmotic stress (Hampsey, 1997).

Growth on KCl, another indicator for osmotic stress resistance, is not inhibited for *Δpaa1*, indicating specific sensitivity of *Δpaa1* to NaCl in particular. It has been shown previously that growth on NaCl leads to vacuolar fragmentation in *Δisw1* and *Δpaa1* (Michaillat and Mayer, 2013). This indicates that the effect we observe for *Δpaa1* on NaCl might be caused by vacuolar fragmentation, as it does not occur on KCl. However, growth of *Δisw1* is unaffected by NaCl. Growth of the double mutant on media containing NaCl is improved compared to growth on control media and to growth of the single mutants. This indicates that *Δisw1* can rescue the growth defect of *Δpaa1* on NaCl, although we cannot determine the precise nature of the process.

3.2.3 *Δisw1 Δpaa1* is deficient for DNA replication

Single deletion of *PAA1* also shows growth defects on hydroxyurea, a phenotype also previously described by (Liu et al., 2005). We could confirm this phenotype in our experiment (Figure 2-3). This phenotype is further exacerbated in *Δisw1 Δpaa1* cells, to a point where the strain is incapable of growth. Hydroxyurea leads to the arrest of cells at the G1/S-phase checkpoint, by preventing the accumulation of dNTPs, which are required for transition into S-phase (Koc et al., 2004). Sensitivity to hydroxyurea is an indicator for strains that are defective in DNA replication. For *PAA1* it has been observed that it shows genetic interactions with *RAD53*, a gene that is essential for the S-phase checkpoint (Liu et al., 2005). The phenotype caused by *rad53-21* mutation is greatly exacerbated by additional deletion of *PAA1*. Liu et al., (2005) have also shown that the increase of polyamine levels on chromatin might directly influence replication. More polyamines binding DNA possibly increases the burden already imposed by hydroxyurea, therefore exacerbating sensitivity to HU. This would also explain the slow growth phenotype of *Δisw1 Δpaa1*.

In fact, *PAA1* also shows genetic interaction with several genes that indicate *PAA1* plays a role in transcriptional repression. Specifically, *PAA1* displayed genetic interactions with

GCN5 and *SPT8*, both encoding proteins that are part of histone acetyltransferase complexes important for transcription activation. This is thought to be an effect of changes in polyamine levels upon deletion of *PAA1*. Loss of Paa1 leads to accumulation of unacetylated polyamines, which are then able to bind chromatin at higher levels. This increased binding to chromatin leads to a further slowing of replication, exacerbating the effect of hydroxyurea in *Δpaa1* (Liu et al., 2005). Further removal of remodeler ISWI increases the burden, leading to a worsening phenotype. This result sits opposed to our previous observations, were removal of Isw1 lead to an improvement.

Polyamine levels have complex effects on chromatin. Low polyamine levels stimulate histone acetylation, whereas high levels inhibit acetylation (Burgio et al., 2016). For *Δpaa1* we cannot observe a large effect on overall transcription. For *Δisw1 Δpaa1* we see great changes in both directions. This can be explained by Isw1 generally having a repressive effect on transcription, therefore deletion of *ISW1* leads to increase of transcription. This phenotype is exacerbated by deletion of *PAA1*. It seems, the interplay between remodeler and polyamine levels is more complex than previously assumed.

3.3 Cryptic transcription is increased in *Δisw1 Δpaa1*

Another phenotype we could observe is that of cryptic transcription. In wild type cells, cryptic transcription is repressed due to the activities of remodelers Isw1b and Chd1. Together they retain K36me3 hypoacetylated histone H 3 in the wake of RNAPII. These histones have reduced levels of acetylation that leads to stronger interactions between histones and DNA. This maintains a tight chromatin structure, and subsequently prevents the activation and expression from cryptic promoter sites that can be found in the ORF of certain genes (Carrozza et al., 2005). H3K36me3 is also recognized by the histone deacetylase complex Rpd3S which then removes acetylation marks from surrounding histones. This increases compaction of chromatin and prevents cryptic transcription (Carrozza et al., 2005; Keogh et al., 2005; Joshi and Struhl, 2005) Around 20% to 30% of genes possess such a cryptic promoter site (Venkatesh et al., 2016).

It has been previously observed that in a mutant lacking both Chd1 and Isw1, the suppression of cryptic transcription is perturbed and cryptic promoters are active (Smolle et al., 2012). During transcription in this strain, the K36me3 hypoacetylated histones are no longer retained, and instead new histones with acetylation marks are incorporated into chromatin. This leads to a loosening of chromatin structure and increased accessibility of cryptic promoter sites. A comparable effect can be observed in a single Δisw1 mutant, albeit to a weaker extent.

We investigated several different genes for cryptic transcription using two separate methods. In the first method we used a reporter strain showing cryptic transcription on *FLO8*, in the second method we utilized northern blots to examine cryptic transcription on PCA1 and *SSK22*. Cryptic transcription is increased in the *Δisw1 Δpaa1* mutant on all of our target genes, *FLO8* (Figure 2-5A), *PCA1* and *SSK22* (Figure 2-7). This effect is stronger than it is in the single mutant *Δisw1*. This indicates a synthetic interaction between *ISW1* and *PAA1*, as the combined effect of their deletion is stronger than the individual deletions. Effects of deletion

mutants on cryptic transcription were more easily shown by northern blotting, which is therefore the focus of our cryptic transcription studies.

Cryptic transcription on *PCA1* and *SSK22* occurred in *Δisw1 Δpaa1*.Deletion of *ISW1* alone has been previously shown to increase cryptic transcription of *PCA1* and *SSK22* (Smolle et al., 2012). Isw1 is the catalytic subunit of two separate complexes. Deletion of *ISW1* removes both complexes.

Deletion of either *IOC2* or *IOC3* abrogates formation of the Isw1a and Isw1b remodelers respectively. Hence an *Δioc2 Δioc3 Δpaa1* mutant strain would be expected to mimic the phenotype of the *Δisw1 Δpaa1* mutant. However, we could not observe such an effect. This could have several causes. Isw1 might be acting on its own, as has been previously shown by Mueller and Bryk, (2007), who have observed Isw1 to regulate transcriptional silencing on ribosomal DNA. Also, since Isw1 carries the catalytic subunit the effect may be stronger, because of potential residual recruitment to some target sites, even without Ioc subunits. It also seems as though Isw1a plays a potential role in suppression of cryptic transcription, as seen for *SSK22* in the *Δioc3* mutant, also based on other unpublished observations from the lab. In the future, a new protocol will be used in the lab to look at antisense transcription by qPCR at sets of ten different genes, to reassess the effects of *Δioc2* and *Δioc3* in a *Δpaa1* background. The change in cryptic transcription is therefore specifically caused by absence of Isw1 alone.

On *SSK22*, deletion of *IOC3* leads to an almost *Δisw1 Δpaa1* like increase of cryptic transcription. This effect is not influenced by additional deletion of *PAA1* or *IOC2* (Figure 2-8B and D). Absence of Ioc3 means absence of Isw1a, but might also free up more of Isw1 to form more Isw1b complexes. It is difficult to say at this point, if the effect we observe is because of either change in remodeler concentration or a combined effect of both.

Isw2 is a functional homolog to Isw1 and Chd1, while belonging to a different family has overlapping functions with Isw1. Neither *Δchd1* nor *Δisw2*, however show any combinatorial effect with *Δpaa1*, making this effect strictly specific to *ISW1*. It is clear however that changes of cryptic transcription are specific for each transcript and are likely dependent on several different factors. Very little is known so far about the function of cryptic transcripts. It is known that some cryptic transcripts are in fact translated into peptides, but the function of these peptides is unknown (Cheung et al., 2008). Cheung et al., 2008 also observed an increase of cryptic transcription for wild type yeast strains when grown on SD medium compared to YPD.

Some cryptic transcripts have been tied to stress response, in particular heat stress response (Garcia-Martinez et al., 2012). Garcia-Martinez et al., 2012 have observed an increase of cryptic transcription in certain genes upon heat stress, although evidence points to this being a response to changes in mRNA stability rather than a direct effect of heat shock exposure. The double deletion of *ISW1* and *PAA1* causes significant stress for the cell. It is possible that increase of cryptic transcription might also be an indirect effect of this stress, rather than a direct response.

Other functions of non-coding transcripts have been previously discovered. Such as regulation of *IME4* by antisense strand encoded *RME2* (Hongay et al., 2006), or the expression of *IME1* by *IRT1* (van Werven et al., 2012).

3.4 Analysis of genome-wide expression levels

From the northern blots in 2.2.4 we observed a general effect on transcription in *Δisw1 Δpaa1*, when investigating cryptic transcription. Full-length transcription of *PCA1* was increased in *Δisw1 Δpaa1*, whereas canonical transcription of *SSK22* was unaffected. This indicates a selective effect of transcription regulation on certain genes. We performed strand-specific RNA-seq to get an overview of changes in gene expression in *Δisw1 Δpaa1* in both sense and antisense direction. We evaluated expression in the double and single mutants as $\log_2$ fold changes of wild type expression. This gives us a good understanding of which genes are changed in expression in these specific mutants. This somewhat mirrors the results we have seen for our analysis of cryptic transcription.

3.4.1 Transcriptional changes are strongest in *Δisw1 Δpaa1*

Expression in the double mutant is affected the strongest, with the majority of changes leading to upregulation of transcription. There is a higher number of up-regulated genes than down-regulated genes (Figure 2-10).

Deletion of *PAA1* affected relatively few genes. Regarding canonical sense transcripts, 76 genes were up- and 62 genes were down-regulated. Also, no large effect on antisense transcription could be observed. As expected, *Δisw1* mutant showed a large number of genes (982) with increased antisense transcription. There were also 180 genes with increased sense transcription in *Δisw1* (Figure 2-10). We know from previous studies that Isw1 and Chd1 are important for long genes with a low transcription rate in order to prevent antisense transcription. We can observe a similar effect here for *Δisw1*, as there is more antisense transcription for long genes and genes with low transcription rates (Figure 2-12B and Figure 2-13B).

For the double mutant there are overall massive changes of transcription. Canonical sense transcripts especially up-regulated transcripts (287), but also down-regulated transcripts (516) are affected. Similarly, antisense transcription has undergone massive changes, with a large number of up-regulated transcripts (1253). Many of these transcripts overlap with genes that showed changes in *Δisw1* (Figure 2-10). The effect of the double mutant is more widespread and more varied than the single deletion. We cannot identify individual groups, based on, for example, gene length or transcription rate that had a specific effect on transcription. Mostly *Δisw1 Δpaa1* leads to much more variation in sense transcription related to wild type and to increased antisense transcription everywhere else we look. Only ribosomal proteins genes are significantly down-regulated, consistent with the fact that the cells are under immense stress. For the double mutant at least, it seems as though most antisense changes occur on genes that are also affected in sense direction (Figure 2-18).

A change of nucleosome occupation could explain the changes in transcription we observed. We could not detect any difference in transcription on genes with increased histone

exchange rate when compared to genes with no change in histone exchange rate (Figure 2-17). This indicates that it is not the change in histone turnover that causes transcriptional changes.

3.4.2 Stress-related changes of expression

Expression of ribosomal protein genes is down regulated in *Δisw1 Δpaa1* (Figure 2-15). This is commonly a sign of stressed cells. Growth of *Δisw1 Δpaa1* is severely impaired even on rich media. The double mutant is defective in respiration and DNA replication. Stress might be a compounding factor influencing genome-wide transcription levels. Expression of ribosomal protein genes was unaffected in either of the single mutants and neither of these strains showed decreased respiratory competence. The increased stress caused by respiratory defects, compounded by defective DNA replication could explain the changes of transcription in *Δisw1 Δpaa1*. It does not explain, however the changes of transcription in *Δisw1*. Previous analysis of transcriptional changes in an *Δisw1* mutant did not show changes stronger than twofold wild type (Vary et al., 2003). Although sensitivity of these experiments was reduced compared to RNAseq. One thing to note is that we generated mRNA by enriching for polyA-tails. This unfortunately leads to a loss of cryptic transcripts that do not possess a polyA tail. This means that many transcripts that are usually degraded quickly by the exosome, like CUTs, are lost completely (Goodman et al., 2013). Analysis of total ribo-depleted RNA may be useful to further shed light on this matter. Furthermore, the pervasive changes caused by the double mutant on a genomic level will also be investigated by the lab using metabolomics, along with the effect of polyamine levels in *Δisw1 Δpaa1*.

3.5 The effect of nucleosome pattern on transcription

Nucleosomes form arrays over gene bodies, many of which have a nucleosome depleted region near the promoter. This NDR is flanked by +1 and -1 nucleosomes. After the +1 nucleosome follows an evenly spaced nucleosome array along the gene body (Lee et al., 2007; Mavrich et al., 2008). These nucleosomes prevent access to DNA by transcription factors and therefore repress unfettered transcription. Active transcription requires sliding or eviction of nucleosomes, in order to free access to underlying DNA. Perturbation of this pattern can also lead to spurious transcription, particularly of cryptic promoter sites (Kaplan et al., 2003; Thompson and Parker, 2007). We hypothesized that changes in nucleosome spacing may correlate with changes of transcription we observed in our RNA-seq data.

3.5.1 Genome-wide analysis of nucleosome spacing revealed polyamine-dependent spacing

We could not detect any changes of nucleosome positioning in *Δisw1* compared to wild type positions. Conversely, in *Δpaa1* spacing of the nucleosome pattern is increased to 170 bp, compared to the 160 bp wild type spacing (Figure 2-19D). This shift of nucleosome repeat length is consistent throughout the entire data set and affects all genes, independent of class.

In *Δisw1 Δpaa1* the entire nucleosome array is moved closer to the TSS (Figure 2-19C). There was no change in average NRL, however. Interestingly, the double mutant does not show

the same effect as *Δpaa1*. This indicates that deletion of *ISW1* is capable of reinstating wild type spacing in a *Δpaa1* mutant.

It has been shown previously, that addition of polyamines to *in vitro* assays increases nucleosome repeat length (Blank and Becker, 1995). Activity of Paa1 leads to the breakdown of polyamines in the cell, therefore deletion of *PAA1* leads to the accumulation of polyamines (Casero and Pegg, 1993). This would explain the increase of spacing in *Δpaa1*. It has been found in mammals that repressed chromatin has increased NRLs compared to transcriptionally active chromatin (Thomas and Thompson, 1977; Villeponteau et al., 1992). This has been confirmed in yeast as well (Feng and Villeponteau, 1992; Norouzi et al., 2015). This would indicate that in a *Δpaa1* mutant transcription is repressed. Our results show neither an increase nor decrease of transcription in *Δpaa1*, therefore we cannot provide any supporting evidence for this observation.

3.5.1.1 The effect of polyamines supersedes the clamping activity of ISWI remodelers

It has been previously shown that nucleosome spacing generated by Chd1 and ISWI is independent of nucleosome density (Lieleg et al., 2015). The NRL generated by these two remodelers remains the same, giving ISWI and Chd1 a clamping activity. This would lead us to expect that spacing in any strain containing both these remodelers would remain comparable to wild type. However, as Ocampo et al., (2016) have shown, removal of each remodeler individually leads to different spacing and NRLs, depending on which remodeler is missing.

However, as we have found, spacing is increased in a *Δpaa1* mutant, despite both remodelers being present. There are several factors that could influence this change of spacing. For one, it has been shown that increase of polyamines *in vitro* also increases NRL (Blank and Becker, 1995). Second, repressed chromatin has increased NRL compared to transcriptionally active chromatin (Feng and Villeponteau, 1992; Norouzi et al., 2015). This might explain why NRLs were increased in *Δpaa1*, as it is less transcriptionally active than the double mutant. However, transcription in *Δpaa1* compares to wild type transcription, but the wild type does not have the same increase of NRL. Therefore, it is unlikely that the change in NRL is a result of repressed chromatin. The nucleosome repeat length in the presence of polyamines was determined *in vitro* and not in the presence of remodelers. It is unclear if this cation-dependent spacing supersedes remodeler activity. Our results suggest that at least in the case of ISWI, cations have a stronger effect.

3.5.1.2 Chd1 can take over spacing duty in the absence of Isw1

Ocampo et al., (2016) have shown that Chd1 and ISWI compete when it comes to spacing. Chd1 creates arrays with shorter spacing, whereas ISWI favors arrays with longer spacing. The combination of these two spacing factors results in an average spacing of about 165 bp observed over the entire yeast genome. Removal of one remodeler should change spacing in favor of the other. Removal of Isw1 would therefore lead to a decrease of nucleosome spacing. If we take the nucleosome positioning data alone, this would explain the effect we could observe. Spacing of *Δisw1* and *Δisw1 Δpaa1* seems to have shifted closer to the TSS (Figure 2-19). However, if looking at the precise nucleosome repeat lengths, we cannot observe any significant changes in

spacing. The NRL favored by ISWI is 160 bp, which only puts it at 5 bp smaller than the genome-wide average of 165 bp in the wild type. It is possible that the difference is simply too small to observe. *Δpaa1* on the other hand shows an increase of spacing, despite both remodelers being present. Polyamines accumulate in the absence of Paa1, leading to an increase of spacing, as observed by (Blank and Becker, 1995). This supports our previous assumption that the presence of polyamines supersedes remodeler activity. Yet, in *Δisw1 Δpaa1* polyamine presence does not affect spacing. This effect could be explained by activity of Chd1.

The functions of Chd1 and Isw1 overlap (Tsukiyama et al., 1999). In the presence of Isw1 and therefore both Isw1 complexes, *Δpaa1* still generates changes in spacing. This indicates that neither Isw1a nor Isw1b are capable of correcting the change in spacing generated by *Δpaa1*. In their absence Chd1 might be able to reinstate proper spacing. Chd1 is recruited to the CTD of RNAPII via its interaction with the PAF complex and therefore primarily associated with genes that are being transcribed (Simic et al., 2003; Quan and Hartzog, 2010).

Our nucleosome spacing data suggests that Chd1 takes over remodeling function in the absence of *Δisw1*, correcting the change of spacing that occurs in *Δpaa1*. More Chd1 is present in genes that are highly transcribed and therefore its activity would have a stronger effect on transcription. Similarly, lowly transcribed genes contain less Chd1 and therefore would be less affected. Interestingly, *Δisw1* does not follow the same pattern of transcriptional regulation dependent on native transcription rate. This means that the absence of Isw1, and subsequently the absence of both remodeler complexes, alone is not sufficient to substitute Chd1 activity for Isw1. That indicates that the absence of Paa1 also has an effect on remodeler activity, its absence leading to direct changes in transcription. This would also explain how *Δisw1 Δpaa1* can rescue growth on NaCl.

3.6 Conclusions and future perspective

We could not confirm physical interaction between Isw1 and Paa1. Instead, we identified largely synthetic genetic interaction between the two. These synthetic effects point towards replication defects and transcription changes.

We observed that deletion of both genes leads to synthetic growth effect on rich media for the double mutant. This might be a result of stress caused by the double deletion, as we could also show that *Δisw1 Δpaa1* leads to respiratory defects. Regarding replication defects, we could observe loss of growth on HU, which is a common marker for defective DNA replication.

Gene expression is also changed in the double mutants, as we could observe in our northern blot and RNAseq experiments. There are some milder effects in *Δisw1* as well, but the effect is stronger in the double mutant. Both cryptic and canonical transcription are affected.

The formation of nucleosome arrays is only affected in *Δpaa1* however, as we could show with our MNase-seq experiments. There are no large transcription changes in *Δpaa1*. Conversely, *Δisw1* and *Δisw1 Δpaa1*, where we could see changes in expression of canonical and cryptic transcripts, had no changes in nucleosome spacing. This is in somewhat contrast to

what has been observed in *Δisw1 Δchd1*, where there is a loss of arrays, but a strong increase of transcription.

One possible explanation could be changes of polyamine levels, which are affected by Paa1. It seems as though spacing is not responsible for the changes we observe. It could be that there are differences in nucleosome accessibility, which cannot be observed by MNase-seq. Other methods could be employed to examine nucleosome accessibility, for example assay for transposase-accessible chromatin (ATAC-seq). Alternatively, polyamines could play a role. In *Δpaa1* levels of polyamines are increased, which might have an effect on nucleosome spacing. To compare polyamine levels between the double mutant and *Δpaa1* the lab will perform metabolomics in the future. This should provide better understanding if polyamine levels are in fact responsible for changes in nucleosome spacing.

Δisw1 has increased levels of acetylated H4 over ORFs, caused by the loss of function of Isw1. Isw1 together with Chd1 prevents incorporation of hyperacetylated histones (Smolle et al., 2012). Given the large transcription changes in the double mutants, even compared to changes in *Δisw1*, it would be useful to determine levels of H4 acetylation in *Δisw1 Δpaa1* with ChIP-seq experiments. We would expect more histone acetylation compared to wild type, influenced by polyamine levels, or a direct effect of polyamine levels on chromatin organization. For example, as polyamines bind DNA, increase of polyamines could further influence chromatin organization. It is also possible that polyamine levels influence activity of HDAC.

To further understand if and how polyamines are responsible for these changes, additional experiments are necessary. Overexpression of polyamine synthases in the wild type should mimic *Δpaa1* in regards to polyamine levels. Conversely, overexpression of polyamine synthases in *Δpaa1 Δisw1* might be able to rescue the transcription phenotype. This should give confirmation if indeed polyamine levels are responsible for the observed effects.

Another approach is a catalytic dead mutant of Paa1. The polyamine levels should be the same as for *Δpaa1*. If it mimics the growth phenotypes and changes of transcription and nucleosome spacing, we observe in *Δpaa1* this would mean that indeed polyamines are responsible.

It would also be interesting to further examine the accessibility of chromatin. The overall accessibility could be determined with ATAC, which could give the precise sequence of nucleosome positions and give an overview of chromatin accessibility. Furthermore, it would be interesting to see what happens to histone turnover in a *Δpaa1* or *Δisw1 Δpaa1* mutant. This could be achieved by ChIP experiments for H3K56ac, since H3K56 can only be acetylated when histones are soluble and not already incorporated in chromatin.

Additionally, precision nuclear run-on sequencing (PRO-seq) and global run-on sequencing (GRO-seq) could show RNAPII positioning during transcription, which would give more insights into quickly degrading transcripts.

4 Materials and Methods

4.1 Materials

4.1.1 Chemicals

All chemicals and reagents used in this study, unless stated otherwise, were purchased from New England Biolabs, Sigma-Aldrich, BioRad, Invitrogen, VWR, Merck, Thermo Fisher Scientific or Roth.

4.1.2 Enzymes and Kits

DNA isolation and purifications were carried out using the mi-PCR Purification Kit (Metabion). Plasmid purifications were carried out using mi-Plasmid Miniprep Kit (Metabion). RNAseq library preparations were carried out with NEBNext® Ultra™ II Directional RNA Library Prep Kit for Illumina® (New England Biolabs) and polyA enrichment was carried out with NEBNext® Poly(A) mRNA Magnetic Isolation Module (New England Biolabs). NEBNext® Multiplex Oligos for Illumina® (Index Primers Set 1) (New England Biolabs) was used for both RNAseq and MNase-seq library preparations. All Kits were used according to manufacturer's instructions unless stated otherwise.

4.1.3 Escherichia coli (E. coli) cell culture

4.1.3.1 Grow up of E. coli

Bacterial cells were grown in Lysogeny Broth (LB) liquid media (0.5% (w/v) yeast extract, 1% (w/v) bacto-tryptone, 1% (w/v) NaCl) at 37°C at constant agitation. If grown on plates, 2% (w/v) agar was added to LB media. Media was autoclaved at 120°C for 15 minutes and 100 µg/ml ampicillin was added prior to use. Growth of *E. coli* was measured with a photometer to determine optical density at 600 nm. Bacteria strains used in this thesis are listed in Table 4-1.

Table 4-1: Bacterial strains used in this thesis

Strain	Genotype	Application
DH5α	F^- *endA1 glnV44 thi-1 recA1 relA1 gyrA96 deoR nupG purB20* Φ80d*lacZ*ΔM15 Δ(*lacZYA-argF)U169*, hsdR17(r_K-m_K+), λ-	Plasmid propagation

4.1.3.2 Transformation of E. coli

200 µl of chemically competent DH5α *E. coli* cells (Table 4-1) were thawed on ice. Mixed with approximately 100 ng of plasmid DNA and incubated on ice for 20 minutes. The cells were then heat shocked at 42°C for 45 seconds. 400 µl of LB-media without antibiotics were added, before 100 µl of the reaction were streaked on an LB-Amp plate. The plate was then incubated overnight at 37°C. Plasmids used to transform *E coli* are listed in Table 4-2.

Table 4-2: Plasmids used in this thesis

Name	Description	Marker in *E. coli*	Marker in *S. cerevisiae*	Reference
pFA6a-HIS3MX6	HIS3 deletion cassette	Amp	HIS3	Longtine 1998
pFA6a-kanMX6	KanMX deletion cassette	Amp	KAN^R	Longtine 1998
pFA6a-TRP1	TRP1 deletion cassette	Amp	TRP1	Longtine 1998
pSJ1348	mCherry-tagged Pus1	Amp	LEU2	Gifted by Sue Jasperson
pUG27	HIS5 deletion cassette	Amp	HIS5	Gueldener 2002
pUG72	URA3 deletion cassette	Amp	URA3	Gueldener 2002
pUG73	LEU2 deletion cassette	Amp	LEU2	Gueldener 2002
pYM-hphNT1	Hygromycin deletion cassette	Amp	hph	Janke 2004
pYM13-AP	AP-tagging cassette	Amp	KAN^R	Gifted by Matias Capella
pYM16 BirA-HA	BirA tagging cassette	Amp	HYG	Gifted by Matias Capella

4.1.4 *S. cerevisiae* cell culture

4.1.4.1 Growth of S. cerevisiae

S. cerevisiae cells were grown in Yeast extract–Peptone–Dextrose (YPD) liquid media (1% (w/v) yeast extract, 2% (w/v) peptone, 2% (w/v) glucose) at 30°C with constant agitation. If grown on plates, 2% (w/v) agar was added to YPD media. Media was autoclaved at 120°C for 15 minutes prior to use. Growth of *S. cerevisiae* was measured with a photometer to determine optical density at 600 nm. Parental yeast strains are listed in Table 4-3.

4.1.4.2 Yeast strains

Table 4-3: List of parental yeast strains used in this thesis

Strain	Genotype	Selection marker	Reference
BY4741	*MATa his3Δ1 leu2Δ0 met15Δ0 ura3Δ0*		Open Biosystems
FY2712	*MATa his3D200 leu2D1 lys2-128D trp1D63 ura3-52 kanMX-GAL1pr-FLO8-HIS3*	KAN^R	Cheung 2008
YMS277	*PAA1-GFP::HIS3MX6*	HIS3	Invitrogen, Huh 2003

Yeast strains used by, or generated for this thesis are listed in Table 4-4.

Table 4-4: Yeast strains generated for this study

Strain	Parent strain	Genotype	Selection marker	Reference
YAF007	BY4741	*Δpaa1::KAN^R Δisw1::URA3*	KAN^R, URA3	A. Fritsch
YAF008	BY4741	*Δpaa1::KAN^R Δioc3::HIS3*	KAN^R, HIS3	A. Fritsch
YAF023	Paa1-GFP p[PUS1-mCherry::LEU2]	*PAA1-GFP::HIS3MX6 PUS1-mCherry::LEU2*	HIS3, LEU2	A. Fritsch
YAF039	FY2712	*isw1Δ::TRP paa1Δ::hph*	KAN^R, TRP, hph	A. Fritsch
YAF051	BY4741	*ISW1-3xFlag::KAN^R PAA1-TAP::HIS3*	HIS3	A. Fritsch
YAF054	BY4741	*IOC2-3xFlag::KAN^R PAA1-TAP::HIS3*	KAN^R, HIS3	A. Fritsch
YAF057	BY4741	*IOC3-3xFlag::KAN^R PAA1-TAP::HIS3*	KAN^R, HIS3	A. Fritsch
YAF060	BY4741	*IOC4-3xFlag::KAN^R PAA1-TAP::HIS3*	HIS3	A. Fritsch
YAF062	FY2712	*paa1Δ::HYG*	KAN^R, hph	A. Fritsch
YAF079	BY4741	*Δioc2::URA3*	URA3	A. Fritsch
YAF086	BY4741	*Δchd1::KAN^R Δpaa1::LEU2*	KAN^R, LEU2	A. Fritsch
YAF087	BY4741	*Δisw2::KAN^R Δpaa1::LEU2*	KAN^R, LEU2	A. Fritsch
YAF088	BY4741	*Δioc2::KAN^R Δpaa1::LEU2*	KAN^R, LEU2	A. Fritsch
YAF090	BY4741	*Δpaa1::LEU2*	LEU2	A. Fritsch
YAF091	BY4741	*Δioc2::KAN^R Δioc3::HIS3*	KAN^R, HIS3	A. Fritsch
YAF092	BY4741	*ISW1-BirA-HA::HYG*	HYG	A. Fritsch
YAF093	BY4741	*Δioc2::KAN^R Δpaa1::LEU2 Δioc3::HIS3*	KAN^R, LEU2, HIS3	A. Fritsch
YAF098	BY4741	*ISW1-BirA-HA::hph Paa1-AP::KanMX*	hph, KAN^R	A. Fritsch
YAF099	BY4741	*ISW1-BirA-HA::hph Arl1-AP::KanMX*	hph, KAN^R	A. Fritsch
YAF100	BY4741	*ISW1-BirA-HA::hph IOC4-AP::KanMX*	hph, KAN^R	A. Fritsch
YAF105	BY4741	*IOC3-BirA-HA::hph*	hph	A. Fritsch
YAF106	BY4741	*IOC4-BirA-HA::hph*	hph	A. Fritsch
YAF108	BY4741	*IOC3-BirA-HA::hph Arl1-AP::KAN^R*	hph, KAN^R	A. Fritsch
YAF110	BY4741	*IOC3-BirA-HA::hph ISW1-AP::KAN^R*	hph, KAN^R	A. Fritsch
YAF111	BY4741	*IOC4-BirA-HA::hph Arl1-AP::KAN^R*	hph, KAN^R	A. Fritsch
YAF112	BY4741	*IOC4-BirA-HA::hph ISW1-AP::KAN^R*	hph, KAN^R	A. Fritsch
YAF125	BY4741	*IOC4-BirA-HA::hph Paa1-AP::KAN^R*	hph, KAN^R	A. Fritsch
YAF126	BY4741	*IOC3-BirA-HA::hph Paa1-AP::KAN^R*	hph, KAN^R	A. Fritsch

YMS033	BY4741	*Δisw1::KAN^R*	KAN^R	Open Biosystems
YMS038	BY4741	*Δioc3::KAN^R*	KAN^R	Open Biosystems
YMS039	BY4741	*Δioc4::KAN^R*	KAN^R	Open Biosystems
YMS078	BY4741	*ISW1-3xFlag*	KAN^R excised	M. Smolle
YMS279	BY4741	*paa1Δ::KAN^R*	KAN^R	Open Biosystems
YMS298	FY2712	*kanMX-GAL1pr-flo8::HIS3 isw1Δ::TRP*	KAN^R TRP	M. Smolle

4.1.4.3 Transformation of S. cerevisiae

A yeast colony was inoculated in 5 ml YPD liquid media and incubated at 30°C overnight on a rotator wheel. The next day, a 20 ml culture of YPD was inoculated to an OD_{600} of 0.2 and incubated at 30°C in a shaking incubator. Cells were harvested after at least 4 divisions had occurred or at an OD_{600} of ≥ 0.8. Cultures were transferred to a 50 ml conical tube and centrifuged at 4000 rpm for, 3 min at room temperature, washed once with 25 ml of ddH2O once and then centrifuged again. The pellet was resuspended in 1 ml 100 mM lithium acetate and spun down at maximum speed for 15 seconds. The supernatant was then discarded and the pellet resuspended in 100 mM lithium acetate to a final concentration of 2x107 cells/ml. 50 µl aliquots were taken per transformation reaction. To each reaction were added: 240 µl of 50% (w/v) PEG3350, 36 µl of 1 M lithium acetate, 25 µl of single-stranded carrier DNA (2 mg/ml) and 1-2 µg of DNA in 50 µl of ddH_2O. The samples were then vortexed and incubated for 30 minutes at 30°C and then for 20 minutes at 42°C. Samples were then spun down at 8000 rpm for 15 seconds and resuspended in 250 µl ddH_2O and plated on selective agar plates. If antibiotics resistance markers were used, cells were instead resuspended in 500 µl of YPD media and left to recover for 4-16 hours on a rotating wheel at 30°C. Cells where then spun down and resuspended in 250 µl of ddH_2O and plated on antibiotics selective agar plate.

4.1.4.4 Spotting assays

Cells were grown in 5 ml liquid YPD media to an OD_{600} of 0.6-0.8. Enough volume was taken to give an OD_{600} of 1 in 1 ml and the samples centrifuged at 8000 rpm for 30 seconds at room temperature. Samples were washed twice with 1 ml ddH2O and then resuspended in 1 ml ddH2O. Each sample was then diluted 5-fold 6 times in a 96-well cell culture plate (Sigma Aldrich). Samples were then spotted on selective plates as required. Plates were grown at the required temperature and then photographed after 48-96 hours.

4.2 Methods

4.2.1 Molecular Biology Methods

4.2.1.1 Yeast Genomic DNA preparation

A large colony was taken from an agar plate and resuspended in 500 µl buffer A (Table 4.5), by vortexing for 30 seconds. Then 60 µl of buffer B (Table 4-5) was added and the sample again vortexed for 30 seconds. The samples were then incubated at 80°C for 30 minutes. After

incubation, 300 µl of Buffer C (Table 4-5) were added and the samples gently mixed. The samples were cooled on ice for 5 minutes and then centrifuged at full speed for 10 minutes at room temperature. The supernatant was collected and mixed with 600 µl isopropanol and again centrifuged for 10 minutes. The pellet was washed with 500 µl 75% (v/v) EtOH and centrifuged for 5 minutes at room temperature. The supernatant was discarded and the pellet left to dry. Once dried the pellet was resuspended in 50 µl TE buffer (10 mM Tris-HCl, pH 7.4, 1 mM EDTA).

Table 4-5: Buffers used in yeast genomic DNA preparation

Yeast genomic DNA preparation		
Buffer A	50mM	Dextrose
	25 mM	Tris
	10 mM	EDTA
	Adjust pH to 8	
Buffer B	10% (w/v)	SDS
Buffer C	1.3 M	Potassium acetate
	Adjust pH to 4.8	

4.2.1.2 Polymerase Chain Reaction (PCR)

PCR reactions were carried out in 50 µl reactions. They contained 100 ng of template DNA, or 2 µl of genomic DNA, 0.25 µl of 50 µM forward and reverse primers respectively, 1x the appropriate buffer, 0.5 µl of 10 mM dNTPs, 1 U of polymerase. Polymerases were either OneTaq® Hot Start DNA polymerase (New England Biolabs) or Phusion® High-Fidelity DNA polymerase (New England Biolabs). The parameters of the cycling reactions were adjusted according to the primers chosen, the specifications of the polymerase and the length of the DNA template fragment. Primers used for PCR amplification and generation of Northern probes are listed in Table 4-6.

Table 4-6: Primers used in this study

Name	**sequence (5'-3')**	**Description**
ARL1_pYM-F1	TTTAGATTGGTTGATTGATGTTATAAAAGAGGAACAGTTACGTACGCTGCAGGTCGAC	Genetic tagging, *ARL1* - pYM
ARL1_pYM-R1	AAAGTATGCATCTACACTTTTTTTTTGCAAATCTTTATCGCTAATCGATGAATTCGAGCTCG	Genetic tagging, *ARL1* - pYM
dIOC22_seqF	GACATAATTCTTCCTTTCCAGCAAC	*IOC2* sequencing fw
dIOC3_seqF	TCGTGCTTCACGATTTGCTG	*IOC3* sequencing fw
dIOC3_seqR	CTTTTTCGTCCTCACTTTCTACC	*IOC3* sequencing rv
dIOC4_seqF	AAAATATCGTGGCTCCCCG	*IOC4* sequencing fw
dIOC4_seqR	TTGGACTATCAAAGACTGCG	*IOC4* sequencing rv
dISW1_seqF	TTTCACTGCATTTAGTACATCTG	*ISW1*, sequencing fw
dISW1_seqR	TGTCTATAATCAAGCAATTATCCGG	*ISW1*, sequencing rv
dISW1-S2	GGTGTAGGATATATTAAAAAAAATCGAAATATAAAAAAAGAAGGTTTAATCGATGAATTCGAGCTCG	Genetic tagging, *ISW1* - pYM
dPAA1_KIKO-F1	AAAATAACACCAATACATTACGATTAAATAAAAAGTTAAACAGCTGAAGCTTCGTACGC	Genetic deletion, *PAA1* - pUG72
dPAA1_KIKO-F2	AAAATAACACCAATACATTACGATTAAATAAAAAGTTAAACGGATCCCCGGGTTAATTAA	Genetic deletion, *PAA1* - pFA6a
dPAA1_KIKO-R1	TACTTGGCAATTTTAAAATATACAAAAATTATATGTAGTAGCATAGGCCACTAGTGGATCTG	Genetic deletion, *PAA1* - pUG73

dPAA1_KIKO-R2	TACTTGGCAATTTTAAAATATACAAAAATTATATGTAGTAGAATTCGAGCTCGTTTAAAC	Genetic deletion, *PAA1* - pFA6a
dPAA1_KIKO-R3	TTTATAATTAGACATTTGTAAAGTGCGTTAAACTAATGATCTAATCGATGAATTCGAGCTCG	Genetic deletion, *PAA1* - pYM
IOC2dC_seqR	CATTAAGGATGGCCACTGACGA	*IOC2* sequencing rv
IOC4_pYM-F1	TAGTGAAGACGTAAAGGAAGAAGAAAGCAAAGTAGGAGCACGTACGCTGCAGGTCGAC	Genetic tagging, *IOC4* - pYM
IOC4_pYM-R1	TTGTTCAAAAGCAGAGTACATCAACTGCAATAGCAACAGGTCAATCGATGAATTCGAGCTCG	Genetic tagging, *IOC4* - pYM
ISW1_pYM-F1	GTTGGTAGCAGAGAAAATTCCGGAAAACGAAACCACTCATCGTACGCTGCAGGTCGAC	Genetic tagging, *ISW1* - pYM
ISW1-Flag_seqF	GGGATTGTATTGGATGACGCC	*ISW1*, sequencing fw
ISW1d-R1	GGTGTAGGATATATTAAAAAAAATCGAAATATAAAAAAAGAAGGTGAATTCGAGCTCGTTTAAAC	Genetic deletion, *ISW1* - pFA6a
o-ACT1-3	GGTATGTTCTAGCGCTTGCACCATCCCATT	Northern probe
o-ACT1-4	CCAAGGCGACGTAACATAGTTTTTCCTTGA	Northern probe
o-ARL1-1	CAGTGCAATTAAAGGCGAAGGT	*ARL1* sequencing fw
o-ARL1-2	TGTTTGGATAGAGCTCCTTGA	*ARL1* sequencing rv
o-IOC2-1	CTACCAAATGCTTGTGGAAGAATATC	*IOC2* sequencing fw
o-IOC2-2	ACTTGGGAGGAAGAGCCTTC	*IOC2* sequencing rv
o-IOC3-1	ACCTCAATTGCTAAGGATGGC	*IOC3* sequencing fw
o-IOC3-2	GCGAGCTACAAGTCTTAACCGA	*IOC3* sequencing rv
o-IOC3-3	TTGCAGACATGAAGCCAGGC	*ISW1*, sequencing fw
o-IOC4-1	CTCCCGTTCTGAAGTTTCGTAA	*IOC4* sequencing fw
o-IOC4-2	GCTCCAATCTTCATCATCTTCAA	*IOC4* sequencing rv
o-IOC4-3	AAATGGGATCTGTGGGATCG	*IOC4* sequencing fw
o-ISW1-1	AACTGGTTGGTGTCTCTGCATAAG	*ISW1*, sequencing fw
o-ISW1-2	TGATACGACGTAGTAGAAAAGGCTG	*ISW1*, sequencing rv
o-PAA1-1	TCAGAGAGATCGAGGGCAAAG	*PAA1* sequencing, fw
o-PAA1-2	CCACTTGTAATTTGCCCATGCT	*PAA1* sequencing, rv
o-PAA1-3	GTTTTGAACGGGCAAAAATGG	*PAA1* sequencing, fw
o-PAA1-4	CTCCAAGAACTGAAAAGAACCC	*PAA1* sequencing, rv
o-PAA1-5	AGGACAAAAACTTCGCAGAACAG	*PAA1* sequencing, fw
o-PAA1-6	ATCAATGGCTCGTGAGCAAT	*PAA1* sequencing, rv
o-PCA1-15	GTCATAATTCTCAATCTTTGTTGCTTGGAT	Northern probe
o-PCA1-16	CTAGCTTGGCAACCTCACTTCCCTCATTGA	Northern probe
o-SWP82-1	GGCTGTTAAGCTGGACACTG	*SWP82* sequencing, fw
o-SWP82-2	GTTGGTTATGGCATATTACAC	*SWP82* sequencing, rv
PAA1_pYM-F1	CGATATGGAGAGAGAACTAATTAAGGAAGAATACGACAACCGTACGCTGCAGGTCGAC	Genetic tagging, *PAA1* - pYM
SSK22 3' F	GATACTGAAGAGAATATTGATGAAGAGGCC	Northern probe
SSK22 3' R	CTGAAATAGTCTCTGGAGCCATATACATCG	Northern probe
SWP82_pYM-F1	CCTGGCTAACTTCAGCAACGAAGTAGCTATGAATAAT CGTACGCTGCAGGTCGAC	Genetic tagging, *SWP82* - pYM
SWP82_pYM-R1	TTTCTTATTGGAGTGTTCCCTACATTATGTTTTACTTCTTTCA ATCGATGAATTCGAGCTCG	Genetic tagging, *SWP82* - pYM
Abbreviations: fw (forward), rv (reverse).		

4.2.1.3 Agarose gel electrophoresis

DNA fragments were separated according to size by agarose gel electrophorese. Gels contained between 0.8 to 1.5% (w/v) agarose in 1x TAE (Table 4-7) and 0.1% (v/v) 0.25 mg/ml ethidium bromide. 10x DNA gel loading buffer (Table 4-7) was added to DNA samples that were then separated at 100 V for 30 minutes in 1x TAE buffer. DNA was detected with UV-light and documented with a UV-Transillluminator (PeqLab).

Table 4-7: Buffers used for agarose gel electrophoresis

DNA Agarose gel		
10x DNA gel loading buffer	100 mM	Tris
	25% (w/v)	Ficoll 400
	Adjust pH to 6.8	
	Heat to 65°C to dissolve, adjust Volume to 50 ml	
50x TAE buffer	2 M	Tris Acetate
	50 mM	EDTA
	Adjust pH to 8.2 and autoclave	

4.2.1.4 SDS-PolyAcrylamide Gel Electrophoresis (PAGE) and western blotting

Samples were denatured by adding 4x SDS PAGE gel loading buffer (Table 4-8) and boiling for 5 minutes at 96°C. Samples were then loaded onto 10% SDS-PAGE gels (Table 4-8) and separated at 30 mA per gel and 12 W per gel chamber using the Mini-PROTEAN electrophoresis systems (BioRad) in 1x SDS-PAGE running buffer (Table 4-8).

Table 4-8: Gels and buffers used for SDS-PAGE

SDS-Polyacrylamide gel electrophoresis		
Resolving gel (10%)	2.5 ml	Acrylamide (30%)
	1.875 ml	Resolving buffer
	2.74 ml	ddH_2O
	75 µl	10% APS
	15 µl	TEMED
Stacking gel (4%)	200 µl	Acrylamide (30%)
	375 µl	Stacking buffer
	916 µl	ddH_2O
	150 µl	10% APS
	4 µl	TEMED
Resolving buffer	1.5 M	Tris
	Adjust pH to 8.8	
	0.4% (w/v)	SDS
Stacking buffer	0.5 M	Tris
	Adjust pH to 6.8	
	0.4% (w/v)	SDS
10x SDS-PAGE running buffe	250 mM	Tris
	1.92 M	Glycine
	1% (w/v)	SDS
	Add 100-250 mg of Orange G	
5x SDS-PAGE gel loading bu	250 mM	Tris
	10% (w/v)	SDS
	50% (w/v)	Glycerol
	50 mM	EDTA
	Adjust pH to 6.8 and fill up to 50 ml with ddH2O	
	Add 0.25 mg bromophenol blue	

The proteins were then transferred onto a Nitrocellulose membrane (Amersham) at 200 mA at 4°C via wet transfer in a Mini Trans-Blot cell (BioRad) in transfer buffer (Table 4-9). Transfer was verified by staining the blot with 0.1% (w/v) Ponceau S solution, before blocking of the membrane with either 3.5% (w/v) BSA or 2% (w/v) milk in 1x TBS (Table 4-9). Membranes were blocked for 30 minutes to up to an hour at room temperature under constant shaking. Primary antibodies were added in their respective dilutions in either 3.5% (w/v) BSA or 2% (w/v) milk. The membranes were incubated for an hour at room temperature under constant shaking. Membranes were then washed three times with 1x TBS for five minutes each and then incubated with the secondary antibody in BSA or milk for an hour at room temperature, shaking. The membrane was washed three times with 1x TBST (Table 4-9) for five minutes and then developed with Immobilon Western solution (Millipore). Blots were imagined with a Fusion FX chemiluminescence detector (Vilber).

Table 4-9: Buffers used for western blotting

Western blotting		
Transfer buffer	25 mM	Tris
	192 mM	Glycine
	20% (v/v)	Methanol
10x TBS pH 7.5	50 mM	Tris
	150 mM	NaCl
	Adjust pH to 7.5 with HCl	
TBST	1x	TBS
	0.1% (v/v)	Tween-20
Ponceau S	0.1% (w/v)	Ponceau S
	1% (v/v)	Acetic acid

4.2.1.5 Co-Immunoprecipitation assays

Cells were grown overnight in 5 ml liquid YPD media and inoculated into 20 ml cultures at an OD_{600} of 0.2 in the morning. After reaching an OD_{600} of around 1, cells were harvested by centrifugation and pellets washed once with 25 ml of chilled 1x PBS (Table 4-10). Pellets were then resuspended in 500 µl TAP150 extraction buffer (Table 4-10) and added to a 1.5 ml screw-cap tube with 750 µl of 0.5 mm glass beads (Roth). Beads were previously washed twice with 500 µl ddH_2O and then twice with 500 µl TAP150. The screw-cap tube was filled to maximum capacity with TAP150 buffer to prevent bubble formation. The cells were then broken open on a Precellys 24 bead beater (Peqlab), ten cycles of 30 seconds each at 6800 rpm. Samples were cooled on ice in between cycles. The supernatant was then transferred to a fresh tube. Beads were washed with 500 µl TAP150 buffer and the supernatant added to the rest of the sample.7.5 U of Benzonase were added to the samples and they were then incubated for 15 minutes at room temperature. The samples were then spun down for 15 minutes at 14000 rpm at 4°C. The supernatant was transferred to a fresh tube and the protein concentration measured with a Bradford Protein Assay (Bio-Rad). A 50 µl aliquot was taken as input fraction (IN) for later analysis. 60 µl of IgG-Sepharose slurry (GE Healthcare) were washed with 200 µl TAP150 buffer three times and then combined with 2 mg of protein sample to a total volume of 500 µl. The samples were incubated for 4 hours at 4°C under constant rotation. At the end of the incubation a 50 µl aliquot of the supernatant was taken as the unbound (UN) fraction, and the resin were spun down. The sepharose beads were washed three times with 1 ml of TAP150

buffer, before being resuspended in 10 µl of 5x SDS-PAGE loading dye. The samples were then boiled for 5 minutes at 96°C to elute the bound fraction (B) from the beads. All fractions were analyzed by western blotting.

Table 4-10: Buffers used for co-immunoprecipiation assays

10x PBS	137 mM	NaCl
	12 mM	Phosphate
	2.7 mM	KCl
	Adjust pH to 7.4	
TAP150	40 mM	HEPES
	150 mM	NaCl
	10% (v/v)	Glycerol
	0.05% (v/v)	Tween-20
	2.5 mM	DTT
	1 mM	PMSF
	2 µg/ml	Pepstatin A
	1 µg/ml	Leupeptin
	Adjust pH to 7.5 with HCl	

4.2.1.6 Bio-ID super shift assay

Strains were grown for 6 hours in 5 ml liquid YPD media and then harvested by centrifugation. The pellets were resuspended in 1 ml of 1.2 M Sorbitol and incubated at 30°C for 10 minutes shaking at 800 rpm. 1 mM of H_2O_2 (AppliChem) and 1 mM of Biotin (Thermo Fisher Scientific) were added and the samples again incubated for 1 minute at 30°C. Pellets were then resuspended in 150 µl of NaOH/β-mercaptoethanol and incubated on ice for 15 minutes. Then 150 µl of 55% trichloroacetic acid (TCA) were added and the samples incubated on ice for 15 minutes. At the end of the incubation 500 µl chilled ddH_2O were added and the samples centrifuged at 14000 rpm at 4°C for 18 minutes. The supernatant was discarded and the samples centrifuged for 3 more minutes. The remaining liquid was aspirated and the samples resuspended in 50 µl HU buffer (Table 4-11). The samples were then incubated at 65°C for 20 minutes. 10 µl of sample were mixed with 5 µl of either ddH_2O or Streptavidin (Sigma Aldrich) and incubated for 10 minutes at room temperature and then loaded onto a 4–20% Mini-PROTEAN ® TGX™ Precast Protein Gel (BioRad). The gel was run for 45 minutes at 30 mA and was then transferred onto a Nitrocellulose membrane at 200 mA for 1 hour. The membrane was blocked with 5% milk in TBST and then incubated with Peroxidase Anti-Peroxidase Soluble Complex antibody (Sigma Aldrich) in 1% (w/v) milk. The membrane was imaged with a Fusion FX Chemiluminescence detector (Vilber).

Table 4-11: Buffers used for Bio-ID super shift assay

Super shift assay		
HU buffer	200 mM	Phosphate buffer
	8 M	Urea
	5% (w/v)	SDS
	1 mM	EDTA
	100 mM	DTT
Phosphate buffer	38.2 g/l	$Na_2HPO_4•2H_2O$
	37.6 g/l	$NaH_2PO_4•H_2O$
NaOH/β-ME	2 M	NaOH
	1 M	β-Mercaptoethanol

Antibodies used for western blotting are listed in Table 4-12.

Table 4-12: Antibodies used in this study

Name	**Isotype**	**Clonality**	**Working dilution**	**Reference**
Anti-Flag M2	Mouse	Monoclonal	1:1000	Sigma Aldrich (#F3165)
Goat Anti-Mouse IgG (H + L)-HRP Conjugate	Goat		1:5000	BioRad (#1706516)
Goat Anti-Rabbit IgG (H + L)-HRP Conjugate	Goat		1:5000	BioRad (#1706515)
Peroxidase Anti-Peroxidase Soluble Complex Antibody	Rabbit		1:1000	Sigma Aldrich (#P1291)
TAP Tag Antibody	Rabbit	Polyclonal	1:5000	Life Technologies (#CAB1001)

4.2.1.7 RNA extraction

50 ml yeast cultures were harvested at an OD_{600} of around 0.6 by centrifuging for 3 minutes at 4000 rpm. Cells were then washed with 25 ml of ddH_2O and centrifuged again. The cells were resuspended in 400 µl of AE-buffer (50 mM sodium acetate, 10 mM EDTA, pH 5.2). To this, 40 µl of 10% (w/v) SDS and 400 µl phenol (pH 4.5, Roth) were added and the samples vortexed. The samples were then incubated at 65°C for 4 minutes at 1200 rpm and then rapidly chilled in dry ice. Samples were then incubated at 65°C until they were melted and transferred to 2 ml Phase Lock Gel Heavy tubes (VWR). 400 µl of chloroform were added and the samples inverted to mix. Samples were centrifuged for 3 minutes at 6000 *x g* and the upper aqueous phase decanted into a new 2 ml tube. 60 µl of sodium acetate and 1.5 ml of cold absolute ethanol were added and the samples were vortexed. Following 30 minutes of incubation at -80°C, the samples were centrifuged for 30 minutes at 15000 *x g* at 4°C. The pellets were washed with 750 µl of cold 70% (v/v) ethanol and centrifuged for 5 minutes. The supernatant was removed and the pellets dried in a speed vacuum centrifuge (RVC 2-25, Christ) for 5 minutes at room temperature. The pellets were resuspended in 50 µl of RNAse-free ddH_2O and incubated at 65°C, 1200 rpm for 2 minutes. The concentration was measured with a Nanodrop One (Thermo Fisher Scientific).

4.2.1.8 Northern blotting

Prior to use, each piece of equipment was cleaned with RNAse Away (Thermo Fisher Scientific) and all buffers and solutions were prepared with DEPC-treated ddH_2O. A gel chamber (Perfectblue gelsystem mini L, Peqlab) was set up with 16-well, 1mm combs (Peqlab). 1.5% (w/v) agarose ME (Biozym) was prepared in 1x MOPS and 6.66% (v/v) Formaldehyde (Sigma Aldrich) and poured into the gel chamber and covered with 1x MOPS buffer. The gel was then pre-run for 5 minutes at 80V. The Formaldehyde was washed from the wells with a 1 ml pipette. Denaturation reactions were set up as follows: 20 µg of RNA were diluted in 6 µl of ddH_2O and mixed with 1x MOPS, 16% (v/v) Formaldehyde, 40% (v/v) Formamide (Sigma Aldrich) and 8 ng/µl ethidiumbromide (Sigma Aldrich) in nuclease free ddH_2O (Thermo Fischer Scientific). The mix was incubated at 95°C for 5 minutes and for another 5 minutes on ice. 1x FH-loading dye (Table 4-13) was added to each sample afterwards. Samples were loaded onto the gel and run for 2 hours at 100 V. After the run, the gel was removed and visualized on a UV-Transillluminator (Peq-Lab). The gel was then washed four times for five minutes with DEPC-treated ddH2Oshaking at 150 rpm. The gel was then incubated for 20 minutes in 10x SSC buffer (Table 4-13) at 150 rpm. RNA was transferred onto a Zeta probe membrane (BioRad) by overnight capillary transfer. The gel was placed upside down on a piece of absorbent paper (Whatman) covering the casting chamber that was placed in a plastic box filled with 10x SSC buffer and then covered with the Zeta membrane. Four pieces of absorbent paper the size of the gel was added on top. A stack of paper tissue was added on top and a weight placed on top of that. The transfer was left for at least 24 hours before being disassembled. The RNA was UV-crosslinked to the membrane at 120 mJ in a BIO-LINK UV-Crosslinker (Vilber). The membrane was then stained with methylene blue solution to ascertain successful transfer. The membrane was then laminated and stored at 4°C until hybridization.

Table 4-13: Buffers used for northern blotting

1x MOPS	0.2 M	MOPS
	20 mM	Sodium acetate
	1 mM	EDTA
	Dissolve in DEPC treated ddH_2O and adjust pH to 7	
DEPC ddH_2O	1 l	ddH_2O
	1 ml	DEPC
	Stir for one hour and then autoclave	
1x FH-loading dye	50% (v/v)	Glycerol
	10 mM	EDTA
	0.25% (w/v)	Bromophenol blue
	0.25% (w/v)	Xylene cyanol FF
	0.25% (w/v)	Orange G
20x SSC	0.2 M	MOPS
	0.3 M	Trisodium citrate dehydrate
	Dissolve in DEPC treated ddH_2O and adjust to pH 7	
Methylene blue solution	0.03% (w/v)	Methylene blue
	0.3 M	Sodium acetate

Membranes were put into a hybridization tube (Peqlab, VWR) and covered with prehybridization buffer (Table 4-14). The tubes were then put into a hybridization oven (Analytik Jena) and rotated for at least an hour at 65°C. Appropriate probes were generated by

PCR and then radioactively labeled with [α-32P]-dCTP (111TBq/mmol, Hartmann Analytik) using the Megaprime DNA labeling system (GE Healthcare). Unincorporated nucleotides were removed with Illustra MicroSpin s-300 HR columns (GE Healthcare). The labeled probes were boiled for 2 minutes at 96°C and added to the hybridization tubes. Tubes were then incubated at 65°C overnight. The membranes were then rinsed with wash buffer A (Table 4-14) and then washed for 10 minutes at room temperature with the same buffer. The membrane was then washed two more times for 10 minutes at 65°C with wash buffer B (Table 4-14). Lastly, the membranes were rinsed with wash buffer C (Table 4-14). The membranes were then sealed in a plastic sheet and exposed on a phosphor imaging screen (Fujifilm) for 5 days. Northern blots were visualized with a Typhoon FLA 9500 laser scanner (GE Healthcare).

Table 4-14: Buffers used for hybridization

Prehybrididizaiton buffer	5x	Denhardt's reagent
	6x	SSC
	0.5% (w/v)	SDS
	Dissolve in DEPC-treated ddH_2O	
50x Denhardt's reagent	1% (w/v)	Ficol 400
	1% (w/v)	Polyvinylpyrrolidine
	1% (w/v)	BSA fraction V
	Dissolve in DEPC-treated ddH_2O	
Wash buffer A	1x	20x SSC
	0.1% (w/v)	SDS
Wash buffer B	0.5x	SSC
	0.1% (w/v)	SDS
Wash buffer C	2x	SSC

4.2.1.9 RNAsequencing

RNA samples were first cleared of DNA by DNase digestion, using the Turbo DNAfree kit (Life technologies) and following the manufacturer's instructions. Following this the samples were enriched for polyA-tails with the NEBNext® Poly(A) mRNA Magnetic Isolation Module (New England Biolabs). RNA-sequencing libraries were prepared with NEBNext® Ultra™ II Directional RNA Library Prep Kit for Illumina® and NEBNext® Multiplex Oligos for Illumina® Index Primers Set 1 (New England Biolabs), according to the manufacturers' specifications. This generated strand specific reads, allowing detection of sense and antisense transcripts separately. The concentration of the samples were measured on a 2100 Bioanalyzer (Agilent) and samples were handed to LaFuGa for pooling and sequencing.

4.2.1.10 Preparation of yeast nuclei

Strains were inoculated in 5 ml liquid YPD media cultures and grown for 8 hours at 30°C. From this, 1 l cultures were inoculated so that they would reach an OD_{600} of 0.8 the next day after 19 hours. Cultures were harvested by centrifugation at 4000 rpm for 10 minutes at 4°C. The pellet was dissolved in 40 ml ddH_2O and transferred to a 50 ml conical tube (Sarstedt) that had been weighed beforehand. Samples were centrifuged at 4000 rpm for 5 minutes at 4°C. The pellet's wet weight was determined. For each g of pellet, 2 volumes of preincubation buffer (Table 4-15) was added and the sample then incubated at 30°C for 30 minutes with shaking. Pellets were harvested by centrifuging at 4000 rpm for 5 minutes at 4°C and then washed with 40 ml of 1 M Sorbitol. 5 ml of β-ME Sorbitol (Table 4-15) were added per 1 g of pellet. The

OD_{600} was measured, before 100 µl of 10 mg/ml Zymolase 100T (Roth) were added per g of pellet. The samples were incubated for 30 minutes at 30 °C with shaking. The lysis degree was determined by measuring the OD_{600} again. If at least 60% of the initial signal was lost, the digest was deemed successful. Samples were spun down at 4000 rpm for 8 minutes at 4°C and washed with 40 ml of 1M Sorbitol. Samples were then resuspended in 7 ml of Ficoll solution (Table 4-15) per g of pellet and aliquoted into centrifuge tubes (Sarstedt) and centrifuged at 15000 rpm for 30 minutes at 4°C. The samples were frozen for 10 minutes in ethanol/dry ice and stored at -80°C.

Table 4-15: Buffers used for nuclear extraction

Preincubation buffer	0.7 M	β-Mercaptoethanol
	2.8 mM	EDTA
	Adjust pH to 8	
β-ME Sorbitol	1 M	Sorbitol
	5 mM	β-Mercaptoethanol
Ficoll solution	18% (w/v)	Ficoll 400
	20 mM	KH_2PO_4
	1 mM	$MgCl_2$
	0.25 mM	EGTA
	0.25 mM	EDTA
	Dissolve in ddH2O and adjust pH to 6.8	

4.2.1.11 MNase digestion

1 g of nuclei pellets were thawed at room temperature and then dissolved in 6 ml of 1x MNase buffer (Table 4-16) and centrifuged at 4000 rpm for 8 minutes at 4°C. The pellet was resuspended in 1.8 ml of 1x MNase buffer and divided into 300 µl aliquots. Different concentrations of MNase were added to each aliquot and the aliquots incubated for 20 minutes at 37°C. MNase concentrations chosen were 0 U/ml, 16 U/ml, 32 U/ml and 64 U/ml. Reactions were stopped by adding 28.5 µl of STOP buffer (Table 4-16). 30 µl of 20 mg/ml Proteinase K (Sigma Aldrich) were added and the samples incubated for 30 minutes at 37°C. After 30 minutes, 70 µl of 5 M $NaClO_4$ and 400 µl of Phenol, pH 8 (Sigma Aldrich) were added. The samples were then vortexed and 400 µl Isoamyl-alcohol:Chloroform (IAC, 1:24, Sigma Aldrich) were added and again vortexed. The samples were then centrifuged at full speed for 5 minutes at room temperature. The upper aqueous phase was then transferred to a new tube and 400 µl of IAC was added, the tubes inverted and again centrifuged. The upper aqueous phase was transferred to a new tube and 1 ml of 100% cold ethanol and 2.5 µl of 20 mg/ml glycogen added. The samples were then incubated for 10 minutes on ice and then centrifuged at 15000 rpm for 15 minutes at 4°C. The pellet was washed with 1.5 ml of 70% ethanol and centrifuged for 5 minutes. The ethanol was removed and the pellet dried in a speed vacuum centrifuge (RVC 2-25, Christ) for 10 minutes, before being resuspended in 250 µl of TE-buffer. 20 µl of 10 mg/ml RNaseA was added and the samples incubated for 1 hour at 37°C. After incubation, 10 µl of 5 M NaCl and 175 µl of isopropanol were added and the sample was incubated for 5 minutes on ice. The sample was then centrifuged at 15000 rpm for 15 minutes at 4°C. The pellet was then washed with 450 µl of 70% ethanol and centrifuged for 5 minutes. The ethanol was removed and the pellet dried for 10 minutes with a speed vacuum centrifuge (RVC 2-25, Christ). The pellet was then resuspended in 45 µl of TE-buffer. The samples were

run on a 1.5% agarose gel to verify digestion rates. Samples containing ca. 80% mononuclesomes were picked for library preparation.

Table 4-16: Buffers used for MNase digestion

MNase buffer	15 mM	15 mM
	50 mM	50 mM
	1.4 mM	1.4 mM
	0.2 M	0.2 M
	5 mM	5 mM
	5 mM	5 mM
	Adjust pH to 7.5	
STOP buffer	500 mM	Tris
	5% (w/v)	SDS
	40 mM	EDTA

4.2.1.12 Size selection of nucleosomal DNA

Size selection was performed to remove long strands of undigested DNA from samples. The concentration of the nucleosome sample was determined using the Qubit® Fluorometer 2.0 (Invitrogen). 500 ng of nucleosomes were diluted in 50 µl 0.1x TE-buffer, to which 27.5 µl of AMPure beads (Agencourt) were added. The sample was mixed and incubated for 5 minutes at room temperature. The beads were collected using a magnet and the supernatant transferred to a new tube. 104 µl of AMPure beads were added and mixed. The samples were then incubated for 5 minutes at room temperature. The beads were collected using a magnet and the supernatant discarded. The beads were washed twice with 500 µl of freshly prepared 80% ethanol. The beads were then eluted with 25 µl 0.1x TE-buffer and the sample concentrations determined using the Qubit® Fluorometer 2.0 (Invitrogen).

4.2.1.13 Library preparation for MNase-sequencing

50 ng of size selected mononucleosomal DNA were mixed with 10 µl of blunting mix (Table 4-17). The samples were then incubated at 20°C for 30 minutes. 50 µl of AMPure beads (Agencourt) were added to the samples and 75 µl of NaCL/PEG (Table 4-17). The samples were mixed by pipetting up and down and then incubated for 5 minutes at room temperature. Beads were collected with a magnet and the supernatant discarded. The beads were washed twice with 500 µl of freshly prepared 80% (v/v) ethanol. The beads were air-dried and resuspended with 50 µl of dA-tailing mix (Table 4-17). Samples were incubated for 30 minutes at 37°C. 125 µl of NaCl/PEG were added to the samples and pipetted to mix and beads were collected on magnet. The supernatant was discarded and the beads were washed twice with 500 µl of freshly prepared 80% (v/v) ethanol. Beads were then air-dried and resuspended with ligation master mix (Table 4-17). Samples were incubated overnight at 16°C. 3 µl of USER enzyme (NEBNext® Multiplex Oligos for Illumina® Index Primers Set 1, New England Biolabs) were added to the samples and they were incubated for 15 minutes at 37°C. 82.5 µl of NaCl/PEG were added to the samples and mixed by pipetting. Beads were collected on a magnet and the supernatant discarded. The beads were washed twice with 500 µl of freshly prepared 80% ethanol. The beads were air-dried and resuspended in 36 µl of 0.1x TE-buffer to elute the samples from the beads. Samples were placed on magnet and the supernatant collected. The samples were then amplified in a PCR reaction with 10 µl of 5x Phusion buffer, 1.5 µl of dNTP-

Mix, 1 µl Universal-Primer, 1 µl of Index primer (NEBNext® Multiplex Oligos for Illumina® Index Primers Set 1) and 0.5 µl of Phusion polymerase. The reactions were amplified over six cycles. Samples were measured on the Qubit® Fluorometer 2.0 (Invitrogen).

Table 4-17: Buffers used for MNase library preparation

Blunting mix	5 µl	T4 Ligase buffer
	1 µl	T4 DNA polymerase
	1 µl	T4 polynucleotide kinase
	2 µl	dNTPs
	0.2 µl	Klenow
NaCl/PEG	1.25 M	NaCl
	20% (w/v)	PEG8000
dA-tailing mix	1x	NEB 2 buffer
	1 mM	dATP
	1 µl	Klenow-fragment (3'-5' exo-)
	Fill with dH_2O to 50 µl	
Ligation master mix	3 µl	T4 ligase buffer
	1 µl	NEBNext Adapter
	3 µl	T4 ligase
	Fill up to 30 µl with dH_2O	

4.2.1.14 Library purification

A PAGE 5% non-denaturing gel (Table 4-18) was cast in a 1 mm cassette (Invitrogen). The gel was run for a few minutes in 1x TBE-buffer (Invitrogen) to pre-warm the matrix and the slots rinsed afterwards. Samples were prepared by adding 6x DNA Gel Loading Dye (Thermo Fisher Scientific) and split into several pockets. One pocket was loaded with 100 bp ladder (New England Biolabs). The gel was run at 120 V for 40 minutes in the XCell SureLock™ Mini-Cell Electrophoresis System (Invitrogen). After the run, the gel was removed from the chamber and stained in 1x TBE buffer (Invitrogen) with ethidium bromide solution (Sigma Aldrich) before being imaged on a UV-table. DNA bands of the right size (approximately 270 bp) were excised from the gel with a scalpel and placed into a 0.5 ml non-stick DNAse-free tube (Eppendorf). A 0.7 mm hypodermic needle (B.Braun) was heated in a flame and used to stab a hole into the bottom of the 0.5 ml tube. The tube was then placed in a 1.5 ml tube and centrifuged for 2 minutes at 14000 rpm. 400 µl of DNA gel extraction buffer (Table 4-18) was added and the sample placed on a rotating wheel at 4°C overnight. The next day, 30 µg of glycogen and 500 µl Isopropanol were added. The samples were placed at -20°C for 30 minutes. The samples were then spun for 30 minutes at 14000 rpm at 4°C. The supernatant was discarded and 2 ml of 80% ethanol were added. The samples were then centrifuged for 10 minutes at 14000 rpm at 4°C and the supernatant was discarded. The residual ethanol was removed and the pellet was dried and resuspended in 15 µl of 10 mM Tris, pH 8 and transferred to a new tube. The sample concentration was measured by qPCR and samples were handed to Lafuga for pooling and sequencing.

Table 4-18: Buffers used for MNase-sequencing library purification

5% non-denaturing PAG	5%	Polyacrylamide 40% (19:1)
	1x	10x TBE
	0.1%	APS
	0.04%	TEMED
DNA gel extraction buf	300 mM	NaCl
	10 mM	Tris
	1 mM	EDTA
	Adjust pH to 8	

4.2.1.15 Next-generation sequencing

Sequencing of pooled RNAseq libraries was performed on an Illumina Hiseq1500 system (LMU, single read mode). The total number of reads per sample were 20 million, with a coverage of 80 and 50 bp read length. Sequences were mapped against the genome of wild type *S. cerevisiae* as determined by (Xu et al., 2009).

Sequencing of MNase-seq libraries was performed on an Illumina Hiseq1500 system (LMU, paired end mode). The total number of reads per sample were 10 million, with a coverage of 40 and 50 bp read length. Nucleosome occupancy was mapped against genome-wide +1 nucleosome coordinates in *S. cerevisiae*, as determined by (Chereji et al., 2018).

4.2.1.16 Bioinformatic analysis of NGS data

The bioinformatics methods used to analyze RNAseq and MNase-seq data were performed by Tamas Schauer (Biomedical Center Munich, Core Facility bioinformatics). RNAseq data was processed, using the DEseq2 package (Love et al., 2014). MNase-seq data was processed using the tsTools package (https://github.com/musikutiv/tsTools). Nucleosome repeat lengths for individual genes in MNase-seq data was determined using the method developed by Ocampo et al., (2016). Transcript annotations originated from Xu et al., (2009). Data for native transcription rates were taken from Miller et al., (2011). Data for gene lengths were taken from Holstege et al., (1998). Basehoar et al., (2004) provided data on genes with TATA boxes. Graphs and plots were made with R (https://cran.r-project.org/) and RStudio (https://www.rstudio.com/).

5 Abbreviations

ACT	Actin
Amp	Ampicillin
APS	Ammonium persulfate
Arl	ADP-ribosylation factor-like
ATAC-seq	assay for transposase-accessible chromatin
ATP	Adenosine triphosphate
bp	Base pair
BSA	bovine serum albumin
CBP	Calmodulin-binding peptide
CHD	Chromodomain-helicase-DNA-binding
ChIP	Chromatin immunoprecipitation
CLB	Coil-linker-DNA-binding motif
Co-IP	Co-immunoprecipitation
CTD	C-terminal domain
CUT	Cryptic unstable transcript
Cys	Cysteine
ddH_2O	Double distilled water
DEPC	Diethyl pyrocarbonate
DNA	Deoxyribonucleic acid
DTT	Dithiothreitol
E. coli	*Escherichia coli*
EDTA	Ethylenediaminetetraacetic acid
EGTA	Ethylene glycol-bis(β-aminoethyl ether)-N,N,N′,N′-tetraacetic acid
FH	Formaldehyde
FLO	Flocculation
Gcn	General control nonderepressible
GNAT	GCN5-related N-acetyltransferase
GRO-seq	Global run-on sequencing
H3K36me3	Trimethylated lysine 36 on histone 3
H3K4me3	Trimethylated lysine 4 on histone 3
H3K9ac	Acetylated lysine 9 on histone 3
H4K20me3	Trimethylated lysine 20 on histone 4
HCl	Hydrochloric acid
HDAC	Histone deacetylase

His	Histidine
HLB	Helical-linker-DNA-binding domain
HSS	HAND SANT SLIDE
HU	Hydroxyurea
IAC	Isoamyl-ethanol chloroform
IME	Inducer of meiosis
INO	Inositol requiring
Ioc	ISWI one complex
IRT	IME1 regulatory transcript
ISWI	Imitation switch
kb	Kilobase
KH_2PO_4	Monopotassium phosphate
LB	Lysogeny broth
LiAc	Lithium acetate
MET	Methionine
$MgCl_2$	Magnesium chloride
MNase-seq	Mnase-sequencing
MOPS	3-(N-morpholino)propanesulfonic acid
mRNA	Messenger RNA
MS	Mass spectometry
NaCl	Sodium chloride
NDR	Nucleosome-depleted region
NGS	Next generation sequencing
NLS	Nuclear localization signal
NRL	Nucleosome repeat length
OD	Optical density
ORF	Open reading frame
Paa	Polyamine acetyltransferase
PAGE	Polyacrylamide gel electrophoresis
PBS	Phosphate-buffered saline
PCA	P-type cation-transporting ATPase
PCR	Polymerase chain reaction
PHD	Plant homeodomain
PRO-seq	Precision nuclear run-on sequencing
PWWP	Proline-tryptophane-tryptophane-proline

RME	Regulator of meiosis
RNA	Ribonucleic acid
RNA-seq	RNA-sequencing
RPL9A	Ribosomal Protein of the Large subunit
RPolII	RNA Polymerase II
S. pombe	*Schizosaccharomyces pombe*
S.c.	*Saccharomyces cerevisiae*
SD	Synthetic defined
SDS	Sodium dodecyl sulfate
SLIDE	SANT-like_ISWI domain
SPT	Suppressor of Ty
SSAT	Spermidine/spermine N^1-acetyltransferase
SSC	Sodium chloride trisodium citrate dihydrate
SSK	Suppressor of sensor kinase
STE	Sterile
SUT	Stable unannotated transcripts
SWI/SNF	Switch/sucrose non-fermentable
TAE	Tris-acetate-EDTA
TAP	Tandem affinity purification
TBS	Tris-buffered saline
TE	tris-EDTA
TES	Transcription end site
TEV	Tobacco Etch virus
tRNA	transfer RNA
TSS	Transcription start site
wt	Wild type
YPD	Yeast extract peptone dextrose
YPG	Yeast extract peptone glycerol
YPGal	Yeast extract peptone galactose
YPLac	Yeast extract peptone Lactate
YPRaff	Yeast extract peptone raffinose
β-ME	β-mercaptoehanol

6 Bibliography

1. Akey, C. W. and K. Luger (2003). "Histone chaperones and nucleosome assembly." Curr Opin Struct Biol **13**(1): 6-14.
2. Allan, J., N. Harborne, D. C. Rau and H. Gould (1982). "Participation of core histone "tails" in the stabilization of the chromatin solenoid." J Cell Biol **93**(2): 285-297.
3. Allfrey, V. G., R. Faulkner and A. E. Mirsky (1964). "Acetylation and Methylation of Histones and Their Possible Role in the Regulation of Rna Synthesis." Proc Natl Acad Sci U S A **51**: 786-794.
4. Avery, O. T., C. M. Macleod and M. McCarty (1944). "Studies on the Chemical Nature of the Substance Inducing Transformation of Pneumococcal Types : Induction of Transformation by a Desoxyribonucleic Acid Fraction Isolated from Pneumococcus Type Iii." J Exp Med **79**(2): 137-158.
5. Bakshi, R., T. Prakash, D. Dash and V. Brahmachari (2004). "In silico characterization of the INO80 subfamily of SWI2/SNF2 chromatin remodeling proteins." Biochem Biophys Res Commun **320**(1): 197-204.
6. Balasundaram, D., C. W. Tabor and H. Tabor (1993). "Oxygen toxicity in a polyamine-depleted spe2 delta mutant of Saccharomyces cerevisiae." Proc Natl Acad Sci U S A **90**(10): 4693-4697.
7. Balasundaram, D., C. W. Tabor and H. Tabor (1996). "Sensitivity of polyamine-deficient Saccharomyces cerevisiae to elevated temperatures." J Bacteriol **178**(9): 2721-2724.
8. Bannister, A. J. and T. Kouzarides (2011). "Regulation of chromatin by histone modifications." Cell Res **21**(3): 381-395.
9. Bannister, A. J., P. Zegerman, J. F. Partridge, E. A. Miska, J. O. Thomas, R. C. Allshire and T. Kouzarides (2001). "Selective recognition of methylated lysine 9 on histone H3 by the HP1 chromo domain." Nature **410**(6824): 120-124.
10. Basehoar, A. D., S. J. Zanton and B. F. Pugh (2004). "Identification and distinct regulation of yeast TATA box-containing genes." Cell **116**(5): 699-709.
11. Belmont, A. S., M. B. Braunfeld, J. W. Sedat and D. A. Agard (1989). "Large-scale chromatin structural domains within mitotic and interphase chromosomes in vivo and in vitro." Chromosoma **98**(2): 129-143.
12. Billett, M. A. and J. M. Barry (1974). "Role of histones in chromatin condensation." Eur J Biochem **49**(3): 477-484.
13. Blank, T. A. and P. B. Becker (1995). "Electrostatic mechanism of nucleosome spacing." J Mol Biol **252**(3): 305-313.
14. Bolton, P. H. and D. R. Kearns (1977). "Effect of magnesium and polyamines on the structure of yeast tRNAPhe." Biochim Biophys Acta **477**(1): 10-19.
15. Bork, P. and E. V. Koonin (1993). "An expanding family of helicases within the 'DEAD/H' superfamily." Nucleic Acids Res **21**(3): 751-752.
16. Brocks, D., C. R. Schmidt, M. Daskalakis, H. S. Jang, N. M. Shah, D. Li, J. Li, B. Zhang, Y. Hou, S. Laudato, D. B. Lipka, J. Schott, H. Bierhoff, Y. Assenov, M. Helf, A. Ressnerova, M. S. Islam, A. M. Lindroth, S. Haas, M. Essers, C. D. Imbusch, B. Brors, I. Oehme, O. Witt, M. Lubbert, J. P. Mallm, K. Rippe, R. Will, D. Weichenhan, G. Stoecklin, C. Gerhauser, C. C. Oakes, T. Wang and C. Plass (2017). "DNMT and HDAC inhibitors induce cryptic transcription start sites encoded in long terminal repeats." Nat Genet **49**(7): 1052-1060.
17. Bryson, K. and R. J. Greenall (2000). "Binding sites of the polyamines putrescine, cadaverine, spermidine and spermine on A- and B-DNA located by simulated annealing." J Biomol Struct Dyn **18**(3): 393-412.

18. Burgio, G., D. F. Corona, C. M. Nicotra, G. Carruba and G. Taibi (2016). "P/CAF-mediated spermidine acetylation regulates histone acetyltransferase activity." J Enzyme Inhib Med Chem **31**(sup3): 75-82.
19. Capili, A. D., D. C. Schultz, I. F. Rauscher and K. L. Borden (2001). "Solution structure of the PHD domain from the KAP-1 corepressor: structural determinants for PHD, RING and LIM zinc-binding domains." EMBO J **20**(1-2): 165-177.
20. Carrozza, M. J., B. Li, L. Florens, T. Suganuma, S. K. Swanson, K. K. Lee, W. J. Shia, S. Anderson, J. Yates, M. P. Washburn and J. L. Workman (2005). "Histone H3 methylation by Set2 directs deacetylation of coding regions by Rpd3S to suppress spurious intragenic transcription." Cell **123**(4): 581-592.
21. Casero, R. A., Jr. and A. E. Pegg (1993). "Spermidine/spermine N1-acetyltransferase--the turning point in polyamine metabolism." FASEB J **7**(8): 653-661.
22. Celano, P., S. B. Baylin and R. A. Casero, Jr. (1989). "Polyamines differentially modulate the transcription of growth-associated genes in human colon carcinoma cells." J Biol Chem **264**(15): 8922-8927.
23. Chaiet, L. and F. J. Wolf (1964). "The Properties of Streptavidin, a Biotin-Binding Protein Produced by Streptomycetes." Arch Biochem Biophys **106**: 1-5.
24. Chattopadhyay, M. K., W. Chen, G. Poy, M. Cam, D. Stiles and H. Tabor (2009). "Microarray studies on the genes responsive to the addition of spermidine or spermine to a Saccharomyces cerevisiae spermidine synthase mutant." Yeast **26**(10): 531-544.
25. Chattopadhyay, M. K., C. W. Tabor and H. Tabor (2006). "Polyamine deficiency leads to accumulation of reactive oxygen species in a spe2Delta mutant of Saccharomyces cerevisiae." Yeast **23**(10): 751-761.
26. Chavez, M. S., J. K. Scorgie, B. K. Dennehey, S. Noone, J. K. Tyler and M. E. Churchill (2012). "The conformational flexibility of the C-terminus of histone H4 promotes histone octamer and nucleosome stability and yeast viability." Epigenetics Chromatin **5**(1): 5.
27. Chereji, R. V., S. Ramachandran, T. D. Bryson and S. Henikoff (2018). "Precise genome-wide mapping of single nucleosomes and linkers in vivo." Genome Biol **19**(1): 19.
28. Cheung, V., G. Chua, N. N. Batada, C. R. Landry, S. W. Michnick, T. R. Hughes and F. Winston (2008). "Chromatin- and transcription-related factors repress transcription from within coding regions throughout the Saccharomyces cerevisiae genome." PLoS Biol **6**(11): e277.
29. Clapier, C. R. and B. R. Cairns (2012). "Regulation of ISWI involves inhibitory modules antagonized by nucleosomal epitopes." Nature **492**(7428): 280-284.
30. Clark, D. (2015). „Chromatin Remodeling and Gene Activation" National Institute of Health http://grantome.com/grant/NIH/ZIA-HD008775-11
31. Collins, K. A., S. Furuyama and S. Biggins (2004). "Proteolysis contributes to the exclusive centromere localization of the yeast Cse4/CENP-A histone H3 variant." Curr Biol **14**(21): 1968-1972.
32. Cronan, J. E., Jr. and J. C. Wallace (1995). "The gene encoding the biotin-apoprotein ligase of Saccharomyces cerevisiae." FEMS Microbiol Lett **130**(2-3): 221-229.
33. Cuperus, G. and D. Shore (2002). "Restoration of silencing in Saccharomyces cerevisiae by tethering of a novel Sir2-interacting protein, Esc8." Genetics **162**(2): 633-645.
34. Daban, J. R. and A. Bermudez (1998). "Interdigitated solenoid model for compact chromatin fibers." Biochemistry **37**(13): 4299-4304.
35. Dhayalan, A., A. Rajavelu, P. Rathert, R. Tamas, R. Z. Jurkowska, S. Ragozin and A. Jeltsch (2010). "The Dnmt3a PWWP domain reads histone 3 lysine 36 trimethylation and guides DNA methylation." J Biol Chem **285**(34): 26114-26120.

36. Dod, B., A. Kervabon and J. Parello (1982). "Effect of cations on the acetylation of chromatin in vitro." Eur J Biochem **121**(2): 401-405.
37. Drouin, S., L. Laramee, P. E. Jacques, A. Forest, M. Bergeron and F. Robert (2010). "DSIF and RNA polymerase II CTD phosphorylation coordinate the recruitment of Rpd3S to actively transcribed genes." PLoS Genet **6**(10): e1001173.
38. Durrin, L. K., R. K. Mann, P. S. Kayne and M. Grunstein (1991). "Yeast histone H4 N-terminal sequence is required for promoter activation in vivo." Cell **65**(6): 1023-1031.
39. Eisen, J. A., K. S. Sweder and P. C. Hanawalt (1995). "Evolution of the SNF2 family of proteins: subfamilies with distinct sequences and functions." Nucleic Acids Res **23**(14): 2715-2723.
40. Eisenberg, T., H. Knauer, A. Schauer, S. Buttner, C. Ruckenstuhl, D. Carmona-Gutierrez, J. Ring, S. Schroeder, C. Magnes, L. Antonacci, H. Fussi, L. Deszcz, R. Hartl, E. Schraml, A. Criollo, E. Megalou, D. Weiskopf, P. Laun, G. Heeren, M. Breitenbach, B. Grubeck-Loebenstein, E. Herker, B. Fahrenkrog, K. U. Frohlich, F. Sinner, N. Tavernarakis, N. Minois, G. Kroemer and F. Madeo (2009). "Induction of autophagy by spermidine promotes longevity." Nat Cell Biol **11**(11): 1305-1314.
41. Elfring, L. K., R. Deuring, C. M. McCallum, C. L. Peterson and J. W. Tamkun (1994). "Identification and characterization of Drosophila relatives of the yeast transcriptional activator SNF2/SWI2." Mol Cell Biol **14**(4): 2225-2234.
42. Feng, J. and B. Villeponteau (1992). "High-resolution analysis of c-fos chromatin accessibility using a novel DNase I-PCR assay." Biochim Biophys Acta **1130**(3): 253-258.
43. Fernandez-Suarez, M., T. S. Chen and A. Y. Ting (2008). "Protein-protein interaction detection in vitro and in cells by proximity biotinylation." J Am Chem Soc **130**(29): 9251-9253.
44. Ferreira, H., A. Flaus and T. Owen-Hughes (2007). "Histone modifications influence the action of Snf2 family remodelling enzymes by different mechanisms." J Mol Biol **374**(3): 563-579.
45. Fukuchi, J., K. Kashiwagi, K. Takio and K. Igarashi (1994). "Properties and structure of spermidine acetyltransferase in Escherichia coli." J Biol Chem **269**(36): 22581-22585.
46. Gangaraju, V. K. and B. Bartholomew (2007). "Dependency of ISW1a chromatin remodeling on extranucleosomal DNA." Mol Cell Biol **27**(8): 3217-3225.
47. Ganguly, S., P. Mummaneni, P. J. Steinbach, D. C. Klein and S. L. Coon (2001). "Characterization of the Saccharomyces cerevisiae homolog of the melatonin rhythm enzyme arylalkylamine N-acetyltransferase (EC 2.3.1.87)." J Biol Chem **276**(50): 47239-47247.
48. Garcia-Martinez, J., G. Ayala, V. Pelechano, S. Chavez, E. Herrero and J. E. Perez-Ortin (2012). "The relative importance of transcription rate, cryptic transcription and mRNA stability on shaping stress responses in yeast." Transcription **3**(1): 39-44.
49. Garinther, W. I. and M. C. Schultz (1997). "Topoisomerase function during replication-independent chromatin assembly in yeast." Mol Cell Biol **17**(7): 3520-3526.
50. Gelbart, M. E., T. Rechsteiner, T. J. Richmond and T. Tsukiyama (2001). "Interactions of Isw2 chromatin remodeling complex with nucleosomal arrays: analyses using recombinant yeast histones and immobilized templates." Mol Cell Biol **21**(6): 2098-2106.
51. Gkikopoulos, T., P. Schofield, V. Singh, M. Pinskaya, J. Mellor, M. Smolle, J. L. Workman, G. J. Barton and T. Owen-Hughes (2011). "A role for Snf2-related nucleosome-spacing enzymes in genome-wide nucleosome organization." Science **333**(6050): 1758-1760.
52. Goldmark, J. P., T. G. Fazzio, P. W. Estep, G. M. Church and T. Tsukiyama (2000). "The Isw2 chromatin remodeling complex represses early meiotic genes upon recruitment by Ume6p." Cell **103**(3): 423-433.

53. Goodman, A. J., E. R. Daugharthy and J. Kim (2013). "Pervasive antisense transcription is evolutionarily conserved in budding yeast." Mol Biol Evol **30**(2): 409-421.
54. Gregory, T.R. (2018). “Animal Genome Size Database.” http://www.genomesize.com.
55. Grune, T., J. Brzeski, A. Eberharter, C. R. Clapier, D. F. Corona, P. B. Becker and C. W. Muller (2003). "Crystal structure and functional analysis of a nucleosome recognition module of the remodeling factor ISWI." Mol Cell **12**(2): 449-460.
56. Guillemette, B., A. R. Bataille, N. Gevry, M. Adam, M. Blanchette, F. Robert and L. Gaudreau (2005). "Variant histone H2A.Z is globally localized to the promoters of inactive yeast genes and regulates nucleosome positioning." PLoS Biol **3**(12): e384.
57. Guschin, D., T. M. Geiman, N. Kikyo, D. J. Tremethick, A. P. Wolffe and P. A. Wade (2000). "Multiple ISWI ATPase complexes from xenopus laevis. Functional conservation of an ACF/CHRAC homolog." J Biol Chem **275**(45): 35248-35255.
58. Hampsey, M. (1997). "A review of phenotypes in Saccharomyces cerevisiae." Yeast **13**(12): 1099-1133.
59. Hassan, A. H., K. E. Neely and J. L. Workman (2001). "Histone acetyltransferase complexes stabilize swi/snf binding to promoter nucleosomes." Cell **104**(6): 817-827.
60. Heby, O. and H. Emanuelsson (1981). "Role of the polyamines in germ cell differentiation and in early embryonic development." Med Biol **59**(5-6): 417-422.
61. Hennig, B. P. and T. Fischer (2014). "The great repression." Transcription **4**(3): 97-101.
62. Holstege, F. C., E. G. Jennings, J. J. Wyrick, T. I. Lee, C. J. Hengartner, M. R. Green, T. R. Golub, E. S. Lander and R. A. Young (1998). "Dissecting the regulatory circuitry of a eukaryotic genome." Cell **95**(5): 717-728.
63. Hongay, C. F., P. L. Grisafi, T. Galitski and G. R. Fink (2006). "Antisense transcription controls cell fate in Saccharomyces cerevisiae." Cell **127**(4): 735-745.
64. Hope, I. A. and K. Struhl (1985). "GCN4 protein, synthesized in vitro, binds HIS3 regulatory sequences: implications for general control of amino acid biosynthetic genes in yeast." Cell **43**(1): 177-188.
65. Igarashi, K. and K. Kashiwagi (2010). "Modulation of cellular function by polyamines." Int J Biochem Cell Biol **42**(1): 39-51.
66. Iouzalen, N., J. Moreau and M. Mechali (1996). "H2A.ZI, a new variant histone expressed during Xenopus early development exhibits several distinct features from the core histone H2A." Nucleic Acids Res **24**(20): 3947-3952.
67. Jenuwein, T. and C. D. Allis (2001). “Translating the histone code.” Science **293**(5532): 1074-1080.
68. Jiang, C. and B. F. Pugh (2009). "A compiled and systematic reference map of nucleosome positions across the Saccharomyces cerevisiae genome." Genome Biol **10**(10): R109.
69. Joshi, A. A. and K. Struhl (2005). "Eaf3 chromodomain interaction with methylated H3-K36 links histone deacetylation to Pol II elongation." Mol Cell **20**(6): 971-978.
70. Kanno, T., Y. Kanno, R. M. Siegel, M. K. Jang, M. J. Lenardo and K. Ozato (2004). "Selective recognition of acetylated histones by bromodomain proteins visualized in living cells." Mol Cell **13**(1): 33-43.
71. Kaplan, C. D., L. Laprade and F. Winston (2003). "Transcription elongation factors repress transcription initiation from cryptic sites." Science **301**(5636): 1096-1099.
72. Kapranov, P., A. T. Willingham and T. R. Gingeras (2007). "Genome-wide transcription and the implications for genomic organization." Nat Rev Genet **8**(6): 413-423.
73. Kassabov, S. R., N. M. Henry, M. Zofall, T. Tsukiyama and B. Bartholomew (2002). "High-resolution mapping of changes in histone-DNA contacts of nucleosomes remodeled by ISW2." Mol Cell Biol **22**(21): 7524-7534.

74. Kawashima, S., H. Ogiwara, S. Tada, M. Harata, U. Wintersberger, T. Enomoto and M. Seki (2007). "The INO80 complex is required for damage-induced recombination." Biochem Biophys Res Commun **355**(3): 835-841.
75. Kayne, P. S., U. J. Kim, M. Han, J. R. Mullen, F. Yoshizaki and M. Grunstein (1988). "Extremely conserved histone H4 N terminus is dispensable for growth but essential for repressing the silent mating loci in yeast." Cell **55**(1): 27-39.
76. Kent, N. A., N. Karabetsou, P. K. Politis and J. Mellor (2001). "In vivo chromatin remodeling by yeast ISWI homologs Isw1p and Isw2p." Genes Dev **15**(5): 619-626.
77. Keogh, M. C., S. K. Kurdistani, S. A. Morris, S. H. Ahn, V. Podolny, S. R. Collins, M. Schuldiner, K. Chin, T. Punna, N. J. Thompson, C. Boone, A. Emili, J. S. Weissman, T. R. Hughes, B. D. Strahl, M. Grunstein, J. F. Greenblatt, S. Buratowski and N. J. Krogan (2005). "Cotranscriptional set2 methylation of histone H3 lysine 36 recruits a repressive Rpd3 complex." Cell **123**(4): 593-605.
78. Kim, S. H., G. Quigley, F. L. Suddath and A. Rich (1971). "High-resolution x-ray diffraction patterns of crystalline transfer RNA that show helical regions." Proc Natl Acad Sci U S A **68**(4): 841-845.
79. Kim, T. S., C. L. Liu, M. Yassour, J. Holik, N. Friedman, S. Buratowski and O. J. Rando (2010). "RNA polymerase mapping during stress responses reveals widespread nonproductive transcription in yeast." Genome Biol **11**(7): R75.
80. Knezetic, J. A. and D. S. Luse (1986). "The presence of nucleosomes on a DNA template prevents initiation by RNA polymerase II in vitro." Cell **45**(1): 95-104.
81. Koc, A., L. J. Wheeler, C. K. Mathews and G. F. Merrill (2004). "Hydroxyurea arrests DNA replication by a mechanism that preserves basal dNTP pools." J Biol Chem **279**(1): 223-230.
82. Krajewski, W. A. (2014). "Yeast Isw1a and Isw1b exhibit similar nucleosome mobilization capacities for mononucleosomes, but differently mobilize dinucleosome templates." Arch Biochem Biophys **546**: 72-80.
83. Krietenstein, N., M. Wal, S. Watanabe, B. Park, C. L. Peterson, B. F. Pugh and P. Korber (2016). "Genomic Nucleosome Organization Reconstituted with Pure Proteins." Cell **167**(3): 709-721 e712.
84. Krogan, N. J., J. Dover, A. Wood, J. Schneider, J. Heidt, M. A. Boateng, K. Dean, O. W. Ryan, A. Golshani, M. Johnston, J. F. Greenblatt and A. Shilatifard (2003). "The Paf1 complex is required for histone H3 methylation by COMPASS and Dot1p: linking transcriptional elongation to histone methylation." Mol Cell **11**(3): 721-729.
85. Kullman, Bellis; Tamm, Heidi; Kullman, Kaur (2005). “Fungal Genome Size Database.” http://www.zbi.ee/fungal-genomesize/
86. Langer, P. R., A. A. Waldrop and D. C. Ward (1981). "Enzymatic synthesis of biotin-labeled polynucleotides: novel nucleic acid affinity probes." Proc Natl Acad Sci U S A **78**(11): 6633-6637.
87. Lee, W., D. Tillo, N. Bray, R. H. Morse, R. W. Davis, T. R. Hughes and C. Nislow (2007). "A high-resolution atlas of nucleosome occupancy in yeast." Nat Genet **39**(10): 1235-1244.
88. Leroy, D., J. K. Heriche, O. Filhol, E. M. Chambaz and C. Cochet (1997). "Binding of polyamines to an autonomous domain of the regulatory subunit of protein kinase CK2 induces a conformational change in the holoenzyme. A proposed role for the kinase stimulation." J Biol Chem **272**(33): 20820-20827.
89. Li, G. and J. Widom (2004). "Nucleosomes facilitate their own invasion." Nat Struct Mol Biol **11**(8): 763-769.

90. Li, J., D. Moazed and S. P. Gygi (2002). "Association of the histone methyltransferase Set2 with RNA polymerase II plays a role in transcription elongation." J Biol Chem **277**(51): 49383-49388.
91. Lickwar, C. R., B. Rao, A. A. Shabalin, A. B. Nobel, B. D. Strahl and J. D. Lieb (2009). "The Set2/Rpd3S pathway suppresses cryptic transcription without regard to gene length or transcription frequency." PLoS One **4**(3): e4886.
92. Lieleg, C., P. Ketterer, J. Nuebler, J. Ludwigsen, U. Gerland, H. Dietz, F. Mueller-Planitz and P. Korber (2015). "Nucleosome spacing generated by ISWI and CHD1 remodelers is constant regardless of nucleosome density." Mol Cell Biol **35**(9): 1588-1605.
93. Liu, B., A. Sutton and R. 28lanz (2005). "A yeast polyamine acetyltransferase." J Biol Chem **280**(17): 16659-16664.
94. Love MI, Huber W, Anders S (2014). "Moderated estimation of fold change and dispersion for RNA-seq data with DESeq2." Genome Biology, 15, 550. doi: 10.1186/s13059-014-0550-8.
95. Luger, K., A. W. Mader, R. K. Richmond, D. F. Sargent and T. J. Richmond (1997). "Crystal structure of the nucleosome core particle at 2.8 A resolution." Nature **389**(6648): 251-260.
96. Lusser, A., D. L. Urwin and J. T. Kadonaga (2005). "Distinct activities of CHD1 and ACF in ATP-dependent chromatin assembly." Nat Struct Mol Biol **12**(2): 160-166.
97. Lutter, L. C. (1978). "Characterization of DNase-I cleavage sites in the nucleosome." Cold Spring Harb Symp Quant Biol **42 Pt 1**: 137-147.
98. Maeshima, K., R. Imai, S. Tamura and T. Nozaki (2014). "Chromatin as dynamic 10-nm fibers." Chromosoma **123**(3): 225-237.
99. Maltby, V. E., B. J. Martin, J. M. Schulze, I. Johnson, T. Hentrich, A. Sharma, M. S. Kobor and L. Howe (2012). "Histone H3 lysine 36 methylation targets the Isw1b remodeling complex to chromatin." Mol Cell Biol **32**(17): 3479-3485.
100. Mani, R., R. P. St Onge, J. L. t. Hartman, G. Giaever and F. P. Roth (2008). "Defining genetic interaction." Proc Natl Acad Sci U S A **105**(9): 3461-3466.
101. Maurer-Stroh, S., N. J. Dickens, L. Hughes-Davies, T. Kouzarides, F. Eisenhaber and C. P. Ponting (2003). "The Tudor domain 'Royal Family': Tudor, plant Agenet, Chromo, PWWP and MBT domains." Trends Biochem Sci **28**(2): 69-74.
102. Mavrich, T. N., I. P. Ioshikhes, B. J. Venters, C. Jiang, L. P. Tomsho, J. Qi, S. C. Schuster, I. Albert and B. F. Pugh (2008). "A barrier nucleosome model for statistical positioning of nucleosomes throughout the yeast genome." Genome Res **18**(7): 1073-1083.
103. McConnell, A. D., M. E. Gelbart and T. Tsukiyama (2004). "Histone Fold Protein Dls1p Is Required for Isw2-Dependent Chromatin Remodeling In Vivo." Molecular and Cellular Biology **24**(7): 2605-2613.
104. McGhee, J. D. and G. Felsenfeld (1980). "Nucleosome structure." Annu Rev Biochem **49**: 1115-1156.
105. McKinley, K. L. and I. M. Cheeseman (2016). "The molecular basis for centromere identity and function." Nat Rev Mol Cell Biol **17**(1): 16-29.
106. Michaillat, L. and A. Mayer (2013). "Identification of genes affecting vacuole membrane fragmentation in Saccharomyces cerevisiae." PLoS One **8**(2): e54160.
107. Miller, C., B. Schwalb, K. Maier, D. Schulz, S. Dumcke, B. Zacher, A. Mayer, J. Sydow, L. Marcinowski, L. Dolken, D. E. Martin, A. Tresch and P. Cramer (2011). "Dynamic transcriptome analysis measures rates of mRNA synthesis and decay in yeast." Mol Syst Biol **7**: 458.

108. Miller, T., N. J. Krogan, J. Dover, H. Erdjument-Bromage, P. Tempst, M. Johnston, J. F. Greenblatt and A. Shilatifard (2001). "COMPASS: a complex of proteins associated with a trithorax-related SET domain protein." Proc Natl Acad Sci U S A **98**(23): 12902-12907.
109. Milo, R., P. Jorgensen, U. Moran, G. Weber and M. Springer (2010). "BioNumbers--the database of key numbers in molecular and cell biology." Nucleic Acids Res **38**(Database issue): D750-753.
110. Morillon, A., N. Karabetsou, J. O'Sullivan, N. Kent, N. Proudfoot and J. Mellor (2003). "Isw1 chromatin remodeling ATPase coordinates transcription elongation and termination by RNA polymerase II." Cell **115**(4): 425-435.
111. Morrison, A. J., J. Highland, N. J. Krogan, A. Arbel-Eden, J. F. Greenblatt, J. E. Haber and X. Shen (2004). "INO80 and gamma-H2AX interaction links ATP-dependent chromatin remodeling to DNA damage repair." Cell **119**(6): 767-775.
112. Mueller, J. E. and M. Bryk (2007). "Isw1 acts independently of the Isw1a and Isw1b complexes in regulating transcriptional silencing at the ribosomal DNA locus in Saccharomyces cerevisiae." J Mol Biol **371**(1): 1-10.
113. Ng, H. H., F. Robert, R. A. Young and K. Struhl (2003). "Targeted recruitment of Set1 histone methylase by elongating Pol II provides a localized mark and memory of recent transcriptional activity." Mol Cell **11**(3): 709-719.
114. Nicolas, E., T. Yamada, H. P. Cam, P. C. Fitzgerald, R. Kobayashi and S. I. Grewal (2007). "Distinct roles of HDAC complexes in promoter silencing, antisense suppression and DNA damage protection." Nat Struct Mol Biol **14**(5): 372-380.
115. Norouzi, D., A. Katebi, F. Cui and V. B. Zhurkin (2015). "Topological diversity of chromatin fibers: Interplay between nucleosome repeat length, DNA linking number and the level of transcription." AIMS Biophys **2**(4): 613-629.
116. Ocampo, J., R. V. Chereji, P. R. Eriksson and D. J. Clark (2016). "The ISW1 and CHD1 ATP-dependent chromatin remodelers compete to set nucleosome spacing in vivo." Nucleic Acids Res **44**(10): 4625-4635.
117. Olins, A. L. and D. E. Olins (1974). "Spheroid chromatin units (v bodies)." Science **183**(4122): 330-332.
118. Papamichos-Chronakis, M., S. Watanabe, O. J. Rando and C. L. Peterson (2011). "Global regulation of H2A.Z localization by the INO80 chromatin-remodeling enzyme is essential for genome integrity." Cell **144**(2): 200-213.
119. Patrone, E., R. Coradeghini, P. Barboro, C. D'Arrigo, M. Mormino, S. Parodi and C. Balbi (2006). "SCN- binding to the charged lysines of histones end domains mimics acetylation and shows the major histone-DNA interactions involved in eu and heterochromatin stabilization." J Cell Biochem **97**(4): 869-881.
120. Pattenden, S. G., M. M. Gogol and J. L. Workman (2010). "Features of cryptic promoters and their varied reliance on bromodomain-containing factors." PLoS One **5**(9): e12927.
121. Perisic, O., R. Collepardo-Guevara and T. Schlick (2010). "Modeling studies of chromatin fiber structure as a function of DNA linker length." J Mol Biol **403**(5): 777-802.
122. Pinskaya, M., A. Nair, D. Clynes, A. Morillon and J. Mellor (2009). "Nucleosome remodeling and transcriptional repression are distinct functions of Isw1 in Saccharomyces cerevisiae." Mol Cell Biol **29**(9): 2419-2430.
123. Plum, G. E., P. G. Arscott and V. A. Bloomfield (1990). "Condensation of DNA by trivalent cations. 2. Effects of cation structure." Biopolymers **30**(5-6): 631-643.
124. Pokholok, D. K., C. T. Harbison, S. Levine, M. Cole, N. M. Hannett, T. I. Lee, G. W. Bell, K. Walker, P. A. Rolfe, E. Herbolsheimer, J. Zeitlinger, F. Lewitter, D. K. Gifford and

R. A. Young (2005). "Genome-wide map of nucleosome acetylation and methylation in yeast." Cell **122**(4): 517-527.

125. Pollard, K. J., M. L. Samuels, K. A. Crowley, J. C. Hansen and C. L. Peterson (1999). "Functional interaction between GCN5 and polyamines: a new role for core histone acetylation." EMBO J **18**(20): 5622-5633.
126. Prunell, A. and R. D. Kornberg (1978). "Relation of nucleosomes to DNA sequences." Cold Spring Harb Symp Quant Biol **42 Pt 1**: 103-108.
127. Qin, S. and J. Min (2014). "Structure and function of the nucleosome-binding PWWP domain." Trends Biochem Sci **39**(11): 536-547.
128. Qiu, C., K. Sawada, X. Zhang and X. Cheng (2002). "The PWWP domain of mammalian DNA methyltransferase Dnmt3b defines a new family of DNA-binding folds." Nat Struct Biol **9**(3): 217-224.
129. Qiu, Y., R. F. Levendosky, S. Chakravarthy, A. Patel, G. D. Bowman and S. Myong (2017). "The Chd1 Chromatin Remodeler Shifts Nucleosomal DNA Bidirectionally as a Monomer." Mol Cell **68**(1): 76-88 e76.
130. Quan, T. K. and G. A. Hartzog (2010). "Histone H3K4 and K36 methylation, Chd1 and Rpd3S oppose the functions of Saccharomyces cerevisiae Spt4-Spt5 in transcription." Genetics **184**(2): 321-334.
131. Radman-Livaja, M., T. K. Quan, L. Valenzuela, J. A. Armstrong, T. van Welsem, T. Kim, L. J. Lee, S. Buratowski, F. van Leeuwen, O. J. Rando and G. A. Hartzog (2012). "A key role for Chd1 in histone H3 dynamics at the 3' ends of long genes in yeast." PLoS Genet **8**(7): e1002811.
132. Ragvin, A., H. Valvatne, S. Erdal, V. Arskog, K. R. Tufteland, K. Breen, O. Y. AM, A. Eberharter, T. J. Gibson, P. B. Becker and R. Aasland (2004). "Nucleosome binding by the bromodomain and PHD finger of the transcriptional cofactor p300." J Mol Biol **337**(4): 773-788.
133. Ransom, M., B. K. Dennehey and J. K. Tyler (2010). "Chaperoning histones during DNA replication and repair." Cell **140**(2): 183-195.
134. Raspaud, E., I. Chaperon, A. Leforestier and F. Livolant (1999). "Spermine-induced aggregation of DNA, nucleosome, and chromatin." Biophys J **77**(3): 1547-1555.
135. Rawal, Y., R. V. Chereji, H. Qiu, S. Ananthakrishnan, C. K. Govind, D. J. Clark and A. G. Hinnebusch (2018). "SWI/SNF and RSC cooperate to reposition and evict promoter nucleosomes at highly expressed genes in yeast." Genes Dev **32**(9-10): 695-710.
136. Redon, C., D. Pilch, E. Rogakou, O. Sedelnikova, K. Newrock and W. Bonner (2002). "Histone H2A variants H2AX and H2AZ." Curr Opin Genet Dev **12**(2): 162-169.
137. Rigaut, G., A. Shevchenko, B. Rutz, M. Wilm, M. Mann and B. Seraphin (1999). "A generic protein purification method for protein complex characterization and proteome exploration." Nat Biotechnol **17**(10): 1030-1032.
138. Robert, F., D. K. Pokholok, N. M. Hannett, N. J. Rinaldi, M. Chandy, A. Rolfe, J. L. Workman, D. K. Gifford and R. A. Young (2004). "Global position and recruitment of HATs and HDACs in the yeast genome." Mol Cell **16**(2): 199-209.
139. Robinson, P. J. and D. Rhodes (2006). "Structure of the '30 nm' chromatin fibre: a key role for the linker histone." Curr Opin Struct Biol **16**(3): 336-343.
140. Rougemaille, M. and D. Libri (2011). "Control of cryptic transcription in eukaryotes." Adv Exp Med Biol **702**: 122-131.
141. Ruiz-Herrera, J., R. Ruiz-Medrano and A. Dominguez (1995). "Selective inhibition of cytosine-DNA methylases by polyamines." FEBS Lett **357**(2): 192-196.

142. Sanchez, R. and M. M. Zhou (2011). "The PHD finger: a versatile epigenome reader." Trends Biochem Sci **36**(7): 364-372.
143. Santisteban, M. S., T. Kalashnikova and M. M. Smith (2000). "Histone H2A.Z regulats transcription and is partially redundant with nucleosome remodeling complexes." Cell **103**(3): 411-422.
144. Sato, N., Y. Ohtake, H. Kato, S. Abe, H. Kohno and Y. Ohkubo (2003). "Effects of polyamines on histone polymerization." J Protein Chem **22**(3): 303-307.
145. Schulz, D., B. Schwalb, A. Kiesel, C. Baejen, P. Torkler, J. Gagneur, J. Soeding and P. Cramer (2013). "Transcriptome surveillance by selective termination of noncoding RNA synthesis." Cell **155**(5): 1075-1087.
146. Scott, R. H., K. G. Sutton and A. C. Dolphin (1993). "Interactions of polyamines with neuronal ion channels." Trends Neurosci **16**(4): 153-160.
147. Shi, X., T. Hong, K. L. Walter, M. Ewalt, E. Michishita, T. Hung, D. Carney, P. Pena, F. Lan, M. R. Kaadige, N. Lacoste, C. Cayrou, F. Davrazou, A. Saha, B. R. Cairns, D. E. Ayer, T. G. Kutateladze, Y. Shi, J. Cote, K. F. Chua and O. Gozani (2006). "ING2 PHD domain links histone H3 lysine 4 methylation to active gene repression." Nature **442**(7098): 96-99.
148. Simic, R., D. L. Lindstrom, H. G. Tran, K. L. Roinick, P. J. Costa, A. D. Johnson, G. A. Hartzog and K. M. Arndt (2003). "Chromatin remodeling protein Chd1 interacts with transcription elongation factors and localizes to transcribed genes." EMBO J **22**(8): 1846-1856.
149. Smolle, M., S. Venkatesh, M. M. Gogol, H. Li, Y. Zhang, L. Florens, M. P. Washburn and J. L. Workman (2012). "Chromatin remodelers Isw1 and Chd1 maintain chromatin structure during transcription by preventing histone exchange." Nat Struct Mol Biol **19**(9): 884-892.
150. SPELL Version 2.0.3. Hibbs MA, Hess DC, Myers CL, Huttenhower C, Li K and Troyanskaya OG (2007). “Exploring the functional landscape of gene expression: directed search of large microarray compendia.” Bioinformatics 23: 2692-9
151. Stockdale, C., A. Flaus, H. Ferreira and T. Owen-Hughes (2006). "Analysis of nucleosome repositioning by yeast ISWI and Chd1 chromatin remodeling complexes." J Biol Chem **281**(24): 16279-16288.
152. Strahl, B. D., P. A. Grant, S. D. Briggs, Z. W. Sun, J. R. Bone, J. A. Caldwell, S. Mollah, R. G. Cook, J. Shabanowitz, D. F. Hunt and C. D. Allis (2002). "Set2 is a nucleosomal histone H3-selective methyltransferase that mediates transcriptional repression." Mol Cell Biol **22**(5): 1298-1306.
153. Suto, R. K., M. J. Clarkson, D. J. Tremethick and K. Luger (2000). "Crystal structure of a nucleosome core particle containing the variant histone H2A.Z." Nat Struct Biol **7**(12): 1121-1124.
154. Tabor, C. W., H. Tabor, A. K. Tyagi and M. S. Cohn (1982). "The biochemistry, genetics, and regulation of polyamine biosynthesis in Saccharomyces cerevisiae." Fed Proc **41**(14): 3084-3088.
155. Thatcher, T. H. and M. A. Gorovsky (1994). "Phylogenetic analysis of the core histones H2A, H2B, H3, and H4." Nucleic Acids Res **22**(2): 174-179.
156. Thomas, J. O. and R. J. Thompson (1977). "Variation in chromatin structure in two cell types from the same tissue: a short DNA repeat length in cerebral cortex neurons." Cell **10**(4): 633-640.
157. Thompson, D. M. and R. Parker (2007). "Cytoplasmic decay of intergenic transcripts in Saccharomyces cerevisiae." Mol Cell Biol **27**(1): 92-101.

158. Tirosh, I.m N. Sigal and N. Barkai (2010). “Widespread remodeling of mid-coding sequence nucleosomes by Isw1.” Genome Biol **11**(5): R49
159. Tsukiyama, T., J. Palmer, C. C. Landel, J. Shiloach and C. Wu (1999). "Characterization of the imitation switch subfamily of ATP-dependent chromatin-remodeling factors in Saccharomyces cerevisiae." Genes Dev **13**(6): 686-697.
160. Tzagoloff, A. and C. L. Dieckmann (1990). "PET genes of Saccharomyces cerevisiae." Microbiol Rev **54**(3): 211-225.
161. Usherwood, P. N. (2000). "Natural and synthetic polyamines: modulators of signalling proteins." Farmaco **55**(3): 202-205.
162. van Dijk, E. L., C. L. Chen, Y. d'Aubenton-Carafa, S. Gourvennec, M. Kwapisz, V. Roche, C. Bertrand, M. Silvain, P. Legoix-Ne, S. Loeillet, A. Nicolas, C. Thermes and A. Morillon (2011). "XUTs are a class of Xrn1-sensitive antisense regulatory non-coding RNA in yeast." Nature **475**(7354): 114-117.
163. van Holde, K. and T. Yager (2003). "Models for chromatin remodeling: a critical comparison." Biochem Cell Biol **81**(3): 169-172.
164. van Werven, F. J., G. Neuert, N. Hendrick, A. Lardenois, S. Buratowski, A. van Oudenaarden, M. Primig and A. Amon (2012). "Transcription of two long noncoding RNAs mediates mating-type control of gametogenesis in budding yeast." Cell **150**(6): 1170-1181.
165. Vary, J. C., V. K. Gangaraju, J. Qin, C. C. Landel, C. Kooperberg, B. Bartholomew and T. Tsukiyama (2003). "Yeast Isw1p Forms Two Separable Complexes In Vivo." Molecular and Cellular Biology **23**(1): 80-91.
166. Vasicova, P., V. Stradalova, P. Halada, J. Hasek and I. Malcova (2013). "Nuclear import of chromatin remodeler Isw1 is mediated by atypical bipartite cNLS and classical import pathway." Traffic **14**(2): 176-193.
167. Venkatesh, S., H. Li, M. M. Gogol and J. L. Workman (2016). "Selective suppression of antisense transcription by Set2-mediated H3K36 methylation." Nat Commun 7: 13610.
168. Villeponteau, B., J. Brawley and H. G. Martinson (1992). "Nucleosome spacing is compressed in active chromatin domains of chick erythroid cells." Biochemistry **31**(5): 1554-1563.
169. Whitehouse, I., A. Flaus, B. R. Cairns, M. F. White, J. L. Workman and T. Owen-Hughes (1999). "Nucleosome mobilization catalysed by the yeast SWI/SNF complex." Nature **400**(6746): 784-787.
170. Whitehouse, I., O. J. Rando, J. Delrow and T. Tsukiyama (2007). "Chromatin remodelling at promoters suppresses antisense transcription." Nature **450**(7172): 1031-1035.
171. Whitehouse, I., C. Stockdale, A. Flaus, M. D. Szczelkun and T. Owen-Hughes (2003). "Evidence for DNA translocation by the ISWI chromatin-remodeling enzyme." Mol Cell Biol **23**(6): 1935-1945.
172. Witkowski, L. and W. D. Foulkes (2015). "In Brief Picturing the complex world of chromatin remodelling families." Journal of Pathology: 403-406.
173. Wong, H., J. M. Victor and J. Mozziconacci (2007). "An all-atom model of the chromatin fiber containing linker histones reveals a versatile structure tuned by the nucleosomal repeat length." PLoS One **2**(9): e877.
174. Woodage, T., M. A. Basrai, A. D. Baxevanis, P. Hieter and F. S. Collins (1997). "Characterization of the CHD family of proteins." Proc Natl Acad Sci U S A **94**(21): 11472-11477.
175. Workman, J. L. and R. E. Kingston (1998). "Alteration of nucleosome structure as a mechanism of transcriptional regulation." Annu Rev Biochem **67**: 545-579.

176. Wyers, F., M. Rougemaille, G. Badis, J. C. Rousselle, M. E. Dufour, J. Boulay, B. Regnault, F. Devaux, A. Namane, B. Seraphin, D. Libri and A. Jacquier (2005). "Cryptic pol II transcripts are degraded by a nuclear quality control pathway involving a new poly(A) polymerase." Cell **121**(5): 725-737.
177. Xu, Z., W. Wei, J. Gagneur, F. Perocchi, S. Clauder-Munster, J. Camblong, E. Guffanti, F. Stutz, W. Huber and L. M. Steinmetz (2009). "Bidirectional promoters generate pervasive transcription in yeast." Nature **457**(7232): 1033-1037.
178. Yadav, T. and I. Whitehouse (2016). "Replication-Coupled Nucleosome Assembly and Positioning by ATP-Dependent Chromatin-Remodeling Enzymes." Cell Rep **15**(4): 715-723.
179. Yamada, K., T. D. Frouws, B. Angst, D. J. Fitzgerald, C. DeLuca, K. Schimmele, D. F. Sargent and T. J. Richmond (2011). "Structure and mechanism of the chromatin remodelling factor ISW1a." Nature **472**(7344): 448-453.
180. Yen, K., V. Vinayachandran, K. Batta, R. T. Koerber and B. F. Pugh (2012). "Genome-wide nucleosome specificity and directionality of chromatin remodelers." Cell **149**(7): 1461-1473.
181. Yun, M., J. Wu, J. L. Workman and B. Li (2011). "Readers of histone modifications." Cell Res **21**(4): 564-578.
182. Zhao, Y. and B. A. Garcia (2015). "Comprehensive Catalog of Currently Documented Histone Modifications." Cold Spring Harb Perspect Biol **7**(9): a025064.
183. Zhu, P. and G. Li (2016). "Structural insights of nucleosome and the 30-nm chromatin fiber." Curr Opin Struct Biol **36**: 106-115.

7 Supplementary

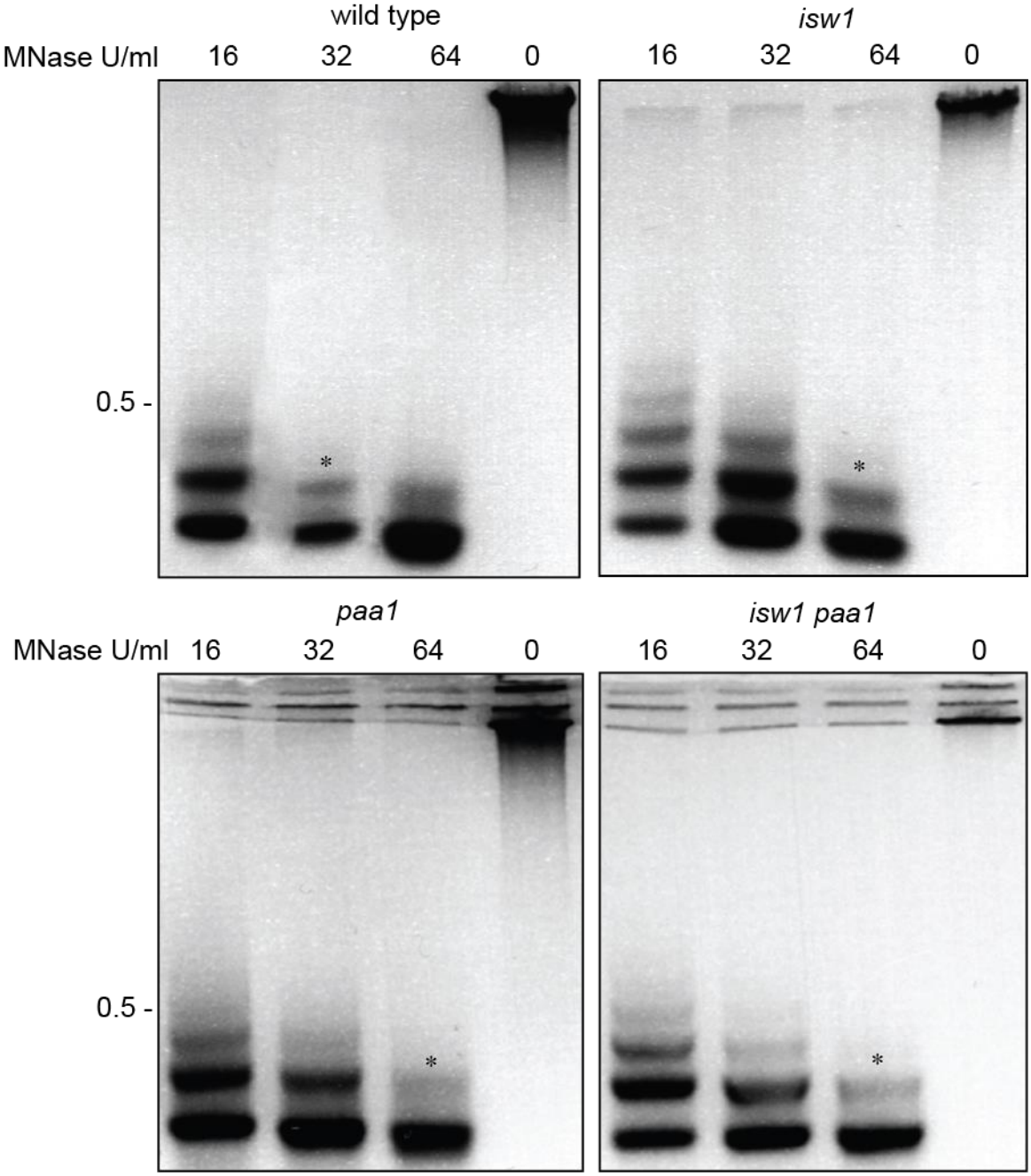

Figure S1: Agarose gel of MNase-digested nuclear extractions. Nuclear extracts of each strain were digested with different amounts of MNase and separated on an agarose gel for comparison. MNase concentrations were 16, 32, 64 and 0 U/ml. This was used to determine the optimal rate of digestion for subsequent MNase-seq experiments.

8 Acknowledgements

This project could not have been done without Prof. Michaela Smolle, who not only provided me with the opportunity to work on the project, but also lent her ear for any troubles I might encounter. She consistently supported me with her advice, but also gave me the freedom to develop myself.

I would like to extend my gratitude to the members of my thesis advisory committee, Prof. Andreas Ladurner, Dr. Jürg Müller and Dr. Wolfgang Zachariae, for their feedback and advice.

Special thanks to the members of the ISWI-club meetings; PD Dr. Philipp Korber, Dr. Felix Müller-Planitz, Dr. Christoph Kurat and all the members of their groups. I have lost count of how often they gave me a push in the right direction, offered new ways or were simply there to support my efforts.

I wish to extent a heartfelt thanks to Dr. Tamas Schauer, who performed most of the computational work for me and was always willing to answer my many naïve questions about R. I would also like to thank Dr. Helmut Blum and Dr. Stefan Krebs from LAFUGA, who performed all the sequencing and were of great and invaluable help when it came to troubleshooting.

Next, I would like to thank the members of the Department of Physiological Chemistry for their help, their support and for providing a nourishing atmosphere that encourages growth. Specifically, I would like to thank Dr. Matias Capella for suggesting the Bio-ID based assay to me, and generally being a great help with anything yeast-related. Dr. Magdalena Murawska for her support and feedback regarding library preparations. Marianne Köber, Zdenka Stanic, PD Dr. Anton Eberharter and Christine Werner for their invaluable support. And I would especially like to thank the current and past members of the Smolle group, Lisa Schuster, Ina Koeva, Osman Mohammed, Dieter Kamp, Lena Bergmann, Julia Schluckebier and Ameirika. Especially Ina Koeva and Julia Schluckebier, who were of great help and took some of the load off my shoulders.

Lastly, I would like to thank my family for their continued support and love.